

UNCLASSIFIED

AD NUMBER
AD909325
NEW LIMITATION CHANGE
TO Approved for public release, distribution unlimited
FROM Distribution authorized to U.S. Gov't. agencies only; Test and evaluation; 26 Apr 1973. Other requests shall be referred to Director, USA Ballistic Research Laboratories, Attn: AMXBR-XM-SE, Aberdeen Proving Ground, MD 21005.
AUTHORITY
USAARDC ltr, 8 Mar 1978

THIS PAGE IS UNCLASSIFIED

THIS REPORT HAS BEEN DELIMITED
AND CLEARED FOR PUBLIC RELEASE
UNDER DOD DIRECTIVE 5200.20 AND
NO RESTRICTIONS ARE IMPOSED UPON
ITS USE AND DISCLOSURE.

DISTRIBUTION STATEMENT A

APPROVED FOR PUBLIC RELEASE;
DISTRIBUTION UNLIMITED.

BRL MR 2276

BRL

AD

MEMORANDUM REPORT NO. 2276

MUZZLE DEVICES, A STATE-OF-THE-ART SURVEY VOLUME I: HARDWARE STUDY

by

Edward M. Schmidt

February 1973

D D C
RECEIVED
APR 26 1973
R
C

26 APR 1973

Distribution limited to US Government agencies only. *T&E*
Other requests for this document must be referred to
Director, USA Ballistic Research Laboratories, ATTN:
AMXBR-XM-SE, Aberdeen Proving Ground, Maryland 21005.

AD909325

USA BALLISTIC RESEARCH LABORATORIES
ABERDEEN PROVING GROUND, MARYLAND

Destroy this report when it is no longer needed.
Do not return it to the originator.

Secondary distribution of this report by originating or
sponsoring activity is prohibited.

Additional copies of this report may be purchased from
the U.S. Department of Commerce, National Technical
Information Service, Springfield, Virginia 22151

The findings in this report are not to be construed as
an official Department of the Army position, unless
so designated by other authorized documents.

BALLISTIC RESEARCH LABORATORIES

MEMORANDUM REPORT NO. 2276

FEBRUARY 1973

MUZZLE DEVICES, A STATE-OF-THE-ART SURVEY.
VOLUME I: HARDWARE STUDY

Edward M. Schmidt

Exterior Ballistics Laboratory

Distribution limited to US Government agencies only.
Other requests for this document must be referred to
Director, USA Ballistic Research Laboratories, ATTN:
AMXBR-XM-SE, Aberdeen Proving Ground, Maryland 21005.

26 APR 1973

TXE

RDT&E Project No. 1J562604A607

ABERDEEN PROVING GROUND, MARYLAND

BALLISTIC RESEARCH LABORATORIES

MEMORANDUM REPORT NO. 2276

EMSchmidt/so
Aberdeen Proving Ground, Md.
February 1973

MUZZLE DEVICES, A STATE-OF-THE-ART SURVEY.
VOLUME I: HARDWARE STUDY

ABSTRACT

A review of the salient literature addressing the engineering design of muzzle devices is presented. Both theoretical and experimental techniques applicable to specific hardware items are discussed. The types of devices considered include: muzzle brakes, compensators, blast deflectors, blast suppressors, and flash suppressors. The second volume of this report addresses specific gas dynamic theories which are applicable, but, in general, have not been utilized in the analysis of muzzle gas flow fields.

TABLE OF CONTENTS

	Page
ABSTRACT	3
LIST OF ILLUSTRATIONS	7
LIST OF SYMBOLS	11
I. INTRODUCTION	13
II. MUZZLE GAS FLOW	13
III MUZZLE DEVICES: THEORY	19
A. Muzzle Brakes, Compensators and Blast Deflectors	20
B. Flash Suppressors	32
C. Blast Suppressors	37
IV. MUZZLE DEVICES: EXPERIMENTAL TECHNIQUES	45
A. Muzzle Brakes, Compensators, and Blast Suppressors	46
B. Flash Suppressors	49
C. Blast Suppressors	52
V. CONCLUSIONS	54
REFERENCES	101
DISTRIBUTION LIST	109

LIST OF ILLUSTRATIONS

Figure	Page
1. Formation of Precursor Blast and Free Jet	55
2. Photograph of Precursor Flow Field	56
3. (a,b,c, and d) Schematic of Propellant Gas Ejection Flow	57
4. (a,b,c, and d) Photograph of Propellant Gas Ejection Flow	61
5. Schematic of Wave Structure for an Underexpanded, Steady Jet	65
6. Plot of Deflection Angle Versus Pressure Ratio	66
7. Plot of Deflection Angle Versus Pressure Ratio for Various γ_e	67
8. Effect of Pressure Ratio Upon Free Jet Structure	68
9. Categories of Muzzle Devices	69
10. Rateau Muzzle Brake	70
11. Rateau's Calculation of Force on 75mm Gun Muzzle Brake	71
12. German Double Baffle Muzzle Brake	72
13. Oswatitsch Brake Nomenclature	73
14. Optimization Plot for w	74
15. Plot of σ vs α_e for Zero Projectile Hole Loss	74
16. Comparison of Theory and Experiment for Oswatitsch Brake	75
17. Smith Muzzle Gas Flow Nomenclature	76
18. Smith Brake Theory Results	76
19. Pressure Distribution on Brake Surface in a Steady Jet	77
20. Flash Phenomena	78

Figure	Page
21. Flash Preventive Devices	79
22. Watling Flash Suppressor Tests	80
23. Supersonic Diffuser Silencer	81
24. Blast Suppressor Classification	82
25. Furrer Explosive Blast Measurements	83
26. The Effect of Muzzle Brakes on Blast Pressures	83
27. Westine's Universal Gun Blast Plot	84
28. Correlation of Overpressure Factor for Various Weapons	85
29. Universal Impulse Plot and Correlation Plot	86
30. Time of Blast Arrival	87
31. Bixler Blast Suppressor Model	88
32. Sequence of Measured Blasts	89
33. Oswatitsch 2-D Measured Blasts	90
34. Efficiency Factor, Theory and Experiment	91
35. Efficiency Factor of Extended Brake	91
36. Axisymmetric Jet With Baffle	92
37. Cover Types and Effect of Efficiency	92
38. Slade Recoil Measurements	93
39. Slade Water Table	94
40. Slade Optimal Turning Vane	94
41. Smith Muzzle Brake Rig	95
42. Aerodynamic Index Versus Pressure Ratio	96
43. Aerodynamic Index for Multibaffle Brakes	96
44. Smith's Overpressure Measurements	97

Figure	Page
45. Concentration Schematic	98
46. MRI Mach Number Measurements and Comparison With Theory	98
47. Relative Time and Intensity of Flash	99
48. Blast Suppressor Test Rig	100
49. Attention of Constant Length Suppressor	100

LIST OF SYMBOLS

A	area
c	gun caliber
D	diameter
E	propellant energy
F	force
G	mass flux parameter
I	impulse
J	momentum flux parameter
l	gun barrel length
\dot{m}	mass flux
M	Mach number
p	static pressure
p_s	stagnation pressure
Q	charge weight
r	radial distance
R	gas constant
t	time
T	temperature
v	velocity
\bar{w}_e	mean brake exit velocity
W	Oswatitsch momentum parameter
α	co-volume
γ	ratio of specific heats
η	Smith efficiency factor

LIST OF SYMBOLS (continued)

- θ free jet turning angle
 ρ density
 σ Oswatitsch efficiency factor

Superscripts

- $(\bar{\quad})$ mean property
 $(\quad)^*$ sonic quantity

Subscripts

- $(\quad)_e$ exit quantity
 $(\quad)_m$ muzzle quantity
 $(\quad)_o$ side-on quantity
 $(\quad)_\infty$ condition at infinity (ambient)

I. INTRODUCTION

Muzzle devices have been used to control the trajectory of projectiles, the motion of the recoiling gun, and the observable effects of the sudden release of the propellant energy. The shotgun choke is an example of a device which controls projectile ballistics through muzzle contour. In the mid-nineteenth century, the French attempted to control recoil by redirecting propellant gases rearward through a series of holes drilled in the gun barrel near the muzzle. Silencers and blast suppressors began appearing around the turn of the century. The Maxim multi-baffle silencer developed during this time frame is still one of the most effective designs. Flash hiders received considerable attention during the First World War; however, the most effective devices namely, bar-type flash suppressors, did not make an appearance until 1949. At this time, the Franklin Institute accidentally discovered the flash suppression capabilities of bars or prongs placed in the muzzle flow regime.

While the construction and use of muzzle devices has proceeded at a brisk pace, the development of an insight into the physical phenomena occurring within the devices has lagged behind. There are no strong theoretical analyses available which permit the design of devices for a large range of weaponry. What techniques are available are generally empirically based and highly restrictive in nature. It is the purpose of this report to present a state-of-the-art survey of the design techniques applied to these devices. Consideration will be given to the muzzle gas flow phenomena associated with both the bare muzzle and the muzzle device-equipped flow fields. Both experimental and theoretical engineering design analyses will be investigated. To define the flow environment in which the muzzle device is immersed, this report will commence with a discussion of bare muzzle phenomena.

II. MUZZLE GAS FLOW

The development of the flow field associated with the discharge of a gun may be broken into two phases. The first phase involves the formation of the precursor free jet and blast. This flow is induced by projectile in-bore travel forcing the tube air to be ejected. Additionally, imperfect obturation permits the leakage of high pressure propellant gases around the projectile. The second phase consists of the flow field created as the high pressure propellant gases leave the gun tube following projectile uncorking. This phase is of longer duration than the precursor phase. It commences with the formation of a strong blast and a coupled, highly underexpanded jet, continuing through the emptying process wherein the pressure in the gun tube is finally brought to equilibrium with the ambient pressure.

The formation of the precursor effects is depicted schematically in Figure 1. Following ignition of the propellant, the projectile is accelerated down the gun tube, forming compression waves in the quiescent tube air. This is the classical accelerating piston problem from one-dimensional gas dynamics. The first wave propagates at the local speed of sound. As it moves, the air it passes is accelerated in the direction of wave motion, compressed and heated. Since the speed of sound in air is proportional to the square root of the air temperature, waves will propagate at a higher velocity through the compressed medium. This effect, coupled with the velocity imparted to the tube gas, causes the subsequent compression waves to catch the lead wave and eventually coalesce to form a shock. This process is shown in the x-t diagram. As the projectile continues to accelerate and as high pressure propellant gases leak around it, more compression waves propagate down the tube strengthening the shock.

When the shock reaches the muzzle, the lateral constraints are no longer present and the gases can expand in three dimensions. The intrusion of this high pressure, moving tube gas stream into the quiescent atmosphere surrounding the gun causes the still air to be rapidly displaced forming the precursor air blast. The tube gas stream expands forming an axisymmetric free jet. If the flow velocity behind the normal shock is subsonic at the time it reaches the muzzle, a one-dimensional expansion fan will propagate back up the gun tube accelerating the gases to a sonic velocity at the muzzle. If the flow behind the normal shock is supersonic at the time it reaches the muzzle, no waves can propagate back upstream. A spark shadowgraph of the precursor blast and free jet formed about the muzzle of a 5.56mm Mann barrel firing M-16 ammunition is shown in Figure 2. This shadowgraph was taken at the BRL^{1*}, but the technique is an historically proven experimental tool utilized by early investigators²⁻⁵ of muzzle gas flows. The precursor blast is nearly spherical with its center displaced forward of the muzzle. In this case the blast geometric center is located approximately 3.2 calibers forward of the muzzle. The tube gas jet is seen to possess a shock structure typical of underexpanded jets. A point to be emphasized is that the blast and jet formation processes are mutually dependent and occurring in a highly unsteady manner. The jet develops in an environment which has been previously compressed and set in motion by the passage of the precursor blast. In turn, the growth of the jet effects the blast, as can be seen from the waves which are propagating from the jet to the blast in the shadowgraph. An additional complication is introduced if the unsteady nature of the muzzle conditions is considered. The precursor muzzle flow forms the ambient into which the high pressure propellant gases expand once the projectile separates from the muzzle.

The growth and decay of the propellant gas jet and associated blast have been studied by a variety of researchers. Cranz^{3,4} utilized spark Schlieren coupled with selective probing of the flow field. He noted

**References are listed on page 101.*

the qualitative agreement between his experimental results and the linearized jet theory of Prandtl. Quayle⁵ used similar techniques to investigate the muzzle gas flow but did not attempt a discussion of the gasdynamics involved. World War II stimulated interest in muzzle phenomena. Working on blast suppressor design, Slade⁶ investigated the chronological history of muzzle phenomena and presented a qualitative description of these based on spark shadowgraphs of a caliber .30 rifle. Using work performed on muzzle brakes during the war^{7a-7c}, Oswatitsch⁸ analyzed the development of the muzzle gas flow field and attempted to quantify the phenomena occurring. From these works, the following description of the muzzle gas flow field about a small caliber, high velocity weapon is constructed. In particular, the flow from a 5.56mm Mann barrel firing an M-193 projectile at 3200 feet per second is addressed.

Schematics of the salient flow features are presented in Figures 3a - 3d. The first figure in the series shows the propellant gases expanding around the projectile soon after uncorking. A strong blast is formed in the area exterior to the boundary of the tube gas free jet. However, there is no evidence of shock formation at the interface between the flow field of the tube gas jet and the developing propellant gas jet. This may be due to the effect of the rapid expansion around the projectile undergone by the propellant gases combined with the presence of an established velocity field (the tube gas jet); thus, the condition of continuity of pressure and velocity across a contact surface could be satisfied. However, the opaqueness of the propellant gas cloud, which also contains a large amount of particulate matter, prevents penetration and makes observation of the exact interface location impossible.

Figure 3b shows the flow field at a somewhat later time. The propellant gases have moved over the projectile and the interface between the two gas jets has moved forward of the projectile nose. Beginnings of shocks are forming ahead of the interface as the propellant gases move into what was the low velocity region of the tube gas jet (i.e., behind the tube gas jet Mach disc). The momentum of the propellant gases in the axial direction plus the flow paths provided by the precursor flow field have caused the propellant gas jet and blast to become significantly elongated in the axial direction. A shock structure internal to the jet has begun to form. Oswatitsch⁸ has shown that the muzzle velocity of the propellant gases is at least sonic. The flow between the muzzle and the projectile base expands rapidly to supersonic velocities. That these velocities are higher than the projectile velocity is evidenced by the shock standing at its base. The pressure at the base of the projectile in this region is considerably higher than that on the nose, and the projectile continues to accelerate. At the jet boundary, shocks are beginning to form due to a coalescing of waves reflected from the contact surface between the propellant gas jet and the surrounding air. The jet boundary is observed to be highly turbulent indicating that mixing between the propellant gases and air is occurring there. This mixing is an important factor in the examination of flash phenomena.

As the propellant gases expand supersonically, their pressure drops rapidly. It is seen from Oswatitsch that the pressure drops from on the order of 5000 pounds per square inch at the muzzle to 5 pounds per square inch at a distance of 10-15 calibers. Since these sub-atmospheric pressures must eventually recover to near-atmospheric pressure (the exact recovery pressure is determined by compatibility of pressures and velocities at the interface between the jet and blast fields), shocks occur in the flow to recompress the gases. In a highly underexpanded jet structure such as the propellant gas jet, axial recompression occurs through the formation of normal shocks (Mach discs in axially symmetric flow or Riemann waves in planar flow). Early in the muzzle jet development, the projectile provides sufficient obstruction to the flow to bring about recompression; however, as the flow field grows larger relative to the projectile, the influence of the projectile presence diminishes and eventually can no longer recompress the flow to provide recovery. At this point, the Mach disc forms in the jet and becomes the means of pressure recovery.

Figure 3c shows the flow field at this time. Across the Mach disc, the flow is decelerated to subsonic velocity. Since the projectile still moves at roughly the muzzle velocity, it no longer is moving slower than the fluid, and it begins to experience drag rather than thrust. As it moves through the propellant gases, a viscous wake is shed. The blast wave is decelerating due to the effects of radial expansion and the projectile moves through it. As the projectile penetrates the blast, a bow shock forms and the drag increases still further. Simultaneous to and at times preceding projectile penetration of the blast, solid particles are seen to be penetrating the blast and moving at supersonic velocities into the undisturbed air. These are most likely powder particles which may be still burning.

The jet structure at this time is nearly that of the typical underexpanded jet. However, the shock structure possesses an irregular, pentagonal configuration. This may be an effect of the precursor flow influencing the subsequent development of the propellant gas flow field. The precursor tube gas jet has been inundated by the rapid growth of the propellant gas jet. One of the last vestiges of the precursor flow is the precursor blast which will soon be outstripped by the stronger main blast.

Subsequent to the projectile penetration of the main blast, the jet attains its maximum growth, Figure 3d. The jet is now of a structure identical to the highly underexpanded steady jet. The flow within the bounding shocks is supersonic increasing in Mach number along the axis and reaching a maximum just at the normal shock. The thermodynamic properties of the gas, namely, density, pressure, and temperature, drop off rapidly from the muzzle values as the expansion region is traversed. Across the shocks, these properties increase again, reaching a second maximum behind the Mach disc. The flow traverses the peripheral oblique shocks maintaining supersonic velocity; however, maintenance of super-

sonic velocities across a normal shock is not possible. Thus, a contact discontinuity is formed between the flow which traverses the oblique shocks and that which traverses the Mach disc. Across the discontinuity, pressure and flow inclination are maintained while all other properties, such as velocity and density, may be discontinuous. The boundary of the jet is the only area where viscous effects are significant. The turbulent mixing layer and recirculating flow region (smoke ring) bring about rapid mixing of the propellant gas and air. The importance of the nature of the jet boundary on the properties of flow interior to the bounding shocks has been shown in steady jet studies⁹⁻¹³ to be negligible. The development of the propellant gas free jet and blast is vividly illustrated in the series of spark shadowgraphs shown in Figures 4a -4d.

The state-of-the-art of blast and jet theory will be discussed in the second volume of this report; however, since the flow in which a muzzle device is immersed is jet-like over almost all of its duration, it will be informative to consider the results of recent work relating to the parameters influencing jet structure. In his text devoted to jets, Pai¹⁴ presents the status of jet studies through the mid-fifties. Love, et al,⁹ present an updated summary of work in the field in addition to presenting an in-depth study of axisymmetric free jet. The upsurge of the space program in the sixties brought about increased investigation¹⁵⁻²⁵ of rocket plumes, which are effectively underexpanded, axisymmetric free jets. The work of most interest in the investigation of the free jet established at the muzzle of a gun is that of Love⁹. In this paper, supersonic jet flows are examined both theoretically, using the method of characteristics, and experimentally, using Schlieren photographs. Parameters of interest are varied and the effect on jet structure is observed. These parameters are: jet exit Mach number, nozzle contour, ratio of specific heats and pressure ratio. For the time being, it is convenient to assume⁸ that the muzzle velocity becomes sonic upon projectile exit and remains so over the major portion of the jet lifetime. Further, a bare muzzle with zero inclination to the bore axis will be taken as the most straight-forward example of this type flow.

Figure 5 schematically depicts a wave pattern for such an expansion. At each corner, the flow is expanded through a wave fan which may be locally assumed to behave like a two-dimensional, Prandtl-Meyer expansion. Since in inviscid flow theory the condition for a contact surface to be maintained is that pressure and flow inclination be continuous across it, the flow expands through an angle, θ , sufficient to reduce the static pressure from the exit pressure, p_e , to the surroundings pressure p_∞ . However, when the waves from the opposite corner reach the jet boundary, they would overexpand the flow to a pressure below that of the surroundings. In order to maintain pressure equivalence at the boundaries these incoming expansion waves must reflect as compression waves. This does in fact occur and the resulting reflected compression waves eventually coalesce to form the shock structure of the jet.

Treating the corner expansion as two-dimensional, Love computes the effect of variation in the exit-to-surroundings pressure ratio, p_e/p_∞ , on the initial jet deflection angle, θ , Figure 6. The effect of increased pressure ratio is quite obvious. For values less than 200, the deflection angle grows rapidly with increasing pressure ratio. However, further increase causes less rapid changes in deflection angle which approaches the limiting expansion angle (for $\gamma = 1.4$, $\theta_{\max} \approx 130^\circ$) asymptotically. The effect of pressure ratio on the muzzle jet can be noted if the initial inclination of the precursor tube gas jet, Figure 2, and that of the propellant gas jet, Figure 4d, are compared. Love investigated another parameter affecting the initial deflection angle, namely, the ratio of specific heats, γ_e , Figure 7. The strong dependence of the initial deflection angle and therefore the overall jet structure upon the ratio of specific heats, γ_e , indicates the importance propellant chemistry can have upon the jet structure. Love continues his calculation past the initial expansion, calculating the jet boundary shape and constructing the characteristic net. However, the effect of compression wave coalescence into shocks is not treated. This coalescence is treated by other jet analyses^{15,26} and resultant property profiles are presented or discussed.

A shock formation which is difficult to predict is the Mach disc. Pai¹⁴ discusses the evolution of the Mach disc in an underexpanded jet as the pressure ratio is increased, Figure 8. These schematics, taken from the original Schlieren photographs of Hartmann and Lazarus³⁰, show that as the pressure ratio, p_e/p_∞ , increases the flow undergoes a stronger expansion initially and must, therefore, undergo stronger recompressions to satisfy the boundary pressure compatibility condition. In the first instance, the exit and surrounding pressures are identical; thus no pressure waves are generated in the inviscid flow field. As the exit pressure is increased, these pressure waves do evolve. The second schematic shows that for a relatively low overpressure the weakness of the waves and confinement of the flow geometry inhibit coalescence until the compression waves reach the outer boundary. As the pressure increases further, the strength of the waves and geometric scale of the flow increase and the shocks move in toward the axis. Further increase causes a shock reflection at the axis. Eventually a pressure ratio is reached where the oblique shocks become so strong that the flow can not traverse both and remain supersonic. At this point, a Mach reflection occurs and the normal shock or Mach disc is formed. Further increases of pressure cause the compression waves to coalesce sooner, forming the shock bottle, and move the location of the Mach disc further downstream. The position of the Mach disc as a function of exit Mach number, pressure ratio, and ratio of specific heats has been investigated by a variety of researchers^{9,10,13,26-30}. For a sonic nozzle, the location of the Mach disc in the axial direction is given^{27,28} as

$$x/D = 0.69 \left(\gamma_e \frac{p_e}{p_\infty} \right)^{1/2}$$

where

x = axial distance to shock

D = orifice diameter

The applicability of this type of relation to the muzzle jet can be seen in comparing the photographs of the precursor and propellant gas jets. Additionally, in another facet of the jet life cycle, its decay, the analysis of free jet structure indicates what to expect. As the pressure ratio decreases, the shock bottle should shrink in size with the Mach disc moving in toward the muzzle. Thus, a reverse sequence to that shown in Figure 8 would be anticipated. Slade⁶ in his discussion of the muzzle phenomena about a caliber .30 rifle indicates that such a process does occur. In light of the direct relationship between the muzzle phenomena after the bullet leaves the muzzle flow field and free jet flows, it is not surprising that muzzle device research has made extensive use of jet theory.

III. MUZZLE DEVICES: THEORY

A simplistic approach to the categorization of muzzle devices would be to establish two groups; the first would contain devices which seek to control or utilize the momentum of the propellant gas flow, while the second would consist of those which control the rate or distribution of propellant energy release, Figure 9.

Muzzle brakes and compensators redirect the propellant gas from purely axial efflux utilizing the resultant forces generated to modify the recoil characteristics of the weapon. Blast deflectors are designed to ameliorate the effects of the propellant gas ejection upon the surroundings. They may be directed to reduce the dust raised by the muzzle gas jet or to eliminate blast wave impingement on the gunner or nearby structures. Deflectors, like brakes and compensators, are essentially turning vanes and/or channels which redirect the flow momentum to a sector where ejection will give least harmful effects. The second category of devices is concerned with the manner in which the residual propellant energy is released into the atmosphere. Blast suppressors attempt to minimize both the amount of energy released from the weapon and the rate at which it is released. A wide variety of blast suppressors has been designed, including multi-baffle, expansion chamber, energy absorption and energy dissipation devices. Flash suppressors function on the principle of controlling the distribution of propellant gases and their energy such that the elevated energy states required to initiate combustion do not occur simultaneously to or in the vicinity of ignitable propellant gas-air mixtures.

The utilization of any particular muzzle device requires a considerable effort to interface the device to the weapon and to the tactical role of the weapon. A muzzle device is useless if its design is impractical either in terms of cost, weight, bulk or interference with

proper weapon functioning and use. The maintenance associated with certain muzzle device designs makes them impractical for general usage. Consideration must be given in designing a device that can utilize currently available materials and manufacturing techniques to provide sufficient structural strength for a long, failure-free life. With such obvious practical considerations recognized, this report will be directed to the consideration of the gas dynamic and chemical kinetic phenomena associated with projectile ejection from a weapon equipped with various forms of muzzle devices. It must be noted that while practical considerations are important, they are at times a hindrance to theoretical and experimental investigations of the detailed flow phenomena. Thus, investigators are forced to make simplifying assumptions in their analyses which are at odds with practical realities. These assumptions and the necessity of making them will, hopefully, be made clear in the discussions to follow.

The devices will be considered by functional groups. Brakes, compensators and blast deflectors operate on identical principles and will be discussed together. Blast and flash suppressors will be considered separately. Important contributions to the analysis of flow through these devices will be discussed. The fourth section will present related experimental techniques.

A. Muzzle Brakes, Compensators and Blast Deflectors

The most definitive source of information concerning the theory and design of muzzle brakes is the survey performed by Hammer³¹ just after the close of World War II. If consideration is given to the fact that the status of muzzle brake design has not advanced significantly from the time of this report, a phrase from page one of Hammer's work is quite telling: "One of the reasons for initiating this project was to discover design formulas for muzzle brakes. Unfortunately, such formulas were not discovered." While this statement is true, the report does present much valuable information, starting with a state-of-the-art summary and concluding with a collection of translations of significant foreign papers^{7,32-38}. To provide an understanding of the development of muzzle brake technology, select papers from this group will be considered.

A basic problem in the computation of muzzle gas flow fields is the estimation of muzzle flow properties as the gun tube empties. Early researchers utilized the work of Hugoniot³² to obtain this estimate. Hugoniot considered the process of emptying a high pressure reservoir. His analysis assumes quasi-steady flow in that no wave motion is allowed in the reservoir. This implies instantaneous adjustment of the thermodynamic state of the reservoir gases to the effects of outflow. The calculations are carried out for either an isothermal or adiabatic process. The rate of outflow may be computed by assuming a sonic orifice

or, if the pressure ratio across the orifice is too low, by using the steady, quasi-one-dimensional flow equations. Knowing the volume and the initial state of the reservoir gases, it is possible to use the computed rate of outflow to compute the subsequent state of the gases for each type process. Rateau³³ modified the analysis of Hugoniot by considering the effect of gas co-volume and approximating the initial property distribution in the gun tube at the time of shot ejection by one with zero velocity but an elevated pressure and temperature which upon adiabatic expansion to the muzzle pressure produces the muzzle velocity. Corner³⁸ compares the analyses of Hugoniot and Rateau, and presents his own calculations for the emptying problem. His work is based on one-dimensional, unsteady gasdynamics and provides a more satisfactory comparison with theory than either Hugoniot or Rateau. However, he indicates that the analysis of Rateau gives reasonably good results if the assumption of an initial property distribution is dropped. Oswatitsch⁸ utilizes the method of characteristics to calculate the variation of muzzle properties. His main aim in this analysis is to establish the validity of assuming a sonic muzzle and quasi-steady flow conditions rather than providing detailed initial conditions to his muzzle gas flow field calculations. The theory of interior ballistics has developed considerably (e.g., Ref. 39-45) since these works; however, with few exceptions, these advances have not been incorporated into analysis of muzzle gas flow fields. For this reason, they will not be discussed, but it is realized that future efforts which attempt to interface the interior and transitional flow fields must consider these improved techniques.

In addition to modifying Hugoniot's theory, Rateau³³ performed an analysis of the flow through a muzzle brake and provided a technique to calculate the force on the brake. The methods of Rateau are of particular interest since they form the basis for the section on muzzle brakes in the current Army Design Handbook⁴⁶. Rateau is realistic in assessing some of the uncertainties facing analysis of muzzle gas flows; among the difficulties he notes are:

1. Physical properties of the high temperature propellant gases are inadequately known.
2. Chemical state is unknown; relative proportion of hydrogen and water vapor greatly modifies coefficients.
3. The flow is highly unsteady while analyses utilize quasi-steady assumptions.
4. Pressure and temperature of gases at muzzle are not well known.

Rateau defines the gun emptying problem as being analogous to the emptying of a reservoir of volume equal to the volume of the gun containing gas at a pressure and temperature both higher than the gun gas values. The gases then expand adiabatically through a converging

nozzle such that at the throat of the nozzle the flow velocity is equal to the muzzle velocity of the gun and the pressure is equal to the muzzle pressure. Using an equation of state of the form:

$$p(v - \alpha) = RT$$

where :

- p = pressure
- v = specific volume
- α = co-volume of gas
- R = gas constant
- T = temperature

he calculates the property variation at the throat through the emptying process. After the gases pass the throat, they are expanded through a brake of the geometry shown in Figure 10. The conical expansion nozzle has a deflection angle δ which is set⁴⁶ at some value less than 30° . This requirement is made to prevent flow separation at the expansion corner. However, in light of recent work⁹⁻³⁰ on underexpanded free jets, this required angle is much too confining. This can be seen by considering that underexpanded jets have initial deflection angles of 90° or more at high pressure ratios, Figures 6 and 7. Since propellant gas jets have a low ratio of specific heats ($\gamma \sim 1.25$) and high pressure ratios ($p_e/p_\infty \sim O(500)$), large initial deflection angles would be anticipated. Figures 4a - 4d indicate this angle to be roughly 90° . Therefore, assuming a smooth transition section from the muzzle to the conical section, turning angles greater than 30° could easily be obtained. Since the important braking forces occur early in the emptying process while the pressure ratio is on the order of 100, there should be no difficulty in maintaining a $60^\circ - 70^\circ$ turn. There appears to be some confusion as to the role of the conical expansion nozzle; rather than inducing expansion of the flow, the nozzle channels the expansion to insure maximum impingement upon brake surfaces.

Rateau assumes the nozzle to be designed such that adiabatic expansion occurs through it, reducing the reservoir pressure to atmospheric pressure at the entrance to the brake. Using the isentropic flow relations, it is possible to calculate the resulting velocity at the brake. From his reservoir emptying calculations and under the assumption of quasi-steady flow, this velocity may be computed as a function of time. Knowing the mass flow through the muzzle and constraining the channel geometry to be such that a quasi-one-dimensional flow may be assumed, the mass flow into the brake and projectile hole may be divided in direct proportion to their relative areas, Figure 10:

$$\dot{m}_1 = \dot{m}^* \frac{S_1}{S_1 + S_2}$$

$$\dot{m}_2 = \dot{m}^* \frac{S_2}{S_1 + S_2}$$

where \dot{m}^* = mass flux through muzzle
 $\dot{m}_{1,2}$ = mass flux through brake, projectile hole
 $s_{1,2}$ = area of brake, projectile hole entrances.

Rateau equates the force on the muzzle brake to the change in momentum through it, assuming flow properties constant through the turn:

$$F_1 = \dot{m}_1 u + \dot{m}_1 u \sin \alpha_1 = \dot{m}^* \frac{s_1}{s_1 + s_2} u (1 + \sin \alpha_1)$$

where: u = velocity of flow expanded to p_∞

For subsequent baffles, the mass flux is again taken as area dependent and the flow properties remain constant. Thus:

$$\dot{m}_2 = \dot{m}_1 \frac{s_3}{s_3 + s_4} = \dot{m}^* \left(\frac{s_2}{s_1 + s_2} \right) \left(\frac{s_3}{s_3 + s_4} \right)$$

$$F_3 = \dot{m}^* \left(\frac{s_2}{s_1 + s_2} \right) \left(\frac{s_3}{s_3 + s_4} \right) u (1 + \sin \alpha_2).$$

Using this analysis, Rateau calculates the force on a muzzle brake from a 75mm gun, Figure 11. The shaded portion of the curve represents the effect of projectile residence in the brake. While there is not a significant increase in impulse (area under the curve) due to projectile residence, there is an increase in peak force which must be accounted for in the structural strength of the device. Rateau claims, but does not show, good success in comparison between tests and analysis.

Rateau's analysis has several shortcomings. He does not account for non-isentropic effects such as friction and, more importantly, shock formations. His assumption of expansion to atmospheric pressure within the conical nozzle is not substantiated. The assumption of turning through the brake without property change is obviously incorrect. These simplifying assumptions make it difficult to use Rateau's analysis to perform optimization studies. The only parameters to be varied are the relative areas of the brake channels, the number of brakes and the turning angle. This leads to the obvious optimization of turning the maximum amount of flow through the greatest angle. The addition of more brakes can be shown to follow the law of diminishing returns as successive brakes work with a mass flux diminished by the flow-through through its predecessors.

Even with its shortcomings, Rateau's analysis formed a basis for a number of subsequent reports³⁴⁻³⁷. The British improved upon the analysis by including the effect of area variation and radial expansion⁴⁷. This form of Rateau's analysis is essentially that presented in the current Army Design Handbook⁴⁶.

With the approach of World War II, the Germans began research into the design of muzzle brakes. This program was largely experimental and produced an unbelievable number of different brake designs³¹. The design which came into most use both by the Germans and the Allies was the double baffle brake, Figure 12. According to the classification of brakes set forth in Reference 46, this is an open brake since the flow expands freely to the brake; whereas the device of Rateau, Figure 10, is a closed brake since the flow is channeled to the brake surfaces. During the war, the British tested a captured German double baffle brake against a variety of high performance designs⁴⁸. The conclusion was that although better braking action could be obtained through the use of closed type brakes with greater rearward flow deflection, the penalty of increased blast overpressures in the crew area could not be tolerated.

The German research effort also included basic investigations of the gas dynamics of muzzle brakes^{7a-7c}. Oswatitsch assumed that the greatest braking forces were imparted during the high pressure, supersonic portion of the tube emptying cycle and, further, that this flow could be assumed to be quasi-steady. Examining a typical brake, Figure 13, Oswatitsch sought to optimize the design details of the device such as spacing, turning angle, brake contour, etc. To estimate the forces transmitted to the brake surface, Oswatitsch performed a momentum flux calculation:

$$F_x = \iint_{A_1} (p - p_\infty + \rho u^2) dA_1 - \iint_{A_3} (p - p_\infty + \rho u^2) dA_3 + \cos \alpha_e \iint_{A_2} (p - p_\infty + \rho u^2) dA_2$$

At the muzzle and brake projectile opening, $p \gg p_\infty$; therefore neglect p_∞ with respect to p :

$$F_x = \iint_{A_1} (p + \rho u^2) dA_1 - \iint_{A_3} (p + \rho u^2) dA_3 + \cos \alpha_e \iint_{A_2} (p - p_\infty + \rho u^2) dA_2$$

Examine the last integral and introduce mean property values over the discharge cross section:

$$\begin{aligned} \iint_{A_2} (p - p_\infty + \rho u^2) dA_2 &= \iint_{A_2} \rho u^2 \left(1 + \frac{p - p_\infty}{\rho u^2}\right) dA_2 \\ &= \bar{w}_e \left(1 + \frac{\bar{p}_e - p_\infty}{\bar{c}_e \bar{w}_e^2}\right) \iint_{A_2} \rho u dA_2 \end{aligned}$$

Define: $J_{A_i} = \iint_{A_i} (p + \rho u^2) dA_i$

$$G_{A_i} = \iint_{A_i} \rho u dA_i$$

The force equation becomes:

$$F_x = J_{A_1} - J_{A_3} + \cos \alpha_e \bar{w}_e \left(1 + \frac{\bar{p}_e - p_\infty}{\bar{p}_e \bar{w}_e^2} \right) G_{A_2}$$

From conservation of mass:

$$G_{A_2} = G_{A_1} - G_{A_3}$$

and defining an efficiency factor, σ , to be:

$$\sigma = F_x / J_{A_1}$$

or:

$$\sigma = 1 - \frac{J_{A_3}}{J_{A_1}} + \cos \alpha_e \bar{w}_e \left(1 + \frac{\bar{p}_e - p_\infty}{\bar{p}_e \bar{w}_e^2} \right) \left(\frac{G_{A_1}}{J_{A_1}} - \frac{G_{A_3}}{J_{A_1}} \right)$$

Oswatitsch now assumes that the conditions at the muzzle are sonic and uniform across the opening. Under this assumption (asterisks indicate sonic throat properties):

$$\begin{aligned} \frac{G_{A_1}}{J_{A_1}} &= \frac{\iint_{A_1} \rho u \, dA_1}{\iint_{A_1} (p + \rho u^2) \, dA_1} = \frac{\rho^* u^* A_1}{(p^* + \rho^* u^{*2}) A_1} \\ &= \frac{\rho^* u^* / p^*}{1 + \frac{\rho^* u^{*2}}{p^*}} = \frac{\gamma M^* / \sqrt{\gamma R T^*}}{1 + \gamma M^{*2}} \end{aligned}$$

Since $M^* = 1$:

$$\frac{G_{A_1}}{J_{A_1}} = \frac{\gamma}{1 + \gamma} \frac{1}{\sqrt{\gamma R T^*}}$$

For a quasi-one-dimensional flow the maximum expansion that can occur is to a condition of zero static temperature implying a complete conversion of internal gas energy into kinetic flow energy. The energy equation can be used to calculate the maximum velocity that occurs in such an expansion:

$$w_{\max} = \sqrt{\frac{\gamma + 1}{\gamma - 1} \gamma R T^*}$$

Thus:

$$\frac{G_{A_1}}{J_{A_1}} = \sqrt{\frac{\gamma^2}{\gamma^2 - 1}} \frac{1}{w_{\max}}$$

$$\text{and: } \sigma = 1 - \frac{J_{A_3}}{J_{A_1}} + \frac{\bar{w}_e}{w_{\max}} \left[1 + \frac{\bar{p}_e - p_{\infty}}{\bar{p}_e \bar{w}_e^2} \right] \sqrt{\frac{\gamma^2}{\gamma^2 - 1}} \left(1 - \frac{G_{A_3}}{G_{A_1}} \right) \cos \alpha_e$$

To evaluate the efficiency of a particular brake design, it is necessary to obtain estimates of the flow behavior within the brake. The propellant gases leave the muzzle at the velocity of sound and are expanded to supersonic velocities. The deflection of the supersonic stream at the brake surfaces causes shocks to form. Thus, if the deflection is great enough, the flow undergoes a non-isentropic process resulting in a decreased stagnation pressure. This represents a decrease in the effective muzzle pressure. Since the deflection of the flow is not constant at all points in the brake, the effective muzzle pressure varies from point to point. However, as a first approximation, Oswatitsch assumes the flow to compress uniformly through a normal shock resulting in a decrease in effective muzzle pressure from p_{sm} to p_{sm}' . From this condition, it accelerates along the brake surface and is ejected at a supersonic velocity. Examining the efficiency equation, it is apparent that maximization of the third term is essential. For the time being neglect projectile hole losses, i.e., assume $J_{A_3} \equiv G_{A_3} \equiv 0$. Then:

$$\sigma = 1 + \frac{\bar{w}_e}{w_{\max}} \left[1 + \frac{\bar{p}_e - p_{\infty}}{\bar{p}_e \bar{w}_e^2} \right] \sqrt{\frac{\gamma^2}{\gamma^2 - 1}} \cos \alpha_e$$

Define:

$$W = \frac{\bar{w}_e}{w_{\max}} \left[1 + \frac{\bar{p}_e - p_{\infty}}{\bar{p}_e \bar{w}_e^2} \right]$$

$$= \frac{\bar{w}_e}{w_{\max}} \left[1 + \frac{1 - \frac{p_{\infty}}{\bar{p}_e}}{\frac{\bar{p}_e}{\bar{w}_e^2}} \right]$$

$$= \frac{\bar{w}_e}{w_{\max}} \left[1 + \frac{1 - \frac{p_{\infty}}{\bar{p}_e}}{\gamma M_e^2} \right]$$

Oswatitsch examines the maximization of this term. Since shocks occur in the brake, let:

$$\frac{p_\infty}{\bar{p}_e} = \frac{p_\infty}{p'_{sm}} \frac{p'_{sm}}{\bar{p}_e}$$

Assuming an isentropic expansion from p'_{sm} to \bar{p}_e , then \bar{M}_e can be calculated from the isentropic relation:

$$\frac{\bar{p}_e}{p'_{sm}} = \left(1 + \frac{\gamma-1}{2} \bar{M}_e^2 \right)^{-\frac{\gamma}{\gamma-1}}$$

and:

$$\begin{aligned} \frac{\bar{w}_e}{w_{max}} &= \frac{\bar{M}_e \sqrt{\gamma R T_e}}{\sqrt{\frac{\gamma+1}{\gamma-1} \gamma R T^*}} \\ &= \frac{\bar{M}_e \sqrt{\gamma R \frac{T_e}{T_{se}} T_{se}}}{\sqrt{\frac{\gamma+1}{\gamma-1} \gamma R \frac{T^*}{T_s} T_s}} \end{aligned}$$

Since stagnation temperature is constant across a shock, $T_s^* = T_{se}$; thus:

$$\frac{\bar{w}_e}{w_{max}} = \frac{\bar{M}_e \sqrt{\gamma R / (1 + \frac{\gamma-1}{2} \bar{M}_e^2)}}{\sqrt{2\gamma R / \gamma - 1}}$$

Using these relations, Oswatitsch calculates W as a function of p'_{sm}/\bar{p}_e for various p'_{sm}/p_∞ , Figure 14. From the limit of sonic exit flow on the left, the W factor increases to a maximum which occurs when the exit pressure is equal to the ambient pressure, $\bar{p}_e = p_\infty$, and then decreases as the flow is overexpanded, $\bar{p}_e < p_\infty$. The brake efficiency is directly related to W :

$$\sigma = 1 + W \sqrt{\frac{\gamma}{\gamma-1}} \cos \alpha_e$$

To use the curves of Figure 14, it is necessary to be capable of calculating p'_{sm}/\bar{p}_e and p'_{sm}/p_∞ . This requires knowledge of the detailed brake flow. Oswatitsch utilizes a method of characteristics calculation to obtain the variation of Mach number along the centerline of the muzzle jet. Assuming the flow passes through a normal shock at the

location of the brake, p_{sm}^i/p_∞ may be calculated from the Rankine-Hugoniot relations and the known muzzle and ambient pressures. A computation of p_{sm}^i/\bar{p}_e is more difficult as it requires a technique to determine how the flow expands along the brake surface. Oswatitsch does not present such a technique and instead assumes $\bar{p}_e = p_\infty$. This effectively reduces the analysis to a method of accounting for shock losses in a thruster nozzle. Since if the flow passes a strong shock, p_{sm}^i/p_∞ is decreased thereby decreasing σ . The analysis is valuable in that it represents the first attempt to account for internal shocks within a framework of multi-dimensional flow.

Assuming a typical value of $p_{sm}^i/p_\infty = 1000$, Oswatitsch picks $W = 0.87$ and calculates the resultant brake efficiency as a function of the deflection angle, Figure 15. The effect of increased deflection is to increase brake efficiency. It should be noted that the calculations presented by Oswatitsch do not allow a detailed investigation of the brake surface design since they in no way account for the method of turning the flow through the angles depicted.

Oswatitsch recognized that this analysis did not account for projectile hole losses. Thus, examining the momentum flux term under the assumption of uniform properties over the cross section of the muzzle and projectile hole:

$$\begin{aligned} \frac{J_{A_3}}{J_{A_1}} &= \frac{p_3 + \rho_3 u_3^2}{p_1 + \rho_1 u_1^2} \frac{A_3}{A_1} \\ &= \frac{\frac{p_3}{\rho_3 u_3^2} + 1}{\frac{p_1}{\rho_1 u_1^2} + 1} \frac{\rho_3 u_3^2}{\rho_1 u_1^2} \frac{A_3}{A_1} \\ &= \frac{1 + \frac{1}{\gamma M_3^2}}{1 + \frac{1}{\gamma M_1^2}} \frac{G_{A_3}}{G_{A_1}} \frac{u_3}{u_1} \end{aligned}$$

Now if the flow is assumed to pass through a normal shock at the brake, it is decelerated to subsonic velocities. In passing through the projectile hole, it expands to sonic velocity at the throat. Since the flow is steady and since the stagnation temperature is constant across the shock:

$$\frac{T_3^*}{T_{s_3}^*} = \frac{1}{\left(1 + \frac{\gamma-1}{2} M_3^{*2}\right)}$$

and

$$\frac{T_3^*}{T_{s3}^*} = \frac{2}{\gamma+1}$$

$$T_3^* = \frac{2}{\gamma+1} T_{s3}^*$$

but

$$T_{s3}^* = T_s^* = T_{s1}^*$$

$$T_1^* = \frac{2}{\gamma+1} T_{s1}^* = \frac{2}{\gamma+1} T_{s3}^* = T_3^*$$

and

$$u_3^* = a_3^* = \sqrt{\gamma R T_3^*} = u_1^*$$

or, at each subsequent throat in the brake, the flow is sonic with a velocity equal to the muzzle exit velocity. Thus:

$$\frac{J_{A_3}}{J_{A_1}} = \frac{G_{A_3}}{G_{A_1}}$$

but:

$$\frac{G_{A_3}}{G_{A_1}} = \frac{\rho_3^* u_3^* A_3}{\rho_1^* u_1^* A_1} = \frac{\rho_3^* A_3}{\rho_1^* A_1}$$

$$= \frac{\frac{p_3^*}{R T_3^*} A_3}{\frac{p_1^*}{R T_1^*} A_1} = \frac{p_3^* A_3}{p_1^* A_1}$$

$$= \frac{\frac{p_3^*}{p_{t_3}^*} p_{t_3}^* A_3}{\frac{p_1^*}{p_{t_1}^*} p_{t_1}^* A_1}$$

Since $M_3^* = M_1^* = 1$, $\frac{p_3^*}{p_{t_3}^*} = \frac{p_1^*}{p_{t_1}^*}$, and:

$$\frac{G_{A_3}}{G_{A_1}} = \frac{p_{t_3}^* A_3}{p_{t_1}^* A_1} = \frac{p_{s_m}'}{p_{s_m}'} \frac{A_3}{A_1}$$

Substituting into the expression for efficiency:

$$\sigma = 1 - \frac{p'_{S_m}}{p_{S_m}} \frac{A_3}{A_1} + w \sqrt{\frac{\gamma^2}{\gamma^2-1}} \left(1 - \frac{p'_{S_m}}{p_{S_m}} \frac{A_3}{A_1} \right) \cos \alpha_e$$

$$= \left(1 - \frac{p'_{S_m}}{p_{S_m}} \frac{A_3}{A_1} \right) \left(1 + w \sqrt{\frac{\gamma^2}{\gamma^2-1}} \cos \alpha_e \right)$$

This expression indicates that shock losses to the flow passing through the projectile hole have a favorable effect on efficiency. Since p'_{S_m}/p_{S_m} decreases with increasing Mach number and since the Mach number increases along the muzzle jet centerline, this indicates that projectile hole losses can be minimized if the distance from the muzzle to the brake is increased (i.e., with increased brake standoff, the mass flux through the projectile hole decreases). However, this must be balanced by the effect of decreasing W with p'_{S_m}/p_∞ . Ideally, a brake should be designed to induce a normal shock to stand at the projectile hole while inducing minimum shock development on the turning vanes. Obviously, such a device would be impossible to construct. However, utilizing this concept, Oswatitsch designed a "back-effect-free" baffle which he tested and compared with his theory, Figure 16. The agreement is quite good, especially in light of the development of oblique rather than normal shocks in the projectile hole.

Additionally, Oswatitsch^{7c} develops a method of characteristics construction of the flow through a muzzle brake. He develops the shock structure and investigates the effect the first baffle has upon the efficiency of the second. His conclusion is that the efficiency of a second brake suffers from two main causes:

1. Reduced mass flow due to presence of the first brake.
2. Reduced jet pressure ratio due to shock structure.

The reduced pressure ratio results in less expansion in the second jet. This tends to develop a higher concentration of mass flux near the axis thereby allowing for increased projectile hole losses. Thus, to obtain more efficiency from a given diameter second brake, it must be placed further from the projectile hole of the preceding brake than the first brake is from the gun muzzle, note Figure 12. Oswatitsch develops an experimental test facility which he used to corroborate his theory and study the internal brake shock structure. However, a discussion of this facility will be deferred until Section IV.

During the war, research in the United States concentrated on the design of blast deflectors. The motivation of these studies was to

decrease the obscuration generated in firing high velocity guns. The work^{6,49,50} concentrated on experimental investigations which will be discussed in Section IV. Millikan⁴⁹ utilized the work of Corner³⁸ to obtain a relation for the momentum flux from a gun. He then used this to calculate the downthrust on a gun under the assumption of complete gas efflux at sonic velocity through holes of a specified geometry. The analysis was overly simplistic failing to allow identification of significant geometric and gas dynamic influences.

Following World War II, interest in muzzle device research waned. Some reports⁵¹⁻⁵⁶ were produced which considered flow through muzzle brakes. Of these, only the work of Smith⁵³⁻⁵⁶ contains an effort to integrate advances in gas dynamic theory with muzzle gas flows. Smith's approach is similar to that of Oswatitsch. He assumes the flow to be steady and utilizes a method of characteristics construction⁵⁷ of a free jet to obtain the flow properties.

Smith notes that Owen and Thornhill postulate the flow within the first shock bottle to be universal, i.e., independent of the pressure ratio. This statement is substantiated by Ladenberg's⁵⁸ experiments. Smith then assumes the force on a baffle placed within the shock bottle may be estimated by assuming "the flow which would normally pass through the disc is simply removed from the flow picture with a corresponding removal of its thrust component. The same result would be obtained if we considered that this flow were deflected normal to the jet axis, without disturbing the remainder of the flow," Figure 17. Smith notes that an optimal value of the axial brake location exists. For small axial separation from the muzzle, there are large losses through the central core flow. As the brake is moved further from the muzzle, these losses diminish due to greater flow impingement upon the brake surface. However, continued displacement tends to increase the flow outside or around the brake. These two effects must be balanced.

To examine the optimization of brake, Smith calculates the aerodynamic index, n , of a selected brake versus the axial location, \bar{x} , within a jet having $p_e/p_\infty \gg 1.0$. The aerodynamic index, which is identical to the brake efficiency, σ , of Oswatitsch, is defined to be:

$$n = 1 - \frac{T}{T_0}$$

where: T = thrust on barrel with brake

T_0 = thrust on barrel without brake.

The calculated results are shown in Figure 18. Smith compared his theory which was calculated for $p_e/p_\infty \approx \infty$ with results obtained from a steady jet⁵³ which had a pressure ratio $p_e/p_\infty = 53$. Theory and experiment agree well. To assess the effect of variable γ , a computation for $\gamma = 1.67$ was made and shown in Figure 18. It is interesting to note

that the experimental data agree better with this computation. However, a consideration of the earlier discussion on jet flows shows this is not surprising. Since increasing γ or decreasing p_e/p_∞ produce similar changes in the initial jet deflection angle, the jet calculation for $p_e/p_\infty \approx \infty$, $\gamma = 1.67$ should result in a flow more geometrically similar to the finite pressure ratio jet ($p_e/p_\infty = 53$, $\gamma = 1.4$) of the experiments.

In later work⁵⁴, Smith uses the analysis to predict the pressure distribution on the brake and compares this with experiment, Figure 19. The ratio of the pressure difference between the front and back surfaces, Δp , to the reservoir pressure is plotted as a function of radial location. Apparently Smith calculates pressure on the front surface by assuming it equal to the stagnation pressure behind a normal shock standing at the location of the surface in a flow field computed from the method of characteristics. The technique to calculate the pressure on the rear surface is not indicated. Possibly, the rear surface pressure may be assumed to be equal to the ambient pressure.

To validate the use of a steady jet analysis for the computation of brake effectiveness of an actual weapon, Smith compares the value of the aerodynamic index obtained in his steady flow experiments with that obtained in firing a 7.62mm rifle. The comparison is good. Since the unsteady flow experiments compare well with the steady jet theory, Smith concludes that the analysis is valid.

The similarities between the work of Smith and Oswatitsch are quite apparent. Both assume steady flow models, utilize the method of characteristics to construct a flow field, and then evaluate brake effectiveness with identical indices. In Section IV, the similarities of their experimental approaches will be examined. The work of these two men essentially represent the current state of muzzle brake theory.

B. Flash Suppressors

Of all the phenomena occurring at the muzzle of a gun, flash is the most difficult to analyze. Not only must the gas dynamics be investigated, but the chemical kinetics associated with propellant gas/air mixtures must be coupled with the flow field. The Franklin Institute has performed a great deal of flash related research⁵⁹⁻⁶⁵ and, in fact, produced the current Army Handbooks on the subject^{46,66}. Reviews of the research performed both at Franklin Institute and elsewhere are available^{67,68}. These show that flash research is concentrated largely on experimental investigations while theory is quite basic and largely qualitative in nature.

A schematic of the flash phenomena showing its salient features⁴⁰ is shown in Figure 20. As the projectile is forced down the tube, a certain amount of high pressure propellant gases leak around it. The leakage mixes with the tube gas and is ejected from the gun tube forming the precursor flow field, Figure 1. If the tube gas was largely air,

the ejected propellant gas/air mixture could be burning upon exit, or, if the tube gas was mainly the propellant gases remaining from a previously fired round, then mixture with the atmosphere could cause ignition. In any case, the flash which occurs prior to the round breaking the muzzle is known as *preflash*.

With the uncorking of the projectile, the high pressure propellant gases are released. At the muzzle, the propellant gases are at high temperature and are likely incandescent. This bright orange incandescence forms what is known as *primary flash*. As the gases move away from the muzzle, they expand very rapidly experiencing a large drop in temperature. This temperature drop quenches the incandescent radiation. However, a dull reddish glow has been observed within the shock bottle and may be due to energy release from internal energy levels which can not adjust to the rapid changes in flow properties. This continued radiation in the expansion region is known as *muzzle glow*. When the gases pass the normal shock, they are slowed to subsonic velocities, compressed and brought to a high static temperature. This conversion of the kinetic flow energy to internal energy of the gas causes the propellant gas to become incandescent once more. This region is called *intermediate flash*.

By far the most severe flash phenomena is *secondary flash*. This flash results from the combustion of the propellant gas/air mixture at the boundary of the jet. The propellant gases mix with the air in the turbulent shear layer and in the vortex ring. The propellant gases consist largely of carbon monoxide and hydrogen with lesser amounts of carbon dioxide, nitrogen, water vapor, traces of hydrocarbons and nitrogen oxides. Since the propellant gases are oxygen poor, mixing with the oxygen rich air forms a combustible mixture requiring only a suitable source of ignition. Among the possible sources of ignition are:

1. ignition by preflash,
2. spontaneous ignition,
3. ignition by intermediate flash,
4. burning powder particles,
5. hot muzzle,
6. tracer rounds.

An experimental investigation conducted by Stephens⁶⁰ indicated the possibility of ignition by the preflash. In a set of firings of a caliber .50 gun, axial holes of various diameters were drilled in the projectile. As the size of the hole increases, the amount of propellant gas leakage and, thereby, the preflash effects grow stronger. Stephens also observed that the secondary flash increased with increasing hole size indicating a connection between the two phenomena.

Spontaneous ignition was examined by Stephens⁶⁰ who developed a technique to calculate the temperature of the air gas mixture upon ejection from an ideal flash suppressor, i.e., one that ejects the gas at atmospheric pressure. He points out that even under optimal conditions it may not be possible to prevent spontaneous ignition once the propellant gas and air reach a certain mixture ratio. Fay⁶⁹ indicates that spontaneous ignition is the most likely source of ignition.

Ignition by the intermediate flash is also noted as possible by Fay⁶⁹. The effectiveness of bar type suppressors in eliminating intermediate flash^{59,63,68}, and, through it, secondary flash demonstrates the ignition capability of these phenomena. A set of photographs by Hodil⁷⁰ seem to indicate the growth of the secondary flash from the intermediate flash. The remaining sources of ignition have been noted by various researchers^{4,68,71,72}.

The literature on muzzle flash contains no analyses which attempt to model the chemical kinetics of the propellant gas at various points in the flow field. The reason for this is quite readily ascertained. There is no available model which accurately describes the non-reacting flow. Although the method of characteristics has been widely used in muzzle brake analysis, the assumption of an inviscid flow is not applicable if flash is to be modeled. Additionally, the chemistry is dependent upon an accurate appraisal of pressure, temperature and residence times the mixture undergoes. The current state-of-the-art does not appear capable of providing an analysis which could handle all of the phenomena associated with a propellant gas jet.

The consideration of a technique to suppress flash is thus largely a matter requiring empirically based principles. The current suppression techniques may be categorized as:

1. Addition of flash inhibitors to the propellant.
2. Utilization of propellant energy through interior ballistic design to reduce residual, post-ejection propellant gas energy.
3. Utilization of muzzle devices.

The first two techniques will not be considered here. There are two types of muzzle devices used on weapons⁶⁶, the flash hider and the flash suppressor, Figure 21. The flash hider merely covers the light-emitting portion of the muzzle gas flow. The conical flash hider is shown covering the primary flash and the muzzle glow. If made significantly larger, this type of device could also shield against intermediate flash. However, it does not eliminate secondary flash, nor does it prevent observation from the front.

Flash suppressors are active devices. They are utilized to control the efflux of propellant gases. The conical flash suppressor was the

device most surveyed during World War II^{68,73-75}. Supposedly, the device expands the propellant gases until they reach atmospheric pressure at the exit. This prevents the formation of an underexpanded jet and its associated shock structure, eliminating intermediate flash and, hopefully, secondary flash by removing its ignition source. Since the jet is being exhausted at supersonic velocities, and at an initial non-zero deflection angle, shocks will form within it emanating from the viscous mixing layer. However, the shocks will not be as strong as the boundary shocks and Mach disc formed within the bare muzzle jet. A point worthy of note is that a device of this design is essentially a supersonic thruster nozzle, and as such, will increase the recoil of the weapon.

The bar type flash suppressor is similar to the conical suppressor in that it is designed to alter the flow shock structure. The device consists of an odd number of bars placed around the bore-line of the weapon. The slots formed are essentially slit nozzles which allow the flow to expand radially in a quasi-planar manner. The utilization of an odd number of bars prevents symmetric wave reflection, Figure 5, from the centerline which eventually builds up into the boundary and normal shock structure. Both this and the conical flash suppressor control the tendency of the flow to overexpand and then recompress through a normal shock. The elimination of the normal shock prevents intermediate flash and retards secondary flash.

The capabilities of a variety of muzzle devices to suppress the flash from a multiple shot weapon were experimentally examined by Watling⁷⁶. Mounting the devices on a caliber .30 machine gun, he fired a multiple burst sequence which consisted of firing for four seconds, resting for eleven seconds, and recycling. The resultant rate of fire was 150 rounds per minute. He defines an efficiency index:

$$\eta = \frac{\text{number of rounds fired}}{\text{number of rounds that flash}}$$

The optimal value of η is infinity which implies zero flashing, and the worst value is one, implying all rounds flash. A sample of the types of devices he tested and the resulting indices are shown in Figure 22.

The results are somewhat surprising. The standard bar type suppressor does not perform as well as some of the more exotic designs. However, the method of firing must be considered since multiple bursts will heat up the barrel and muzzle device, thereby decreasing the flash suppression capability of the system. Thus a device which is extremely effective for single shot or short burst firing may not work well in a prolonged firing role. Additionally, there is data available which does not completely agree with Watling's results. Bar type suppressors have been shown sufficient for miniguns^{71,72} while the addition of a blast suppressor (silencer slots) to other weapons⁷⁰ did not noticeably effect the flash. These inconsistencies indicate the need to

correlate the available information with respect to the type of device used, the weapon fired, the ammunition, the mode of firing, etc. The lack of this correlation is partially responsible for the lack of firm design principles for flash suppressors.

The last device shown in Figure 22 is interesting. The device has an expansion chamber followed by a converging-diverging nozzle. Apparently the nozzle is to function like the diffuser section of a supersonic wind tunnel. At its optimal condition, the device should operate as shown in Figure 23. The flow expands from a sonic muzzle, then is turned parallel to the chamber walls through a shock. The shock is reduced to a Mach wave through interaction with the reflected expansions (note: waves reflect from solid boundaries as the same type waves). This type of "bounded jet" was investigated by Barakauskas⁷⁷ who claimed the resultant flow was similar to that from a Laval nozzle. If this were the case, an expansion into a chamber with a radius larger than that of the muzzle would produce supersonic flow. This supersonic flow then passes through the diffuser. The diffuser throat must be sufficiently large to pass the mass flux of the propellant gas flow. If not, choking will occur and the chamber will be shocked down to subsonic velocity with sonic conditions at the diffuser throat. The flow would then expand to supersonic velocities in the diverging section of the diffuser which is the situation this design seeks to avoid. Assuming choking does not occur, the ideal case would result in the development of a normal shock downstream of or at the throat which will bring the flow to subsonic velocities behind it. The flow then passes the divergent section subsonically which, according to quasi-one dimensional gas dynamics, decreases the flow velocity and increases the static pressure. Through proper design, such a diffuser would eject the flow at low subsonic velocity and a static pressure which was nearly ambient.

These arguments are somewhat misleading in that they consider a steady flow. On this basis, calculation shows for a chamber-to-muzzle radius ratio of 6.0 that a chamber Mach number of 5.50 results. At this Mach number and with atmospheric ejection, the muzzle stagnation pressure could be only about 350 psi to maintain the ideal state. For higher pressures, the normal shock would be pushed out of the diffuser resulting in supersonic exit. However, the effect of the unsteady nature has not been considered. The expansion of the gases into the nozzle chamber does not occur with steady properties at the muzzle. Rather, the pressure, temperature and density are continually dropping; thereby making it conceivable that while the nozzle-diffuser would be initially supersonic throughout, at later times an ideal flow situation could evolve. However, Watling makes no attempt to analyze the flow through these devices.

The detailed investigation of flash suppressor physics requires more information than is currently available. The basic principles of the devices are only vaguely known. A unified data base would be desirable in order to allow for an identification of significant

parameters effecting flash in various weapons. A technique to mathematically model the flow field within these devices would be extremely useful.

C. Blast Suppressors

Gun blast adversely effects the gunner, his concealment, surrounding personnel and structures. The blast forms when the excess propellant gas energy is released into the atmosphere. The propellant gas energy is transferred to the surrounding air by viscous shear, radiation and heat conduction, but the most rapid transfer of energy occurs as the propellant gas expands into the atmosphere doing work by displacing the surrounding air. This displacement at the muzzle propagates as a series of compression waves to all parts of the fluid. The compression waves coalesce rapidly into a blast wave. The intensity of the blast is greatest near the muzzle and is selective in the sense that the highest intensity occurs where the most air displacement is effected, i.e., to the front of the weapon due to the directed kinetic energy of the propellant gas. As the blast expands radially away from the muzzle, the propellant gas energy is deposited over an ever increasing surface area displacing greater volumes of air. This, coupled with the decreasing rate of energy deposition at the muzzle as the gun tube empties, causes the intensity of the blast to drop rapidly as it travels away from the weapon. At sufficiently large distances, the blast wave decays to a sound wave.

The control of weapon blast centers on the technique of releasing the excess propellant gas energy into the atmosphere. The history of device innovation may be traced through the list of patents⁷⁸ on designs to accomplish this energy control. Basically, the devices attempt to reduce blast through energy absorption, energy dissipation, and energy containment and controlled release, Figure 24. Energy absorbing devices use heat transfer from the hot propellant gases to cold metal fibers or device channel walls. This heat transfer lowers the gas temperature thereby decreasing the amount of energy available to perform work. Dissipative devices attempt to force the propellant gas to perform work on the muzzle device prior to release into the atmosphere. The work can be in the form of viscous shear on channel walls or through fibrous packing, or it may perform work on a movable device such as a rotor. Energy containment devices consist of chambers into which the propellant gas expands, decreasing the volumetric energy concentration and allowing release at reduced pressure, temperature and velocity. These categories are not at all exclusive and many devices utilize combinations of some or all of them.

There is great difficulty in translating basic principles such as these into field-worthy, effective hardware. The state of blast suppressor technology testifies to this fact. Existing theory is largely empirical in nature, being an off-shoot of research into large scale

explosions. Westine^{79,80} develops scaling laws for the blast field about guns based upon a technique presented by Hopkinson⁸¹. The Hopkinson scaling law was for the blast field about conventional explosions. Schlenker^{82,84} devised a technique to compute the blast field around artillery pieces with and without muzzle brakes. His analysis used the theoretical results of Brode^{85,86} which was produced for point and spherical source explosions.

Furrer⁸⁷ produced an interesting report which commences with an experimentally derived scaling law for conventional explosions and then attempts to obtain a similar law for weapon blast. Using quartz microphones, Furrer obtained traces of the blast pressure level at a given location as a function of time, Figure 25. The first plot represents a pressure-time trace for the blast of a spherical charge. Furrer observed that both p_0 and t_0 , the maximum side-on overpressure and positive phase duration, respectively, scale with the charge weight, Q . Additionally, he noted that p_0 drops as the inverse of the distance from the charge. He gives the following scaling law:

$$p_0 = 0.34 \frac{Q^{0.44}}{r}$$

$$t_0 = 2.85 Q^{0.12}$$

where:

$$p_0 - \text{Kg/cm}^2$$

$$t_0 - \text{milliseconds}$$

$$r - \text{meters}$$

$$Q - \text{Kg TNT}$$

Performing the same experiments with a gun, he noted the pressure-time traces were not as simple. Spikes appear on the trace not only due to the main blast arrival, but also due to flash blast and ground reflection. However, he noted that at large distances from the weapon, the blast waves coalesce and resemble the blast from a spherical charge. In firing 2 cm through 15 cm cannon, he noted the following scaling law to be applicable:

$$p_0 = 0.43 \frac{Q^{0.44}}{r}$$

$$t_0 = 1.80 Q^{0.24}$$

where measurements were taken along a line perpendicular to the gun bore and even with the muzzle. Furrer also measured the blast field around a gun with and without a muzzle brake noting the resultant distortion of the pressure contours, Figure 26.

Research conducted in the United States during World War II indicated that the scaling law for gun blast was not as simplistic as Furrer indicates. Westine^{79,80} reviews this research^{88,89} and extends it to develop more comprehensive scaling laws. Both Reynolds⁸⁸ and the Navy⁸⁹ noted from experimental data that the peak overpressures about guns would be equal at identical geometric locations if:

1. All distances were measured in calibers.
2. Projectile (muzzle) velocities were equal.

$$3. \frac{M_1}{M_2} = \frac{E_1}{E_2} = \left(\frac{c_1}{c_2}\right)^3 = \left(\frac{l_1}{l_2}\right)^3$$

where: M = projectile mass
 E = propellant energy
 c = gun caliber
 l = gun barrel length

4. Neglect heat conduction, viscosity and gravitational effects. The Navy noted that the scaling could be extended to the impulse, the area indicated by cross-hatching in Figure 25, if the impulse was divided by the gun caliber. Westine⁷⁹ points out that these scaling laws are similar to the Hopkinson⁸¹ spherical charge scaling law:

$$p_0 = f\left(\frac{r}{d}\right)$$

$$\frac{I_0}{d} = f\left(\frac{r}{d}\right)$$

where: r = radial distance from charge
 d = charge diameter
 I₀ = positive phase impulse.

The principal drawback of the Navy scaling laws is the lack of flexibility. The requirements of equal muzzle velocity and scaled projectile mass, propellant charge and barrel length mean that the blast field about a weapon could not be scaled from existing data unless these exact conditions happened to be available.

Westine notes that Barton, et al⁹⁰, introduce an extension to this scaling law which makes it considerably more flexible. Barton approximates the blast field about a gun by the blast field around a spherical charge of reduced energy, w, located a distance r₀ from the muzzle. The reduced energy is calculated from:

$$w = n (E - 1/2 Mv^2)$$

where: w = reduced energy
 n = empirical correlation factor
 E = propellant energy
 M = projectile mass
 v = muzzle velocity.

The distance r_0 is empirically determined as the approximate location of the center of a gun blast shock envelope. The overpressures were then said to be equal at equivalent geometric locations where the distances were scaled by the cube root of the reduced energy:

$$p_0 = f \left(\frac{x}{w^{1/3}}, \frac{y}{w^{1/3}} \right)$$

This scaling eliminated the restrictions of equal muzzle velocity and scaled projectile mass, propellant energy and barrel length.

Westine⁷⁹ notes that all of the aforementioned scaling laws do not consider the ratio of bore length to diameter as being significant. For this reason, Westine claims the techniques can not scale all types of weapons equally well, i.e., rifles would not scale with mortars or pistols. To alleviate this difficulty, Westine proposes an improved scaling law:

$$\frac{p_0 c^3}{w} = f \left(\frac{x}{c}, \frac{y}{c}, \frac{l}{c} \right)$$

$$\frac{I_0 c^2}{w} = f \left(\frac{x}{c}, \frac{y}{c}, \frac{l}{c} \right)$$

where: $w = E - 1/2 Mv^2$
 x = axial dimension
 y = transverse dimension

The functions are then obtained from experiment and presented as a universal plot of non-dimensional overpressure versus distance in calibers. Westine observed from the experimental results that the overpressure parameter could be approximated as:

$$\frac{p_0 c^2 l}{w} = f \left(\frac{x}{c}, \frac{y}{c} \right)$$

This is seen to be equivalent to multiplying the original parameter by l/c . The resulting relation is seen to be quite general and Westine claims it to be valid to an extremely large variety of guns. His plot of overpressure is shown in Figure 27. As an indication of the range of

applicability possessed by the "universal" pressure field, Westine cross plots his data. Figure 28 presents the results obtained by plotting the overpressure parameter against y/c for $x/c = 0$. Also presented is data from experiments on a wide variety of weapons. The correlation is very good, and the range of weapons considered is obviously extensive. Westine indicates that some of the scatter could be due to the difficulty in calculating the available energy, w . The tests examined were not conducted to specifically examine the Westine scaling law, and, therefore, did not contain all of the data required for the computation, e.g., muzzle velocity and propellant specific energy.

Westine also presents a universal curve for the side-on, positive phase impulse which was experimentally determined to scale according to:

$$\frac{I_0 c^{1.25} z^{.75}}{w} = f \left(\frac{x}{c}, \frac{y}{c} \right)$$

Westine notes that this is not a non-dimensional parameter, but should also contain the speed of sound in air. However, he assumes this to be a constant and does not choose to include it giving the above parameter the dimensions of inverse velocity. His results are shown in Figure 29. Again the data is seen to correlate well when cross plotted and compared with the results of a variety of weapons tests.

The third important blast parameter Westine considers is the time of arrival of the blast front. Westine writes the scaling law for time of arrival as:

$$\frac{T_0}{c} = f \left(\frac{x}{c}, \frac{y}{c}, \frac{z}{c}, \frac{w}{c}^{1/3} \right)$$

Westine assumes this function can be approximated by representing the muzzle blast front as being equivalent to the blast front propagating from a point charge located at some distance, L/c , along the boreline away from the gun muzzle. Thus the blast is assumed spherical and the propagation distance, r , is measured from the center of explosion, $y/c = 0$, $x/c = L/c$. The location of the point charge is empirically determined to be a function of $c/w^{1/3}$. The geometry, point charge location and time-distance results of Westine are shown in Figure 30. The scaling for time of blast arrival is more complex than overpressure and impulse scaling. However, this is in part due to the lack of time of arrival data. Westine's results indicate that once the center of the blast is located as a function of $c/w^{1/3}$ then:

$$\frac{T_0}{c} = f \left(\frac{r}{c} \right) = f \left(\frac{x}{c}, \frac{y}{c}, \frac{z}{c} \right)$$

In this sense the scaling is similar to that previously obtained for p_0 and I_0 . It is interesting to note that the blast data possess a slope

almost equal to the sonic slope. This indicates that after an initial period of propagation at speeds in excess of the local speed of sound in air, the blast strength drops quickly and the wave speed, dr/dt_0 , rapidly approaches sonic velocities.

The scaling laws discussed thus far have been for bare muzzles. The addition of a muzzle device increases the complexity of the problem considerably. Schlenker²⁷⁻³⁴ performs an analysis to approximate the blast field around guns equipped with muzzle brakes. His approach is similar to that of Barton, et al³⁰. A reduced gas energy at the time of shot ejection is computed. This energy is allocated to two point sources located on either side of the muzzle brake. The resultant pressure field is then computed utilizing the point source analysis of Brode³⁵. Levin³¹ performs an analysis similar to that of Schlenker with the exception that Levin allocates the reduced energy not only through the brake ports but also through the projectile orifice. Levin utilizes data obtained from recoilless rifle firings as his basic source of blast information. This data enabled him to include the effects of port flow directionality. Additionally, Levin's analysis allows for the consideration of projectile residency within the brake.

The analysis of the effects of blast suppressor design upon the muzzle blast has not been extensive. No significant attempts at modeling energy absorption or dissipation devices were uncovered. However, attempts have been made in the investigation of devices utilizing energy containment and controlled release. Bixler, et al³², studied multi-baffle devices both theoretically and experimentally. Three theoretical approaches are offered: acoustic theory, blast theory and quasi-one-dimensional flow theory. The acoustic theory, which forms the basis for the design of conventional (e.g., automobile) mufflers, assumes linear or sonic wave motion. This is obviously inapplicable to the strong, non-linear muzzle blast, and Bixler indicates that the resultant application is not valid. The blast theory put forth in this report considers a situation similar to Figure 31.

The blast front expands spherically at a velocity relative to its geometric center equal to v_s . At the same time, the geometric center translates at a constant velocity v_c . This blast expands into a multi-baffle blast suppressor with a geometry as shown. Bixler then applies the quasi-one-dimensional shock propagation theory of Whitham³³ to the multi-chambered channel of the blast suppressor. The application of the Whitham theory to this configuration is somewhat tenuous. In it, area variations are small in order to permit the utilization of one-dimensional characteristic theory. For the geometry considered by Bixler, the area changes occur suddenly, completely destroying the one-dimensionality of the flow. However, Bixler makes use of Whitham's relation for a strong shock expanding into a varying area channel:

$$\frac{p}{p_i} = \left[\frac{A_i}{A} \right]^{2k}$$

where: p = static pressure
 A = area
 K_{∞} = function of shock Mach number
 $= 0.394$ for $M_{\infty} \rightarrow \infty$ and $\gamma = 1.4$

Bixler assumes the blast to propagate as shown in the sequence in Figure 31. The projectile effect is neglected allowing the blast to propagate in accordance with the geometry specified earlier. In a certain time interval, Δt , the blast front reaches the first baffle surface, sequence schematic 3. Since the blast front propagates at a velocity equal to $v_c + v_s$, and since the distance from the muzzle to the first baffle is s , the time interval is calculated to be:

$$\Delta t = \frac{s}{v_c + v_s}$$

To use Whitham's pressure formula, Bixler must calculate an equivalent channel area. This he approximates as being equal to the surface area of a spherical blast front of radius $v_s \Delta t$, less the bore area:

$$A = 4\pi (v_s \Delta t)^2 - \frac{\pi \delta^2}{4}$$

Then utilizing Whitham's strong shock equation, Bixler obtains

$$\frac{p_1}{p_m} = \left[\frac{\pi \delta^2 / 4}{4\pi (v_s \Delta t)^2 - \frac{\pi \delta^2}{4}} \right]^{0.394}$$

where: p_m = muzzle pressure
 p_1 = pressure at the exit of the first chamber.

Substitution of the above relation for Δt allows the equation to be rewritten:

$$\frac{p_1}{p_m} = \left[16 \left(\frac{s}{\delta} \right)^2 \left(\frac{v_s}{v_c + v_s} \right)^2 - 1 \right]^{-0.394}$$

In order to obtain a relation for the pressure drop in expanding into subsequent chambers, Bixler assumes the process occurs identically in all chambers. Thus assuming identical geometry and constant shock propagation velocities, he obtains:

$$\begin{aligned} \frac{p_n}{p_m} &= \frac{p_1}{p_m} \times \frac{p_2}{p_1} \times \dots \times \frac{p_n}{p_{n-1}} \\ &= \left[16 \left(\frac{s}{\delta} \right)^2 \left(\frac{v_s}{v_c + v_s} \right)^2 - 1 \right]^{-0.394 n} \end{aligned}$$

The assumptions used to obtain this expression are not justifiable. His method of sequential expansion of the blast implies that the blast boundaries remain frozen in a chamber once the front of the blast moves into the next chamber. This is not a physical reality. The blast continues to expand, reflecting from chamber boundaries and raising the chamber pressure drastically. Thus the pressure within the chamber is not constant nor is it as low as would be predicted by Bixler's method. This fact is noted by Bixler in his comparison of the theory with experiment. He finds that the predicted attenuation is considerably higher than was experimentally observed.

Bixler's third theory, the shock tube theory, attempts to relate the blast propagation to a diaphragm rupturing at the muzzle causing the shock to propagate at a Mach number, M_{10} , into the first chamber. He notes that the gas is not at rest when the diaphragm bursts (bullet uncorks), but is travelling at the projectile velocity, v_p . He then obtains a shock Mach number at the muzzle by adding the two:

$$M_0 = M_{10} + M_p.$$

This type of addition is deceptive. The fact that the gas has a finite velocity when it breaks the muzzle necessitates that the kinetic energy be accounted for in the calculation of M_{10} , i.e., the effect is not linear. Bixler then applies Whitham's theory to the expansion into the chamber, calculating the resultant shock Mach number:

$$\frac{M_1}{M_0} = \left(\frac{A_m}{A_1} \right)^{K_{\infty}/2}$$

where: M_1 = Mach number at exit to first chamber

A_1 = cross-sectional area of first chamber

A_m = muzzle bore area.

The pressure is then apparently calculated from known conditions at the muzzle and the computed Mach number. This procedure is then continued through subsequent baffles. Again, the assumption of quasi-one-dimensional flow, no reflections of blast and a linear diaphragm velocity addition are not justifiable. The resulting comparisons with experiments reflects the lack of physical reality in this theory.

An additional problem with this analysis is its inability to account for projectile presence in the device. Skochko and Greveris^{7B} conducted extensive tests on a wide variety of suppressor designs. Their results show that projectile presence effects blast in the sense that it presents a significant blockage to propellant gas expansion. This blockage is not complete and part of the high pressure gases leak around the projectile forming a distinct "blow-by" blast measured prior

to the main propellant gas blast. The measured blast structure as constructed from these experiments is shown in Figure 32. The four distinct blast pulses were measured near the muzzle. Further away there is a tendency for them to coalesce into a single disturbance.

Another effect of the bullet presence would be the facilitation of the development of a quasi-steady flow structure within the device. With the bullet standing in the exit from a chamber, the gases would be forced to expand completely into the chamber prior to emergence through the hole. If the gas flow attains supersonic velocity, shock formation would cause a loss in stagnation pressure which, coupled with the volumetric expansion, would attenuate the resultant propellant gas blast strength. Such discussion is largely conjecture as no theoretical model is currently available to handle such a complex gas dynamic problem. The current basis of suppressor design remains to be empirical laws.

IV. EXPERIMENTAL TECHNIQUES

The complex nature of the shot ejection phenomena is reflected not only in the difficulties entailed in obtaining a theoretical model, but also in conducting valid experimental investigations. The fact that ejection phenomena such as turbulent mixing, chemically reacting flows, detonation physics, free jet flows, and blast phenomena are the unresolved subjects of extensive research efforts in fields quite remote from ballistics indicates that the muzzle gas flow field is not in imminent danger of being completely defined. However, judiciously conducted experiments can and have shed light on isolated phenomena which are important to the design of muzzle devices.

An important tool in many experimental studies is the muzzle flow simulator. These simulators may be divided into two main categories, steady and unsteady flow devices. The steady flow devices examine the quasi-steady free jet structure and the interaction of this structure with muzzle devices. The gas tested is generally one of known thermodynamic properties, e.g., air, although trace impurities may be deliberately introduced to examine mixing phenomena. The elimination of time dependence and chemical reaction greatly simplifies the investigation of the flow field. However, care must be taken to insure that the effects of free jet parameters such as pressure ratio, ratio of specific heats, exit Mach number and flow inclination are understood and taken into account. The unsteady flow devices include time dependence but simplify examination of the ejection phenomena through elimination of chemical kinetics, reduction in physical scale or number of dimensions, or control of interior ballistics. Such devices as air guns, light gas guns, and scaled down hardware simulators fall into this category.

The techniques utilized to survey the muzzle gas flow and associated phenomena are not unique to this field being taken directly from the current technology base. The remainder of this Section will be devoted to consideration of research efforts conducted on the various type muzzle devices.

A. Muzzle Brakes, Compensators, and Blast Suppressors

To study the muzzle gas flow through a brake, Oswatitsch⁷ constructed a simulator capable of taking gross force measurements and Schlieren photographs, Figure 33. The device was two-dimensional so that the internal flow could be observed. A problem with this type of two-dimensional device is the influence of wall boundary layer growth. Ladenburg³⁸ noted this problem in his free jet studies. Additionally, Oswatitsch assumed that the forces exerted on the brake could be approximated by a steady flow device. Due to limitations on pumping capacity, the maximum pressure ratio that could be obtained was $p_e/p_\infty = 10.0$. This is two orders of magnitude lower than the actual pressure ratio; however, Oswatitsch presents a comparison between his previously discussed theory with computations based on this pressure ratio and the resulting force measurements obtained with this apparatus, Figure 34. Oswatitsch notes that for small a , i.e., near the muzzle, the measured efficiency factor is greater than the corresponding theoretical calculation. This is due to the brake deflecting the flow through a greater angle than that of the brake surface. At larger values of a , the measured brake efficiency is lower than theory. This effect is attributed to losses around the brake. To examine these effects in detail, Oswatitsch designed an extended brake, Figure 35. The effect at values of a greater than one is as expected. The increased baffle surface results in increased flow deflection and increased efficiency. However, at lower values of a , the brake efficiency is lower than the previous experimental values. This effect is not adequately explained, but it may be due to an over-expansion along the baffle surface.

The results of Oswatitsch's research is a brake design similar to that shown in Figure 34, with a radius increased to 2.4 calibers. This device was fabricated and tested on an actual weapon achieving an efficiency compatible with the steady state theory and experiment, Figure 16.

A practical design feature considered by Oswatitsch was the details of the muzzle brake cover. A cover is necessary in order to connect the brake to the weapon and to selectively direct the exhausting gases preventing dust obscuration or blast damage. Oswatitsch utilized an axisymmetric free jet impinging upon a flat plate baffle, Figure 36. By varying the cover design and separation from the axis, Oswatitsch could measure the variation in brake efficiency from the no cover efficiency, Figure 37. The effect of the covering on the brake efficiency is complicated; however, two main effects are noted. First, the covering decreases the brake impingement area which tends to decrease

efficiency. Second, the cover can direct more flow onto the available brake surface causing greater average rearward deflection. This latter effect is positive in nature, but it must be noted that increased flow also passes the projectile hole under this circumstance. Oswatitsch's result shows cover type IV to be the most effective, and it is this design which is recommended.

Simultaneous to the work of Oswatitsch, researchers^{6,49,50} in the United States were investigating the design of blast deflectors. Although the design of the two types of devices are quite often identical, a detailed study of braking action was not attempted. Rather, various device designs were fired over dust tables and the resulting obscuration estimated. Slade⁶ utilized a caliber 0.30 rifle to simulate the dust obscuration effects of larger caliber weapons. Successful deflectors were constructed full size and tested. Slade noted that such scaling did not always work well. The obscuration caused by dust clouds is a subjective measurement increasing non-linearly with the gun caliber. Thus deflectors which worked well on small caliber weapons were not effective on larger caliber weapons. Slade did note that the effectiveness of a device to deflect blast and thereby reduce obscuration was intimately related to the effectiveness of the device as a muzzle brake. Pursuing this concept, a caliber 0.30 rifle was mounted in a ballistic pendulum and the resultant recoil energy measured. A flat plate baffle was placed on the weapon, the plate diameter and distance from the muzzle was then systematically varied, Figure 38. His measurements show similar behavior to those of Smith^{53,54}, shown in Figure 18. Initially, the curves overlap since each baffle deflects the gases identically and the projectile hole losses are equal. However, at greater distances the inability of the smaller diameter baffles to deflect the gases is shown.

To observe the internal shock structure of the blast deflectors, Slade made use of the free-surface liquid analogy. This analogy is based on the fact that there are similarities between the flow of a compressible fluid and the motion of the surface of a liquid. Cranz⁴ references the analogy in noting the similarities between the wave pattern around a moving ship and the spark shadowgraphs of a supersonic projectile. Slade constructed a water table to allow the observation of the flow patterns associated with the blast deflector, Figure 39. The analogy was quite complete, including the bore/chamber profile, baffle profile, and even a projectile. From water table studies and the braking criterion, Slade arrived at an optimal turning vane shape, Figure 40. The design is similar to the optimum brake design of Oswatitsch, Figure 34, with the addition of a guide nozzle. Slade also noted that the only method to completely eliminate obscuration was to duct the gases rearward and eject them vertically at the trunnions.

Pursuing the same goal as Slade, Millikan⁴⁹ and Robinson⁵⁰ also made use of a muzzle flow simulator. However, the device was an air-powered gun. Later in their programs, a steam-powered gun was

utilized to obtain higher pressure ratios. The air gun consisted of a caliber 0.50 bore separated from the chamber by a diaphragm. The chamber was hydraulically pumped to a maximum pressure of 3000 psi at which time the diaphragm ruptured, and the projectile was accelerated down the bore. Using wooden projectiles, muzzle velocities up to 1200 feet per second were obtained. The main advantage of this device was the elimination of contaminants in the gas thereby allowing Schlieren or shadowgraph techniques to be applied with a resultant optical penetration of the muzzle jet. Robinson⁵⁰ utilized the device over a dust table photographing the resultant dust cloud growth with time. His conclusion was that baffles could be designed which effectively eliminated forward muzzle jet flow; however, obscuration still evolved from venting the gases to the side. Millikan⁴⁹ conducted a two-dimensional Schlieren survey of the flow interior to a blast deflector. He used these results coupled with caliber 0.30 firings to propose certain radical anti-obscuration concepts. These ideas were later tested by Munch, et al⁵¹ and found to be generally impractical.

More recently, Smith⁵³⁻⁵⁶ has performed extensive research on muzzle phenomena and, specifically, on muzzle brakes. Like Oswatitsch, Smith assumes that a good approximation of the thrust on a muzzle brake can be obtained with a steady flow simulator. However, where Oswatitsch utilized a two-dimensional simulator with a maximum pressure ratio of 10, Smith constructed an axially symmetric apparatus with a maximum pressure ratio of 264. Both tested mainly in air; although Smith did attempt testing in nitrogen, he noted no significant effect of the ratio of specific heats. Smith's apparatus is shown schematically in Figure 41. The technique of measuring thrust differs from that of Oswatitsch in that rather than measuring the thrust on the brake, Smith measures the overall thrust on the weapon.

Using this apparatus, Smith conducted extensive tests on a variety of muzzle brake designs, including discs, cusps, reverse cones, cowled brakes, open and closed brakes. He also varied brake dimensions, distance from the muzzle, numbers of brakes and spacing of the brakes. His results for a single brake are presented as plots of his previously defined aerodynamic index versus axial location, Figure 18, and versus pressure ratio, Figure 42. The first plot has been discussed. The second plot is interesting as it shows the effect of jet growth on the brake thrust. At low pressure ratios, the jet has a small diameter, Figure 8, and most of the mass passes through the muzzle brake projectile hole. As the pressure ratio increases, the jet grows resulting in greater flow impingement upon the brake surface and increasing aerodynamic index. However, a maximum is reached as increasing pressure ratio results in spillage around the outer edge of the baffle. With further increase of the pressure ratio this spillage or incomplete deflection effect predominates and the aerodynamic index drops. Additionally, Smith⁵⁴ took pressure measurements on the front and rear surfaces of brakes mounted in this simulator. The resulting measurements compared favorably with his steady flow theory, Figure 19.

Smith's investigation of multi-baffle brakes produced interesting results, Figure 43. This plot illustrates what economists call the law of diminishing returns. Due to the deflection of mass by previous baffles, the additional gain in aerodynamic index by each subsequent baffle diminishes; e.g., in this case $\Delta n_1 = 0.48$, $\Delta n_2 = 0.28$, $\Delta n_3 = 0.10$. A second effect is the decrease in the effect jet pressure ratio at each baffle due to shock losses. This requires increased spacing to achieve maximum efficiency, e.g., in this case $\Delta \bar{x}_1 = 1.10$, $\Delta \bar{x}_2 = 1.30$, $\Delta \bar{x}_3 = 2.10$. These effects were also noted by Oswatitsch; however, Smith's results illustrate them quite clearly.

To check the effect of pressure ratio and the steady flow assumption on the validity of his results, Smith mounted identical muzzle brakes on a 7.62mm rifle. The resulting aerodynamic indices obtained from firings with the rifle mounted in a ballistic pendulum compared favorably with his steady state measurements (generally within 10%). Smith notes that to examine dimensional scaling, large caliber firings would be required.

Recognizing that changes in blast effects due to the utilization of a muzzle brake were important, Smith⁵³ applied a multi-flash shadowgraph technique to obtain estimates of peak overpressure levels. The pressure jump across a shock can be obtained from the Rankine-Hugoniot relations if one is given the shock propagation velocity into a medium of known thermodynamic state. Firing a 7.62mm rifle, Smith took multiple shadowgraphs of the shot ejection phenomena on a single photographic plate. Since the distance travelled by the shock and projectile between flashes can be measured directly and assuming the projectile velocity to be constant (2680 ± 20 FPS), the projectile travel divided by the projectile velocity will give the time between flashes, thus allowing the shock velocity to be calculated. The conditions of the ambient into which the shot is fired are known; therefore, the overpressure contours may be computed, Figure 44. The effect of the brake is seen clearly; the overpressure levels on the lower portion of the figure, i.e., with the brake, are higher further to the rear than are those without the brake. Likewise, in the forward direction, overpressure at a fixed location is decreased with the application of a muzzle brake. This overpressure data suggests an interesting possibility, namely, the combination of the scaling laws of Westine^{79,80} with data such as this to provide a "universal" blast field plot for various muzzle brakes. The inclusion of the brake efficiency into such scaling laws is a further attractive possibility which could yield a single scaled overpressure field of wide applicability.

B. Flash Suppressors

Experimental work with flash and flash suppressors has generally been qualitative in nature, addressing flash largely as a yes-no phenomena. The basic experimental tools are photography and human

observation⁷⁰⁻⁷⁶. With the basic physical principles of the flash phenomena in hand, a muzzle device is designed which will supposedly effect some portion of the flash cycle. The technique to test the device is, first, place it in a dark room and photograph the weapon firing. If no flash shows up, place an observer in the room and fire again. If the observer sees no flash or "reduced" flash then the design is considered verified.

However, research conducted at Franklin Institute⁵⁹⁻⁶⁶ was directed at obtaining quantitative information relating to the nature of gun muzzle flash. Their research is summarized in the Army Handbook on flash⁶⁶ and in the Midwest Research Institute state-of-the-art surveys⁶⁷⁻⁶⁸. The approach taken by these investigators was two-fold, consisting of the utilization of steady flow simulators and actual weapons firings.

The steady flow simulator⁶³ discharges air at a stagnation pressure of 500 psi through a 0.025 inch nozzle into a chamber evacuated to 1.0 psi. This gives a static pressure ratio, p_e/p_∞ , of 264. The simulator was utilized to study both jet mixing and jet structure. Mixing was studied through the use of tracer gases in the evacuated chamber. Both NH_3 and CO_2 were tried, but CO_2 was used more extensively due to its less offensive nature. The CO_2 was introduced into the chamber until a 5% concentration was established in the chamber air. Air from the nozzle is dried in a KOH tower and possesses negligible CO_2 , thus any CO_2 detected in the resulting free jet can be ascribed to entrainment from the chamber atmosphere. The resulting concentration of CO_2 is then indicative of the percent of air which would be entrained by a propellant gas jet.

The CO_2 concentration is determined by drawing gas from selected locations in the jet with a hypodermic needle. The gas is passed through a liquid nitrogen trap in which the CO_2 is frozen. The remaining air is drawn off and the rate of air flow measured. Knowing the sampling time, the mass of air taken can then be computed. The mass of CO_2 can be determined by allowing it to expand into a known volume at a known temperature. The resulting pressure is measured and utilized in the equation of state to calculate the CO_2 density. Since the volume is known, the CO_2 mass is also calculated. With both the mass of air and CO_2 sampled, the CO_2 concentration is calculated. A schematic depicting the results of this study is presented in Figure 45. The inclusion of the gas-air mixture within the shock bottle is somewhat surprising and may be due to probe interference effects.

A similar flow simulator was constructed by the Midwest Institute⁶⁴. However, this device utilized a 0.30 inch nozzle and was unsteady in nature utilizing a burst diaphragm to initiate flow. The flow field produced by this device was surveyed utilizing conical tipped probes to determine local Mach number. This technique, used earlier by Cranz and Glatzel⁷, consists of placing a conical probe in a supersonic flow, taking a Schlieren or shadowgraph picture of the probe in the

flow, and measuring the resultant shock angle produced on the tip. From supersonic flow theory, this angle can be related to the local Mach number for a given tip angle. The resulting Mach number distribution is shown in Figure 46. The results are seen to be highly erratic and comparison with theory is almost non-existent. The reasons for this are first the effect of probe interference is very strong in the vicinity of the Mach disc and possibly throughout the flow field, which was geometrically small. Secondly, the jet was unheated and the resultant expansion undoubtedly caused liquefaction of nitrogen in the test air. These results are presented to indicate the difficulties connected with surveying this flow field and to point out the care that must be given to analysis of experimental results.

In addition to attempting a survey of the local flow properties and mixing of the muzzle gas with air, Franklin Institute⁶⁶ conducted spectroscopic surveys of the muzzle flash. While the data did not yield information on radiation from discrete portions of the flow field, it did provide valuable output concerning the gross emission properties of the various flash phenomena. The radiant energy was concentrated mainly in the infrared region of the spectrum with less than one percent of the energy being in the visible range. Additionally, impurities in the propellant gases such as potassium, sodium and compounds of calcium and copper were primary emitters of distinct spectral bands. Since the visible spectrum is of concern in flash suppressor design, certain results obtained by this research will be considered.

Tests were conducted utilizing a caliber 0.50 barrel connected to a 20mm chamber. To survey intermediate flash, an 85 inch barrel was used in order to provide internal energy absorption sufficient to eliminate secondary flash. The spectral analysis of this flash phenomena indicated that continuum emission was the predominant source of radiation, this shows that the major source of intermediate flash is incandescent solids. The barrel length was then successively decreased and firings conducted at each new length to examine the effect of barrel length upon flash. As expected, secondary flash began occurring more frequently as the barrel was shortened. It should be noted that the occurrence of secondary flash was intermittent until a barrel length of 61 inches was reached at which length all rounds flashed.

The barrel was apparently shortened to 45 inches and a spectral analysis of secondary flash undertaken. The results showed a majority of the radiant energy was emitted in selected bands which are indicated below:

Band	% Visible Energy
CuO, CuOH	50
CaOH	25
Na	7
Continuum	18

The utilization of steel bullets rather than the copper jacketed bullets used in constructing the above table produced an altered distribution curve. The curve reflected the elimination of copper impurities and a drop of radiation in those bands (CuO, CuOH).

A survey of the sequence of flash phenomena was undertaken. Utilizing a piezoelectric transducer mounted in the chamber of the gun, the breech pressure as a function of time was recorded on an oscilloscope. Superimposed on this trace were the flash intensity measured by a photocell and the shot ejection recorded by a microphone close to the muzzle. Two cases were observed: with and without secondary flash, Figure 47. These traces are purely qualitative in nature, but they do indicate the relative intensity and duration of the flash phenomena. The secondary flash is seen to occur relatively late in the tube emptying cycle possessing a great amount of intensity which continues for a long period of time. Measurement of the temperatures of the two flash phenomena using the line reversal method shows that intermediate flash possesses a potassium line temperature of 1250⁰K while the corresponding secondary flash temperature is 2200⁰K. These observations serve to illustrate what is already well known; namely, secondary flash is the most severe flash problem.

No research was uncovered which attempted to apply intensive flow field measurement techniques to the muzzle effluence from weapons equipped with flash suppressors. As stated earlier, flash suppressor effectiveness is largely measured as a yes-no parameter. The investigation of flow through these devices and the effect of design changes on the flow and flash phenomena is definitely a prime requirement for advancing the state of understanding of flash suppression by physical means.

C. Blast Suppressors

The understanding of the weapon blast phenomena requires a comprehensive catalog of information ranging from the detailed interior ballistics of the weapon through blast formation due to gas ejection. Flow through the blast suppressor must be examined, and the resulting modification of gas efflux related to changes in the blast field. This latter requirement is not available in the present technology base. Interior ballistics of small arms are reasonably well in hand, and the measurement of blast fields can be readily accomplished with currently available techniques^{78,87,94-98}. However, there have been few significant efforts uncovered which attempt to examine the gas dynamics of blast suppressors.

This lack of a good data base relating suppressor design to blast prompted Skochko and Greveris⁷⁸ to test a group of silencers. Utilizing condenser microphones, the noise levels five meters to the side of these silenced weapons were measured. Fifteen different silencers were tested; however, the weapons upon which the devices were mounted varied from

test to test. This makes it difficult to obtain definite conclusions as to silencer effectiveness. Additionally, the weapons were firing reduced charge rounds leading to subsonic exit velocities. This condition is not applicable to the typical field blast suppressor. Their work does provide insight into the sources of gas dynamically generated sound, Figure 32, and its inclusion of a multitude of device designs and patents forms a useful compendium.

Bixler, et al⁹² conducted a coordinated experimental investigation attempting to relate internal design changes to sensed changes in the blast field. Utilizing a 7.62mm rifle and a caliber 0.45 pistol, a set of test devices was constructed which allowed systematic variation of geometric parameters. The tests concentrated on multi-baffle devices and of necessity required certain restrictions on the number of parameters considered. To test the effect of varying the number and spacing of the baffles upon the weapon muffling characteristics, Bixler constructed a fixed length test device which allowed baffler rearrangement, Figure 48. Sound levels were measured with a condenser microphone, and the results are shown in Figure 49. The full variations examined by Bixler are not included in this figure in order to simplify its interpretation. The blast attenuation is seen to increase rapidly with the number of baffles. A maximum attenuation is attained and remains constant for a considerable increase in baffles until a gradual decline is experienced as the baffles begin to fill the expansion chamber thereby acting more as a channel rather than flow impediments. Bixler notes that the weight of the device increases with the number of baffles added. From an initial weight of one pound without any baffles, a weight of two pounds is incurred if fifteen baffles are utilized.

Bixler also considered a device which allowed the overall length to vary. As expected, the attenuation increased with increasing length. The diameter of the expansion chamber is also an important parameter. Therefore Bixler tested a chamber which was 12" long by 20" in diameter. The resulting attenuation is shown as the closed data point in Figure 49. The attenuation is quite high. Such a device is obviously impractical; however, this data point can be considered an indicator of the maximum attenuation level which could be achieved for this particular weapon with a well-designed device.

Bixler also presents spark shadowgraphs showing the internal flow through a multi-baffle device. The photographs clearly illustrate the multiple shock reflections from the baffle surfaces and the effect of "blow-by" in the formation of the multi-blast sequence of Skochko and Greveris. Bixler's experimental work is a good example of the type of work which is required in the examination of blast suppression. Control of the test weapon or simulator must be exercised. The blast suppressor designs should then be parametrically controlled in order to establish a set of scaling laws which have general applicability.

V. CONCLUSIONS

Various approaches to the theoretical and experimental analysis of muzzle devices have been presented. However, the complexity of the unsteady, chemically reacting, muzzle gas flow coupled with the numerous types of muzzle device for each functional group have prevented the construction of definitive design criteria. Existing data and techniques suffer from a lack of compilation into a unified, coherent data base. In general, the technology applied to these devices is not apace with the current state-of-the-art.

A majority of the research into muzzle devices is directed to the design of muzzle brakes. The work of Ostwatisch^{7a-7c} and Smith⁵³⁻⁵⁶ represent the most advanced approaches to the problem. Although both are quasi-steady analyses, correlation with experimentally obtained data is excellent. It is noted that these techniques have not been incorporated in current Army design literature⁴⁶. The research into the design of flash and blast suppressors has been largely empirical in nature, producing information applicable to a particular design of muzzle device and class of weapon. In all cases, the most pressing requirement is for a compilation of available data. This data base would permit the development of programs to fill obvious gaps in the design techniques. Another obvious requirement is the accurate definition of the muzzle gas and its flow field. A combined experimental and theoretical approach to provide this essential information utilizing currently available technology is being implemented by the BRL under a SASA-supported muzzle device program.

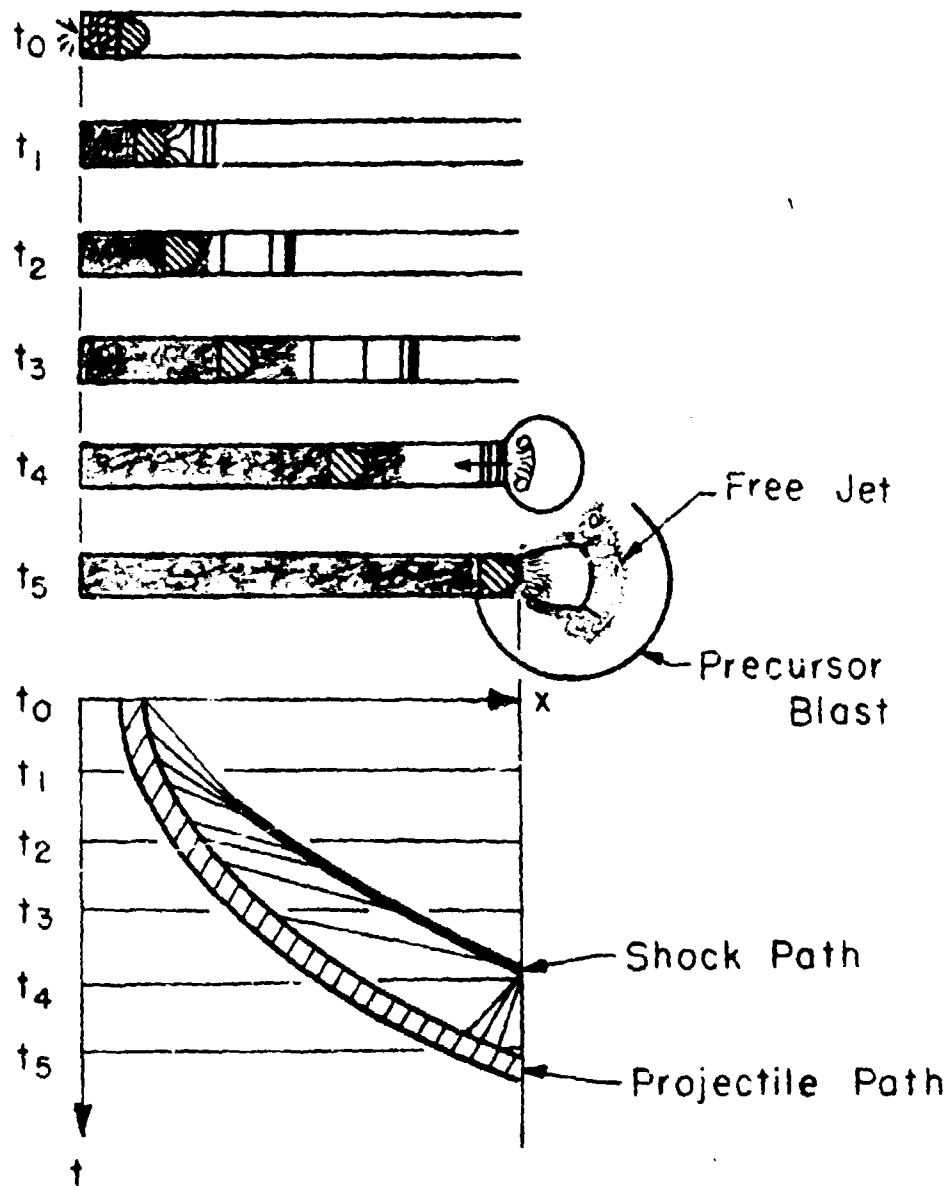


FIGURE 1 FORMATION OF PRECURSOR BLAST AND FREE JET

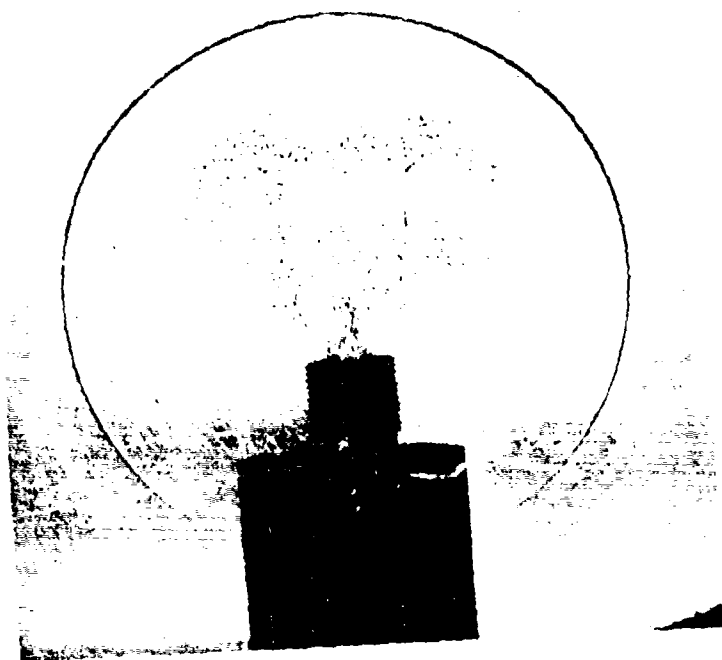


Figure 2. Precursor Flow Field

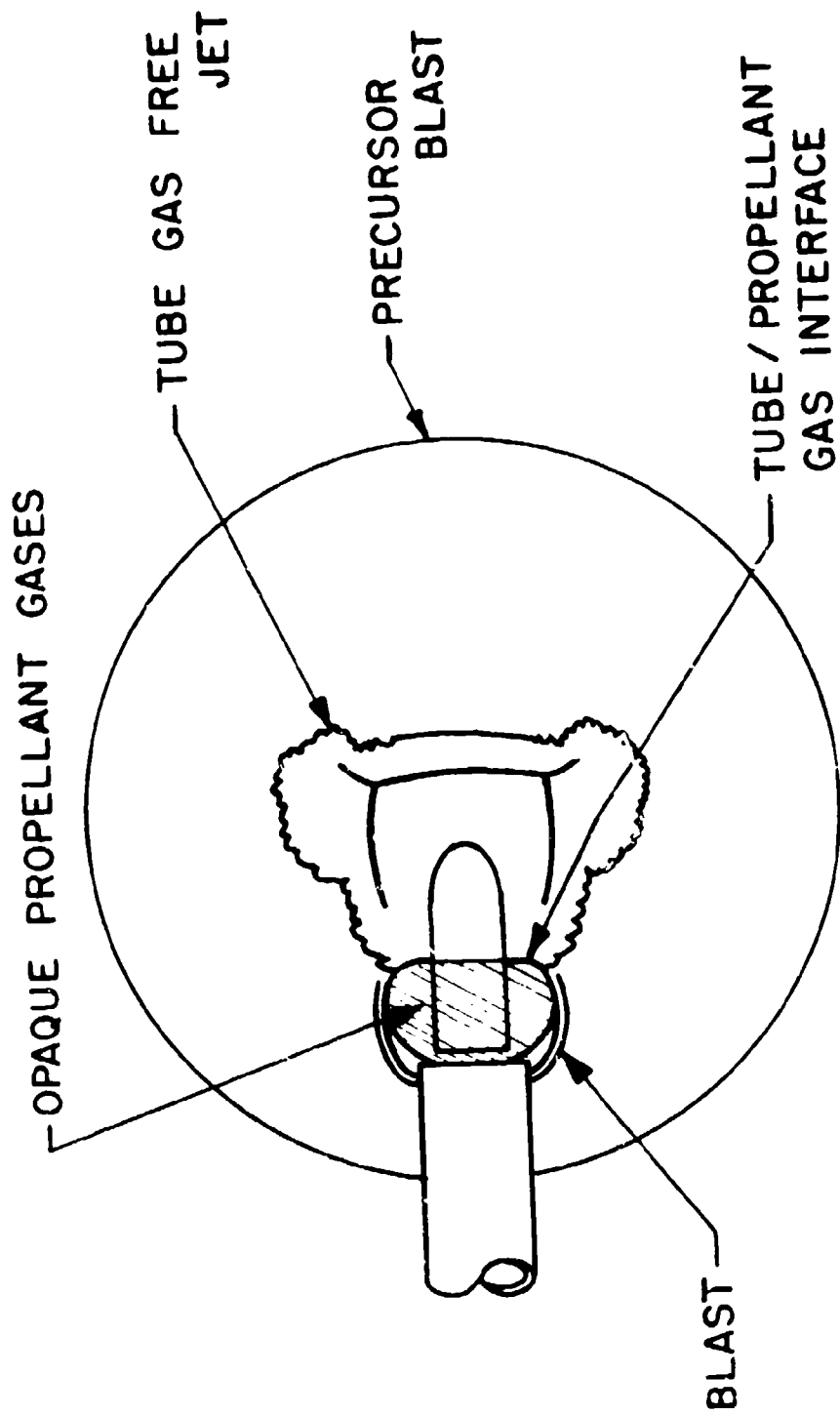


FIGURE 30 SCHEMATIC OF PROPELLANT GAS EJECTION FLOW

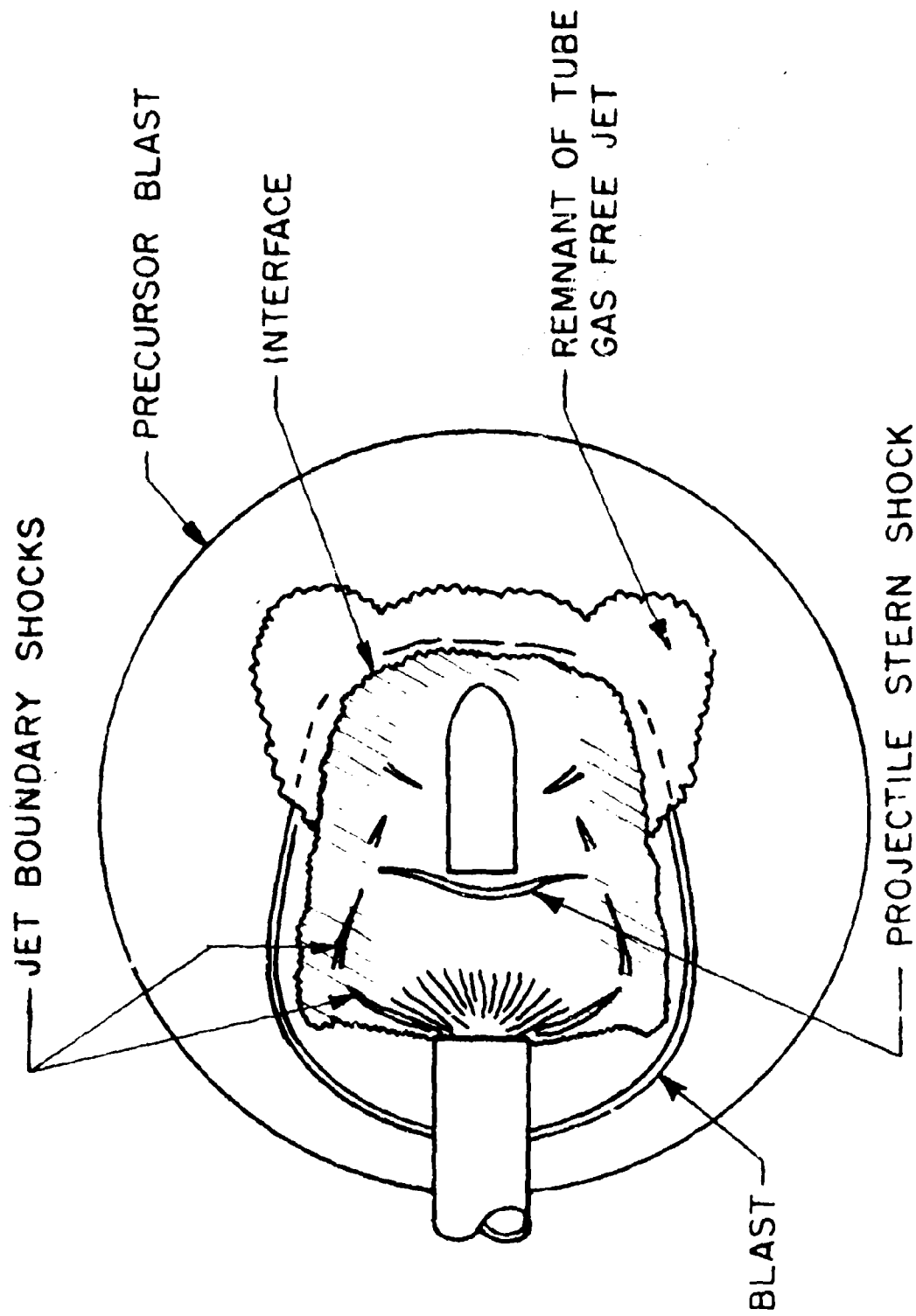


FIGURE 3b SCHEMATIC OF PROPELLANT GAS EJECTION FLOW

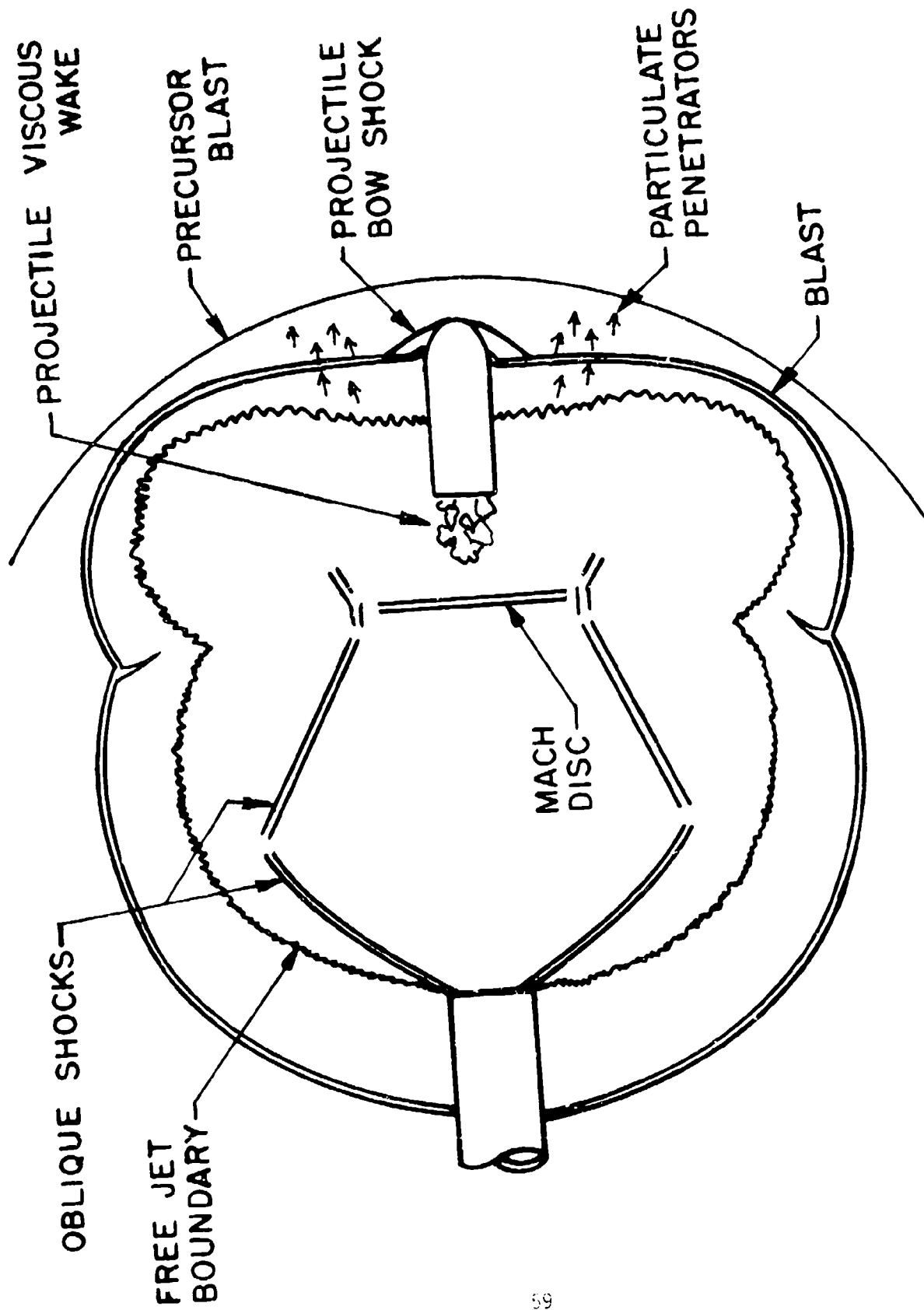


FIGURE 3c SCHEMATIC OF PROPELLANT GAS EJECTION FLOW

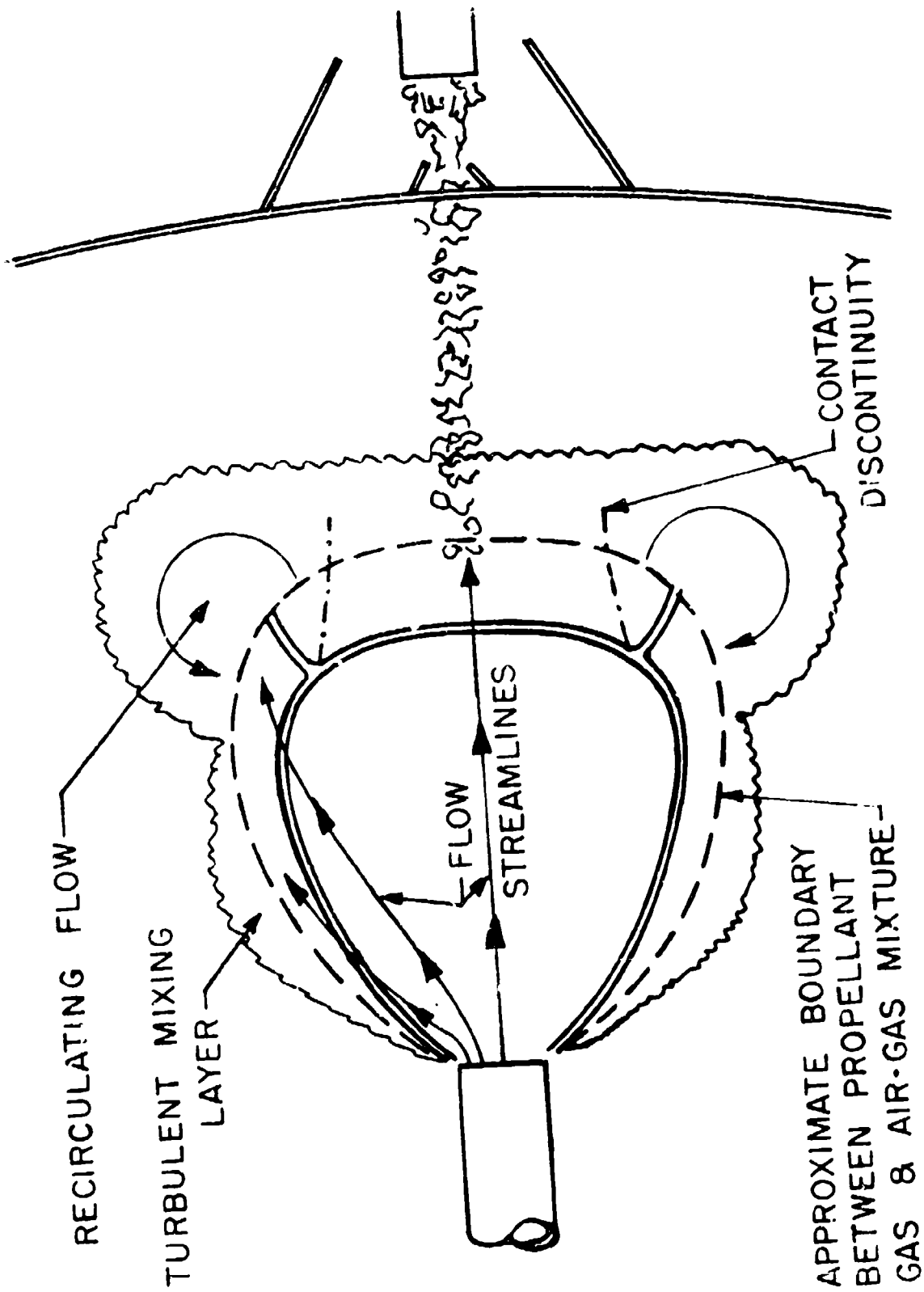


FIGURE 3d SCHEMATIC OF PROPELLANT GAS EJECTION FLOW



Figure 4a. Propellant Gas Flow

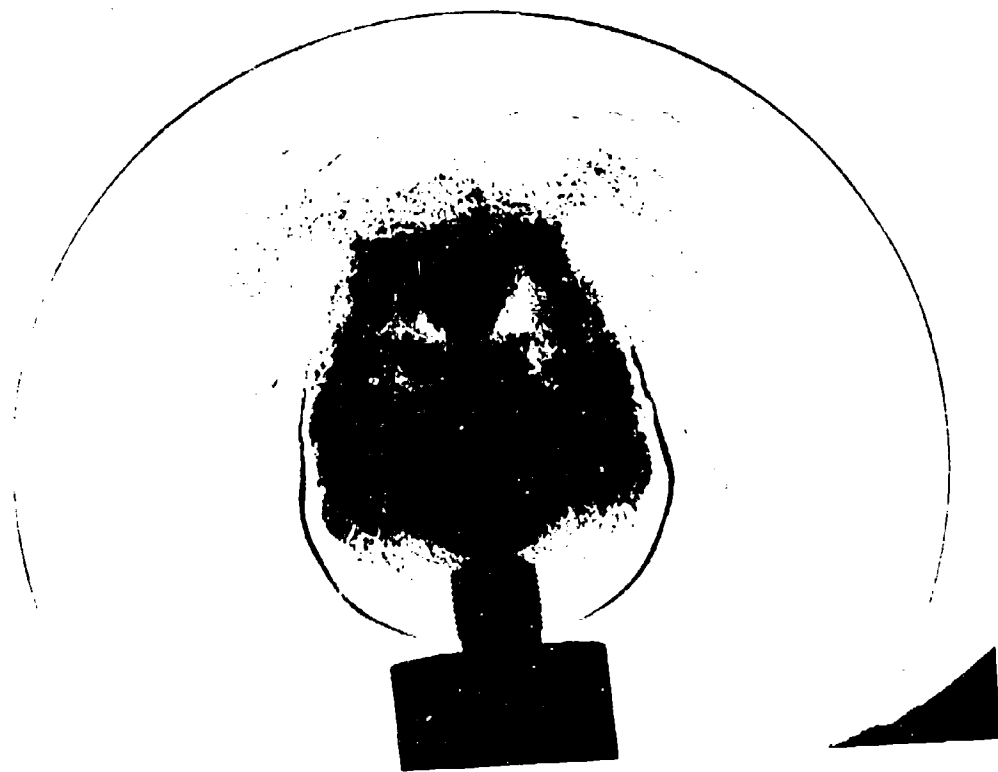


Figure 4b. Propellant Gas Flow

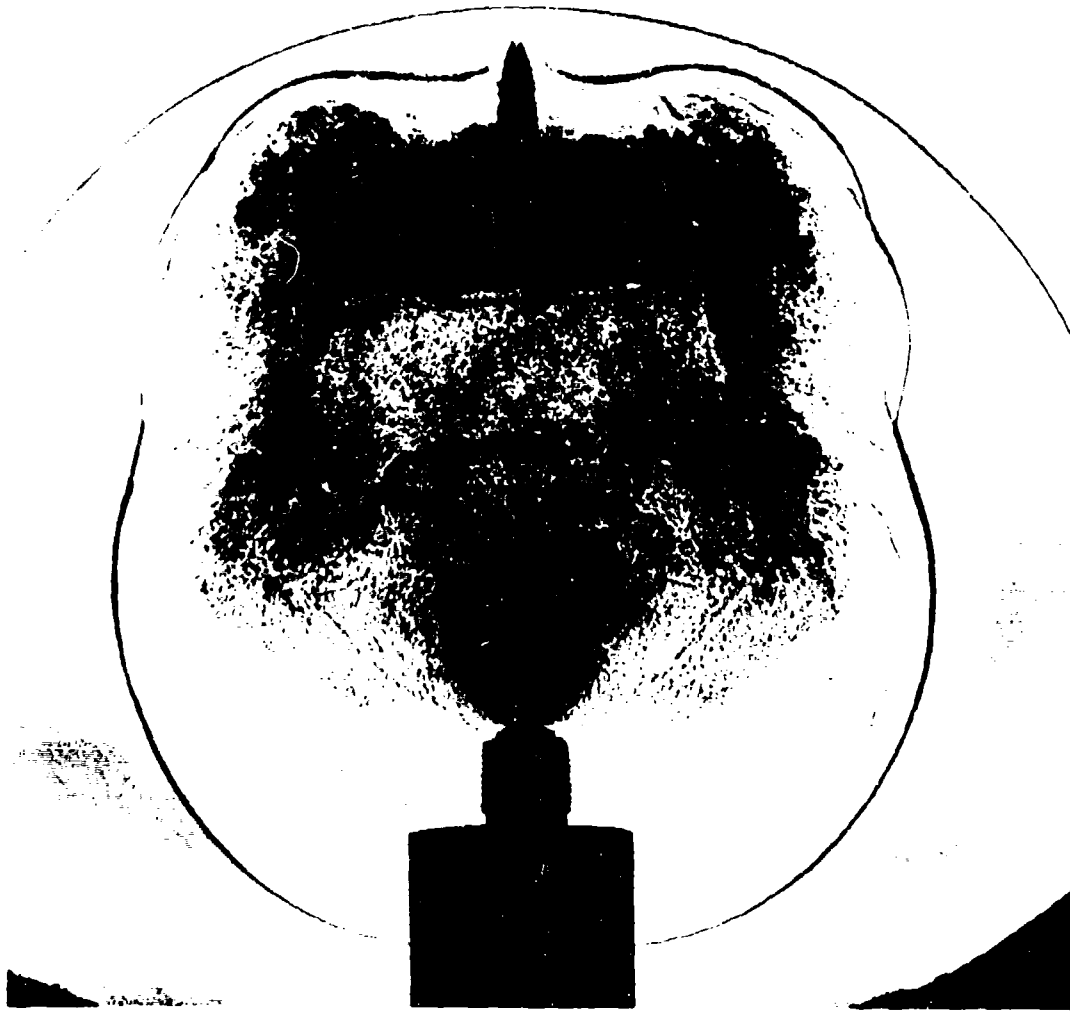


Figure 4c. Propellant Gas Flow

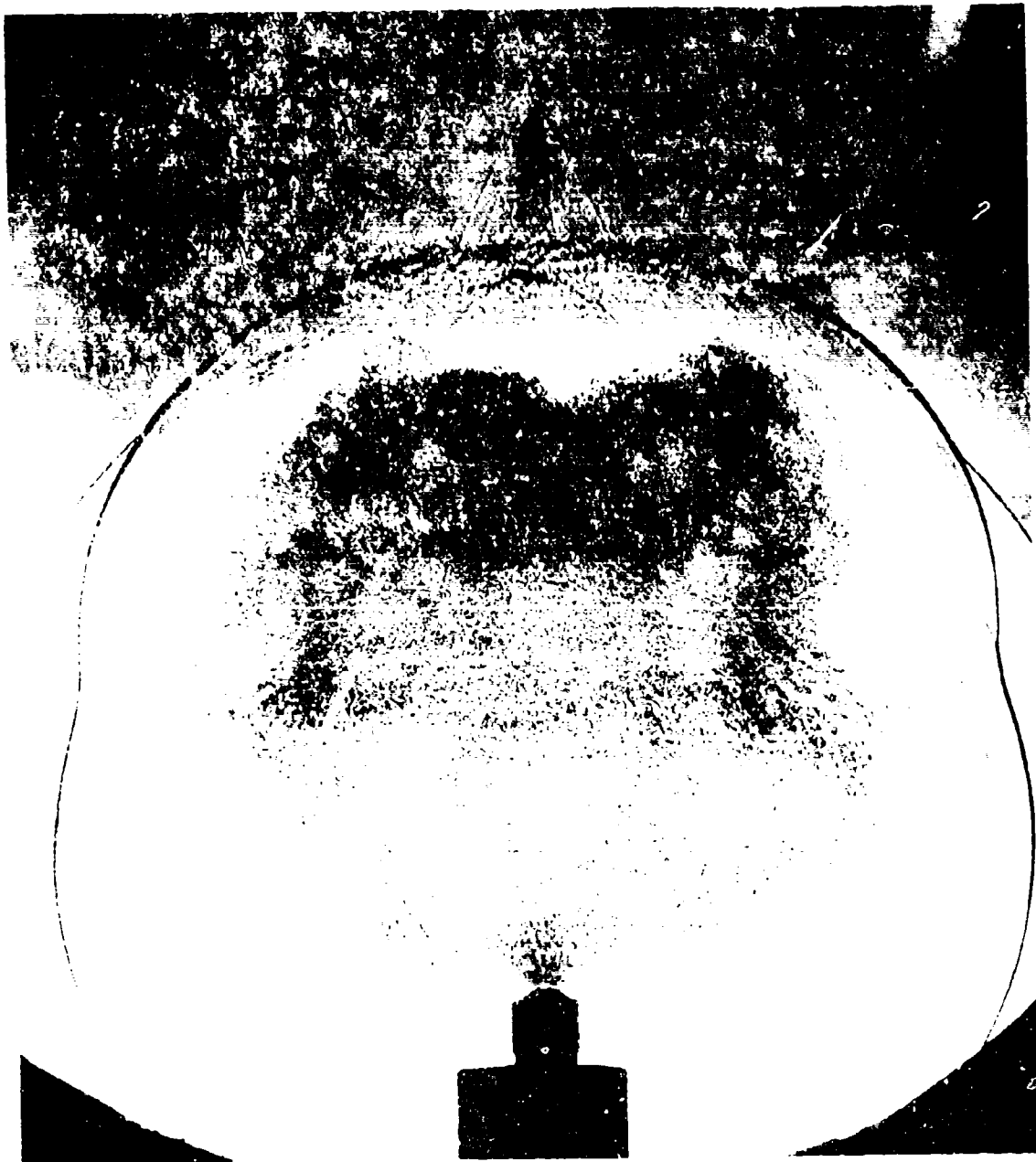


Figure 4d. Propellant Gas Flow

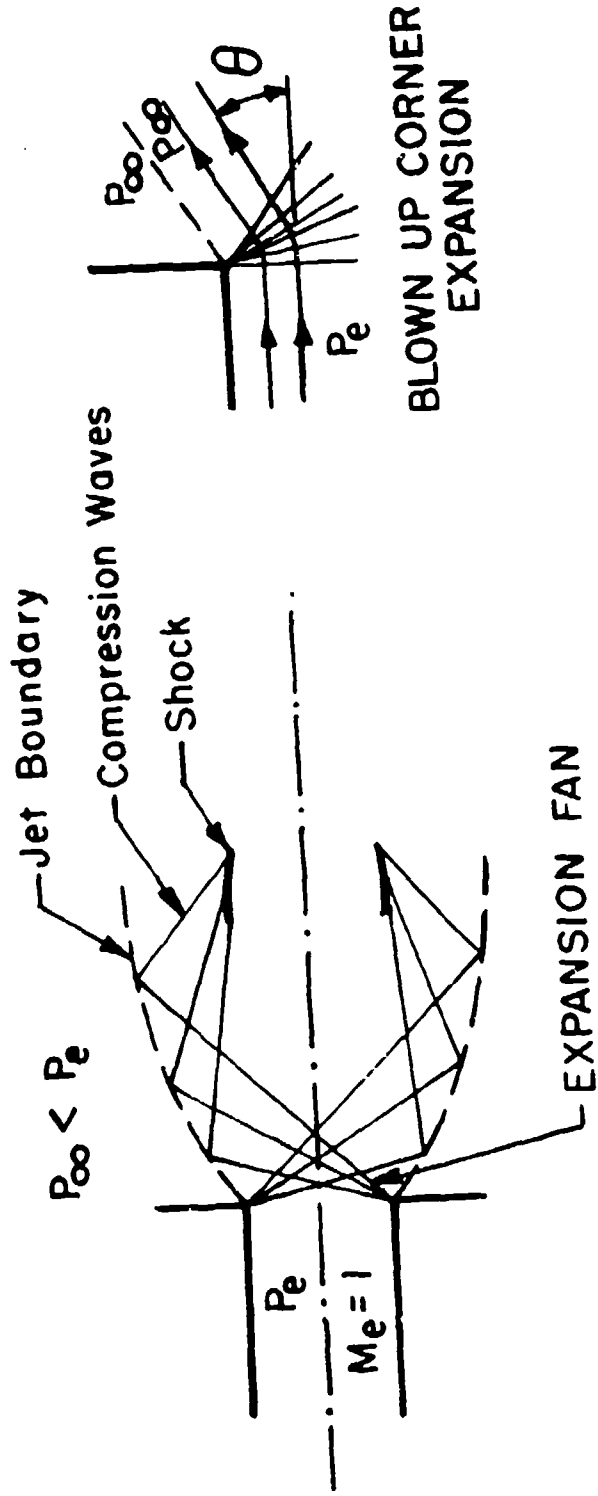


FIGURE 5 SCHEMATIC OF WAVE STRUCTURE FOR AN UNDEREXPANDED, STEADY JET

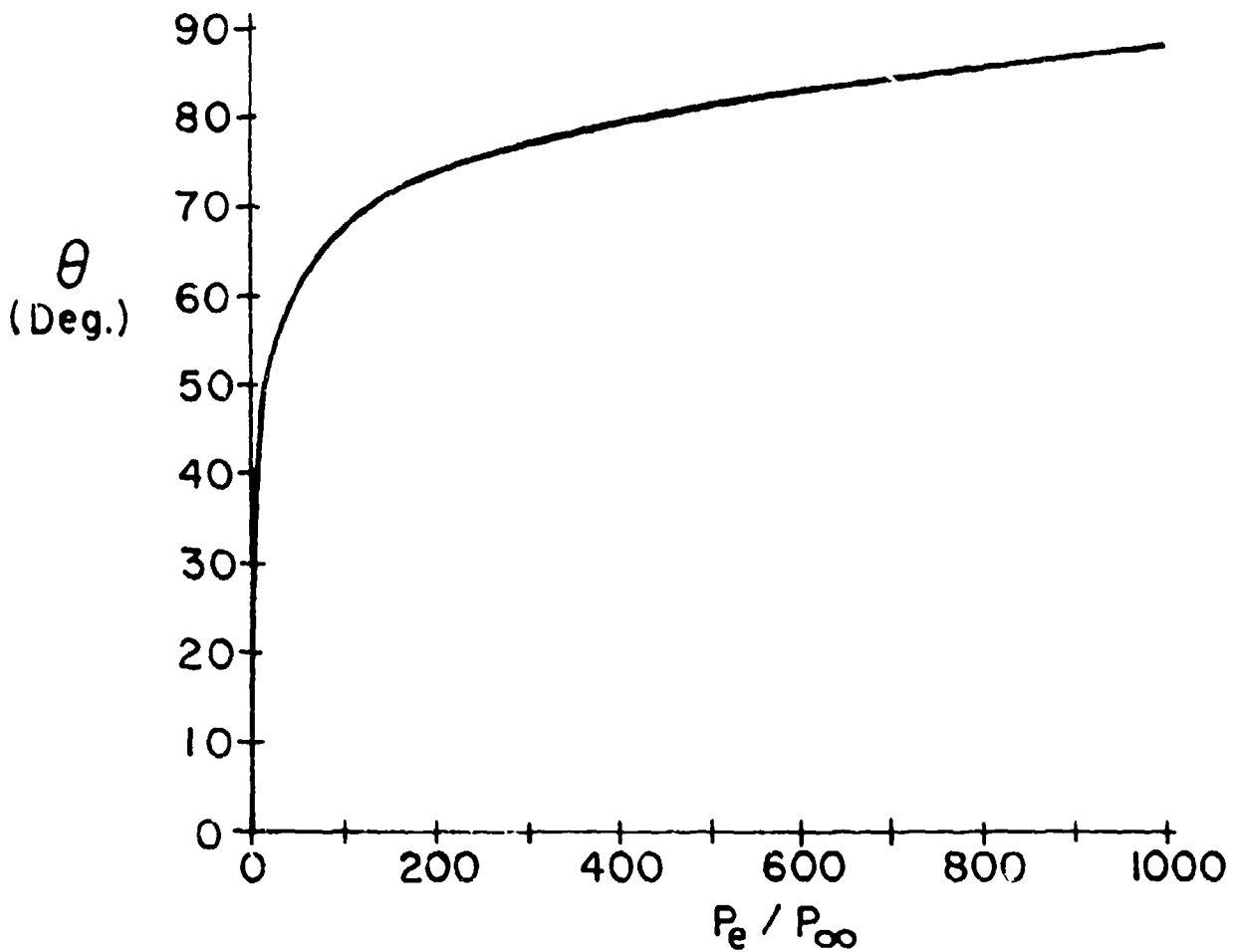
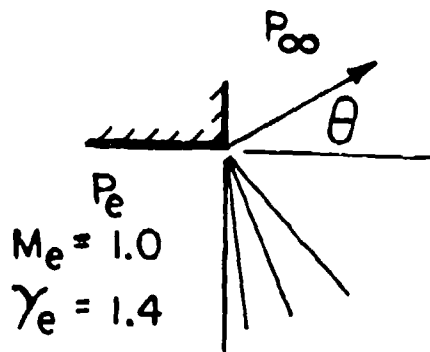


FIGURE 6 PLOT OF DEFLECTION ANGLE VERSUS PRESSURE RATIO

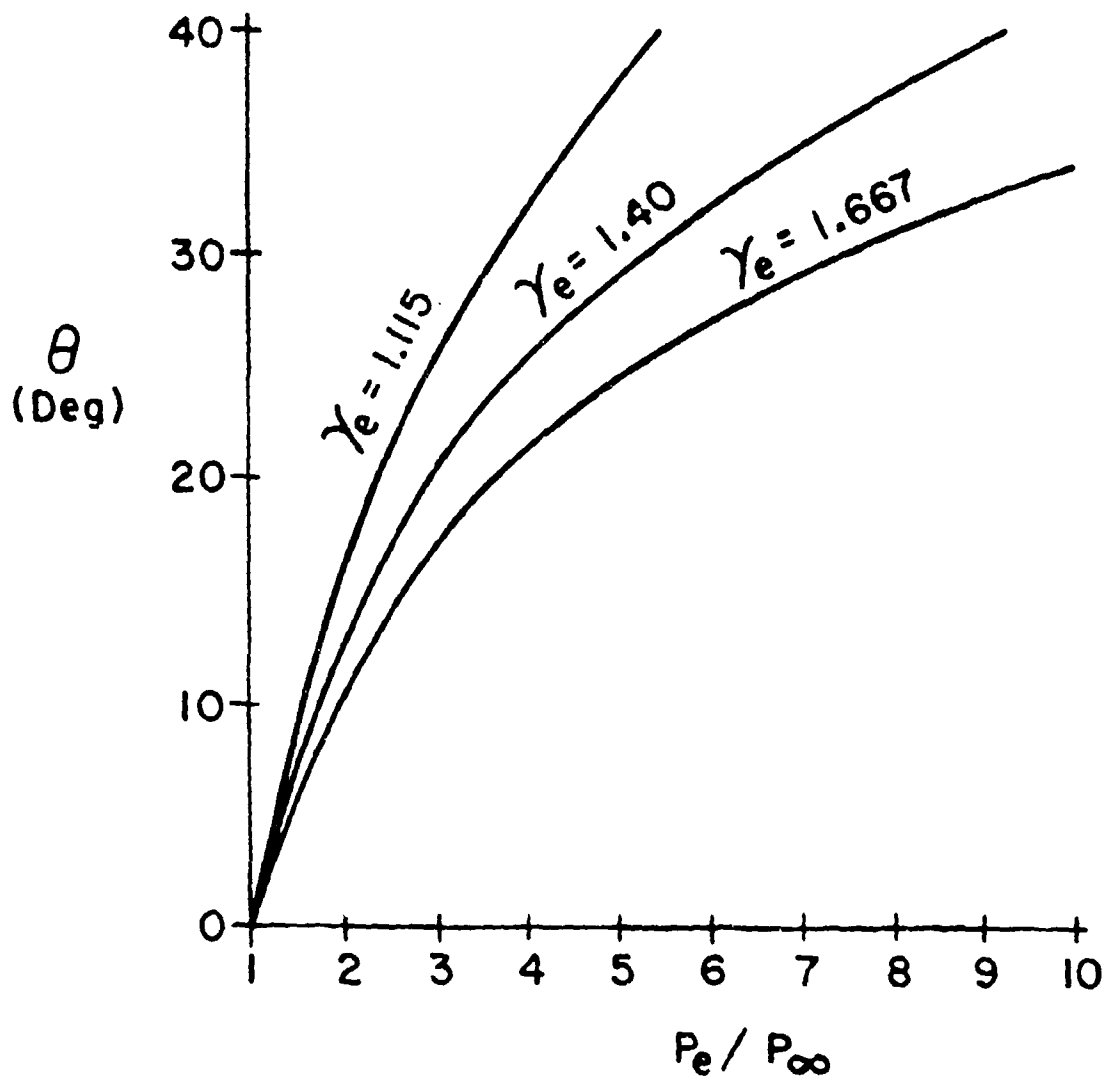
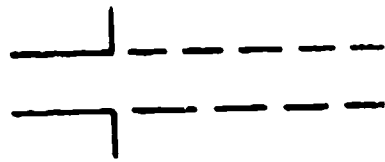


FIGURE 7 PLOT OF DEFLECTION ANGLE VERSUS PRESSURE RATIO FOR VARIOUS γ_e ;
 $M_e = 1.0$, $\theta_e = 0$



$$P_e \sim P_\infty$$



$$P_e \sim 1.8 P_\infty$$



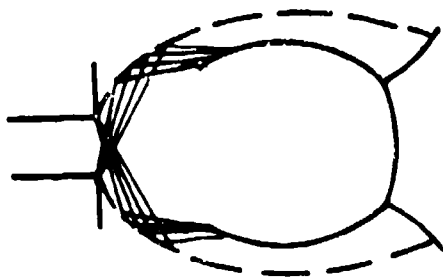
$$P_e \sim 2.3 P_\infty$$



$$P_e \sim 2.5 P_\infty$$



$$P_e \sim 2.8 P_\infty$$



$$P_e \sim 10.0 P_\infty$$

FIGURE 8 EFFECT OF PRESSURE RATIO UPON FREE JET STRUCTURE

I. MOMENTUM

a. UTILIZATION:

**MUZZLE BRAKES
COMPENSATORS**

b. CONTROL:

BLAST DEFLECTORS

2. ENERGY

a. RATE CONTROL:

BLAST SUPPRESSORS (SILENCERS)

b. DISTRIBUTION:

FLASH SUPPRESSORS

FIGURE 9 CATEGORIES OF MUZZLE DEVICES

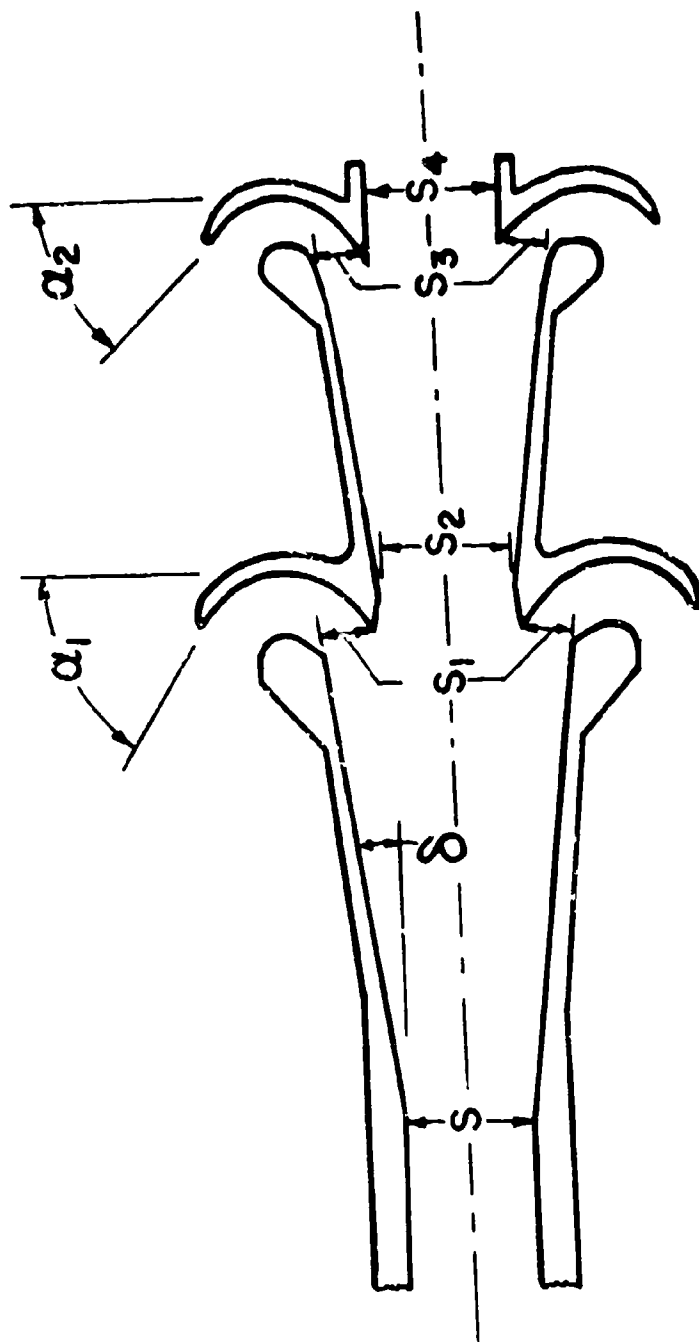


FIGURE 10 RATEAU MUZZLE BRAKE

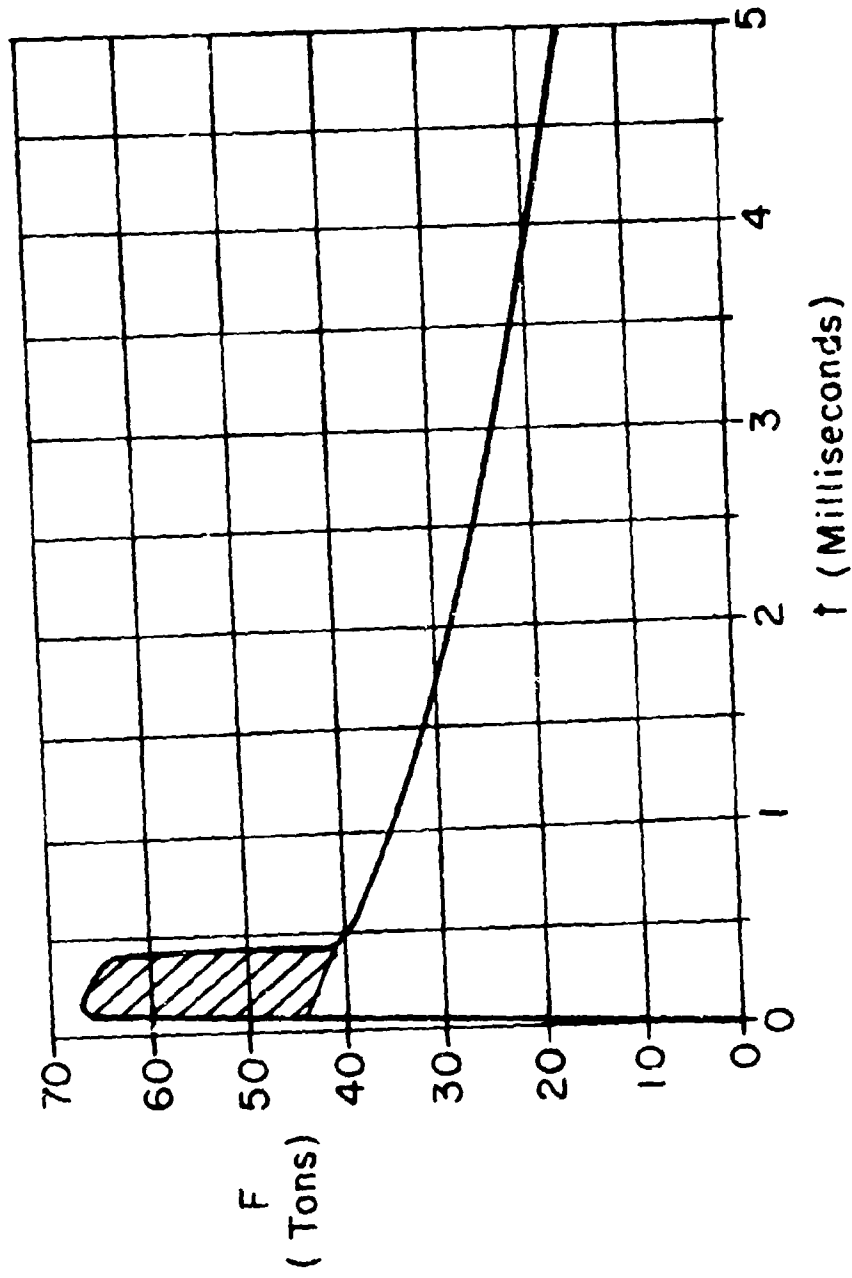


FIGURE II RATEAU'S CALCULATION OF FORCE ON 75 mm GUN
MUZZLE BRAKE

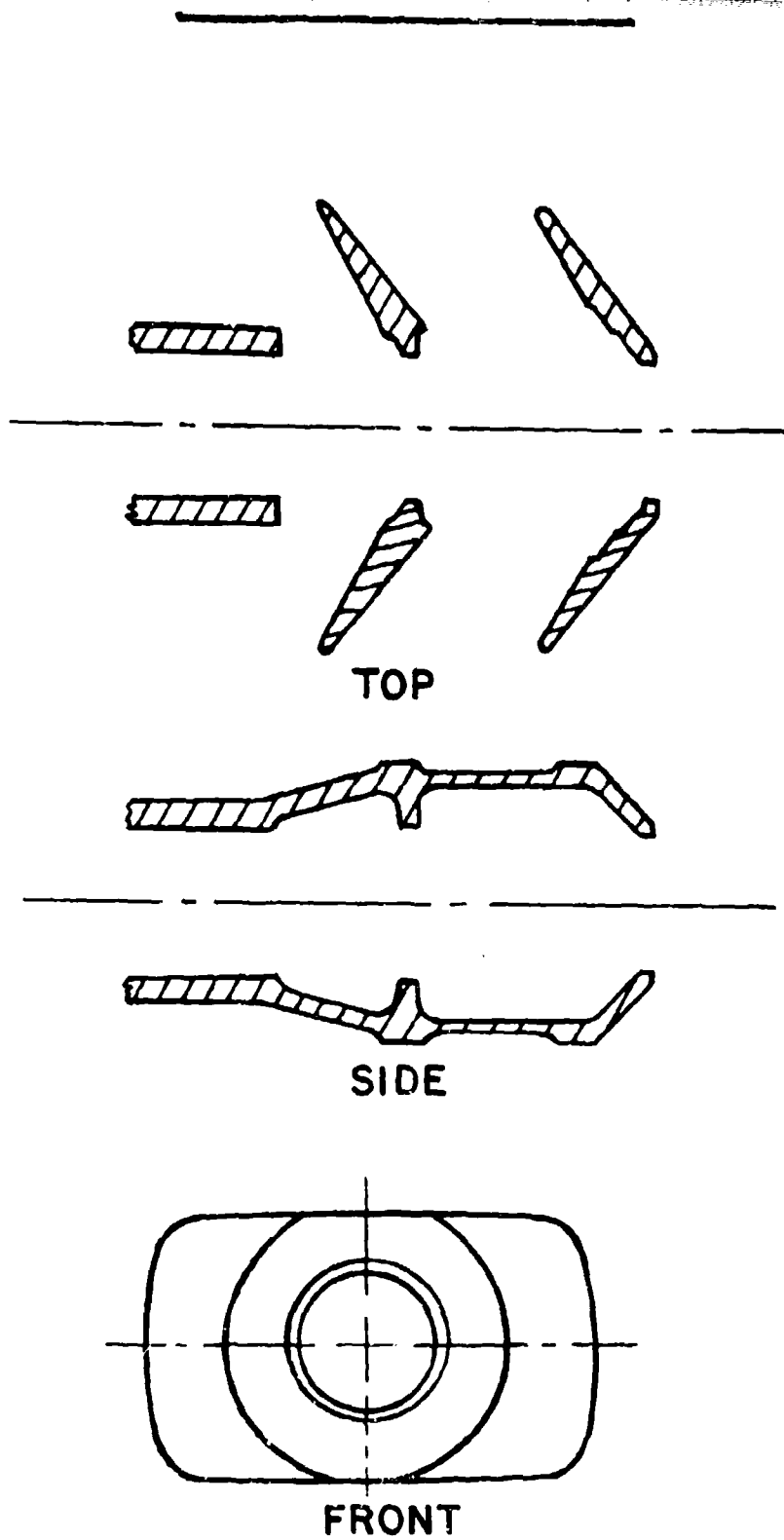


FIGURE 12 GERMAN DOUBLE BAFFLE MUZZLE BRAKE

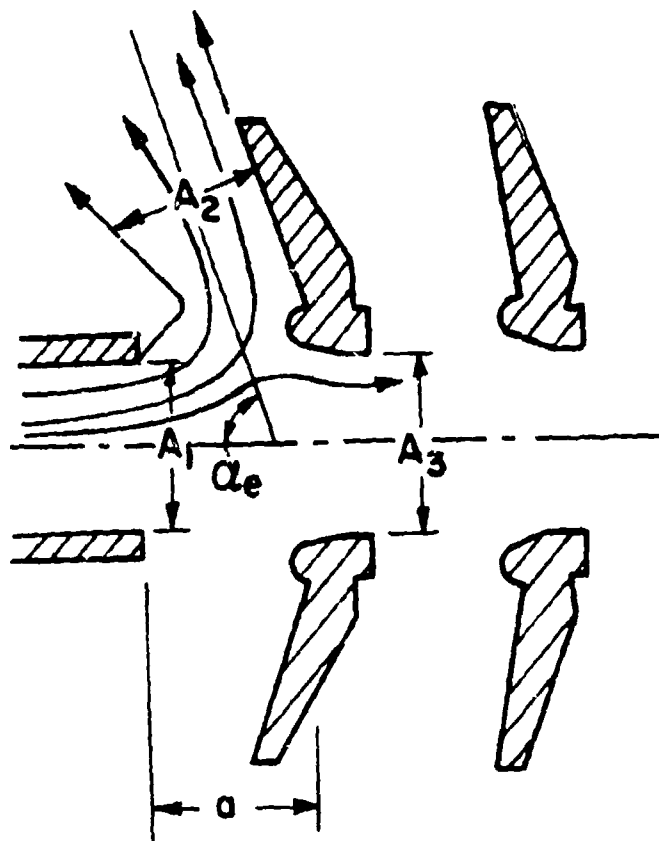


FIGURE 13 OSWATITSCH BRAKE NOMENCLATURE

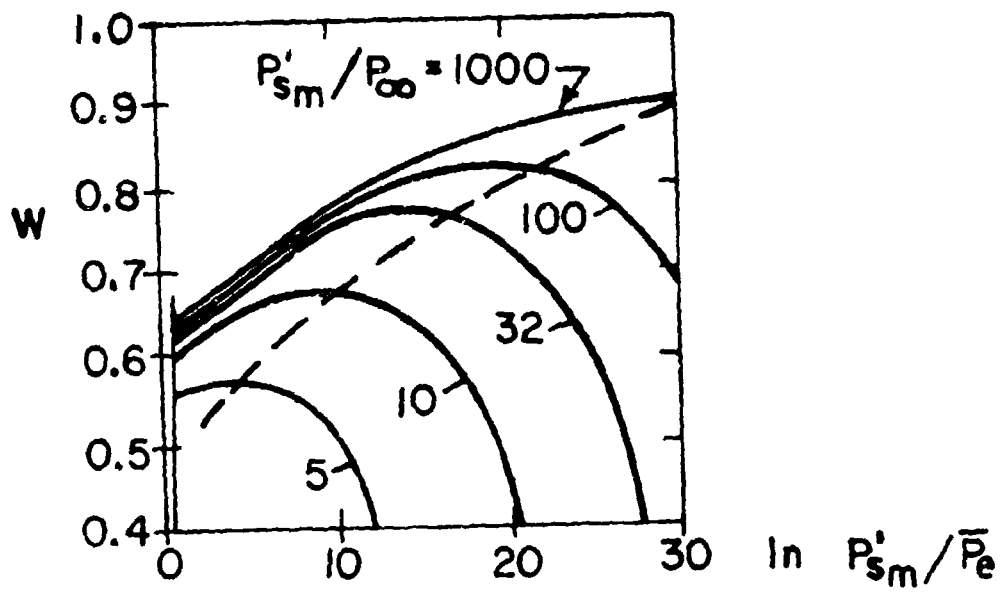


FIGURE 14 OPTIMIZATION PLOT FOR W

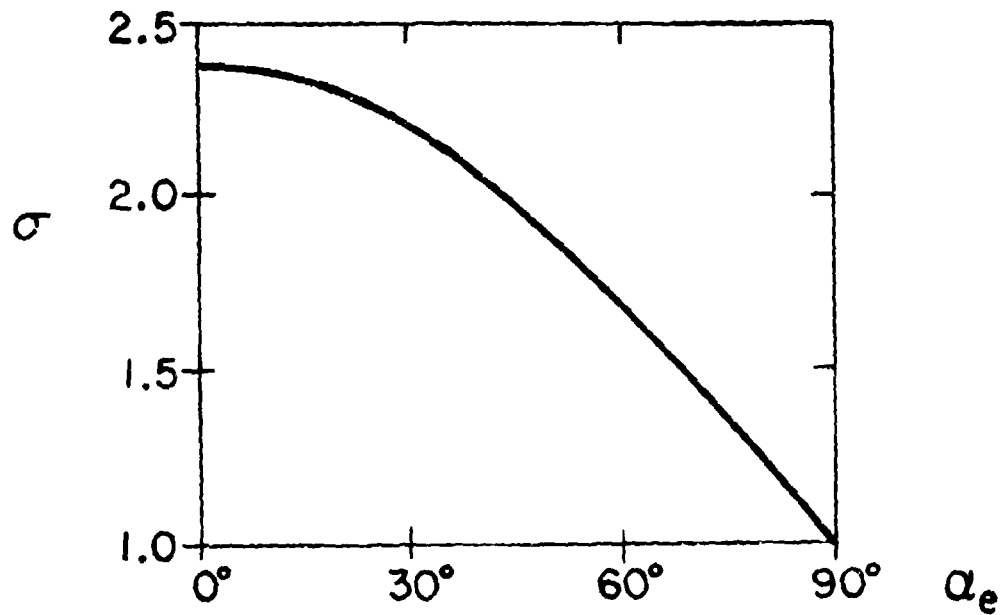


FIGURE 15 PLOT OF σ VS α_e FOR ZERO PROJECTILE HOLE LOSS AND $\gamma = 9/7$

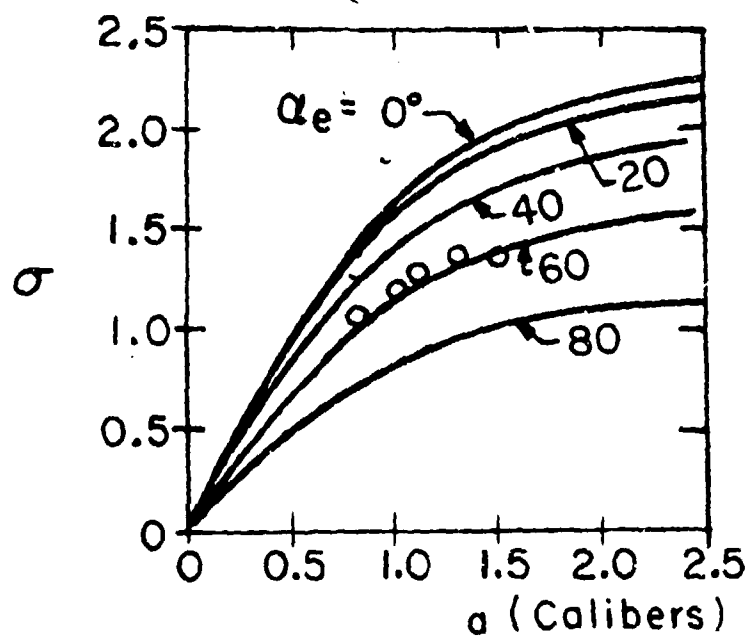
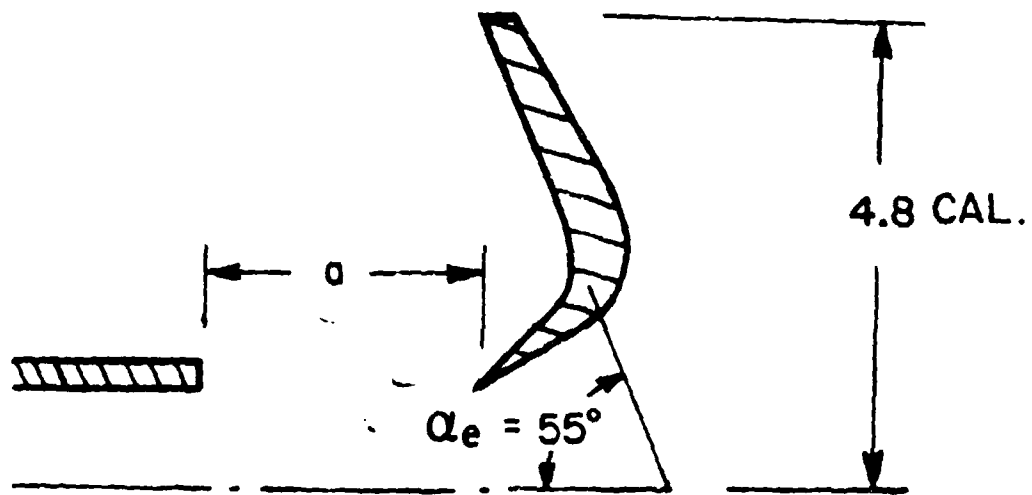


FIGURE 16 COMPARISON OF THEORY AND EXPERIMENT FOR OSWATITSCH BRAKE

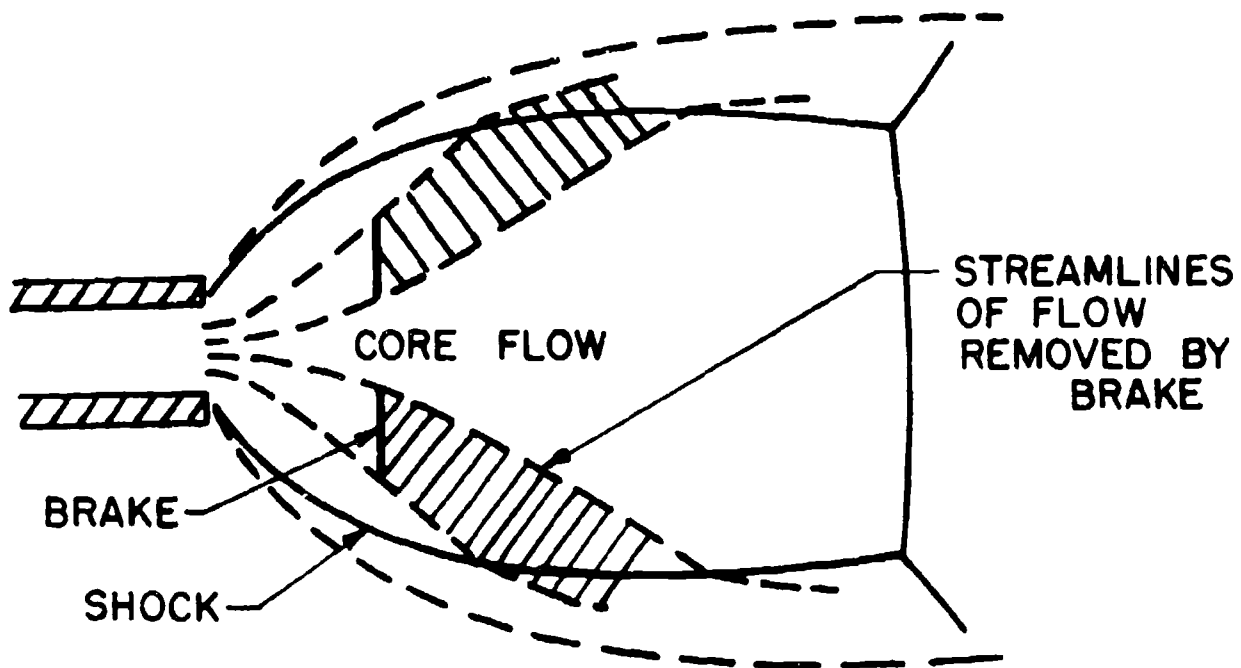


FIGURE 17 SMITH MUZZLE GAS FLOW NOMENCLATURE

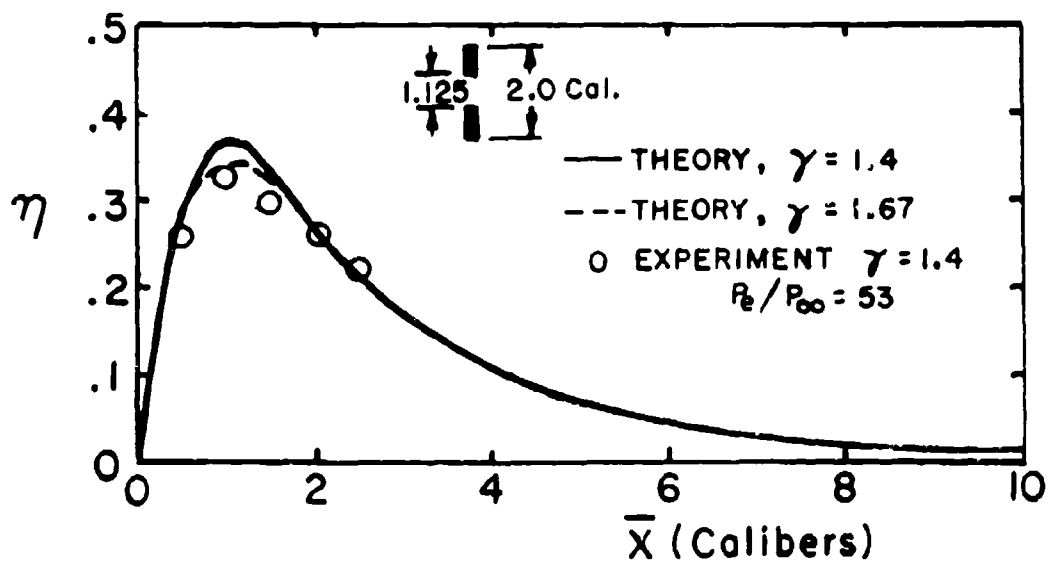


FIGURE 18 SMITH BRAKE THEORY RESULTS

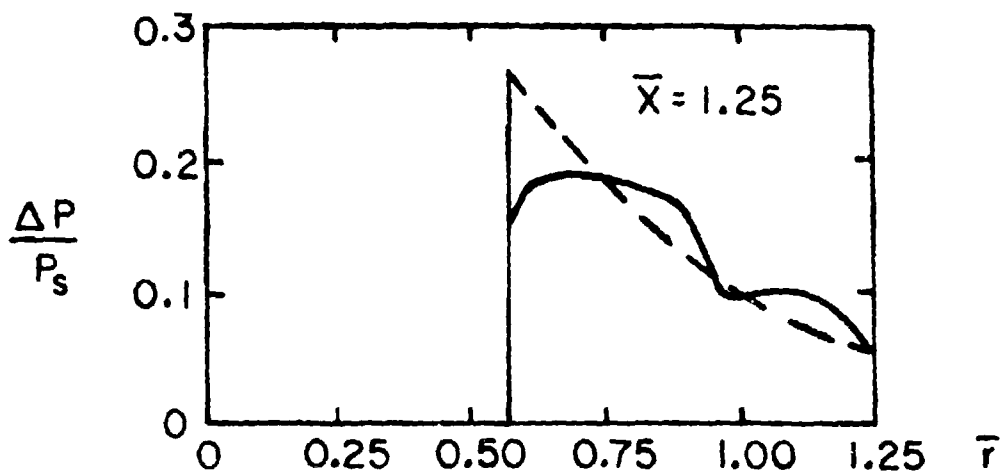
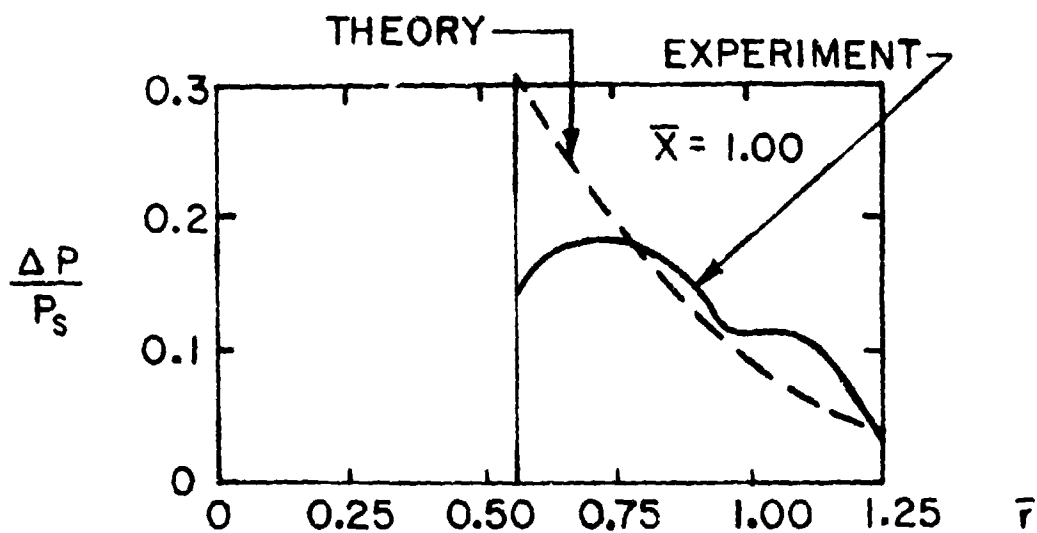
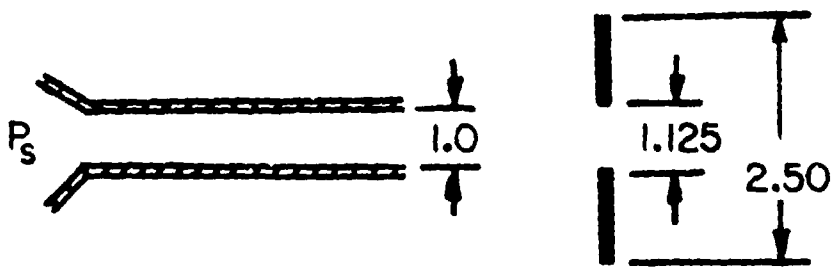


FIGURE 19 PRESSURE DISTRIBUTION ON BRAKE SURFACE IN A STEADY JET

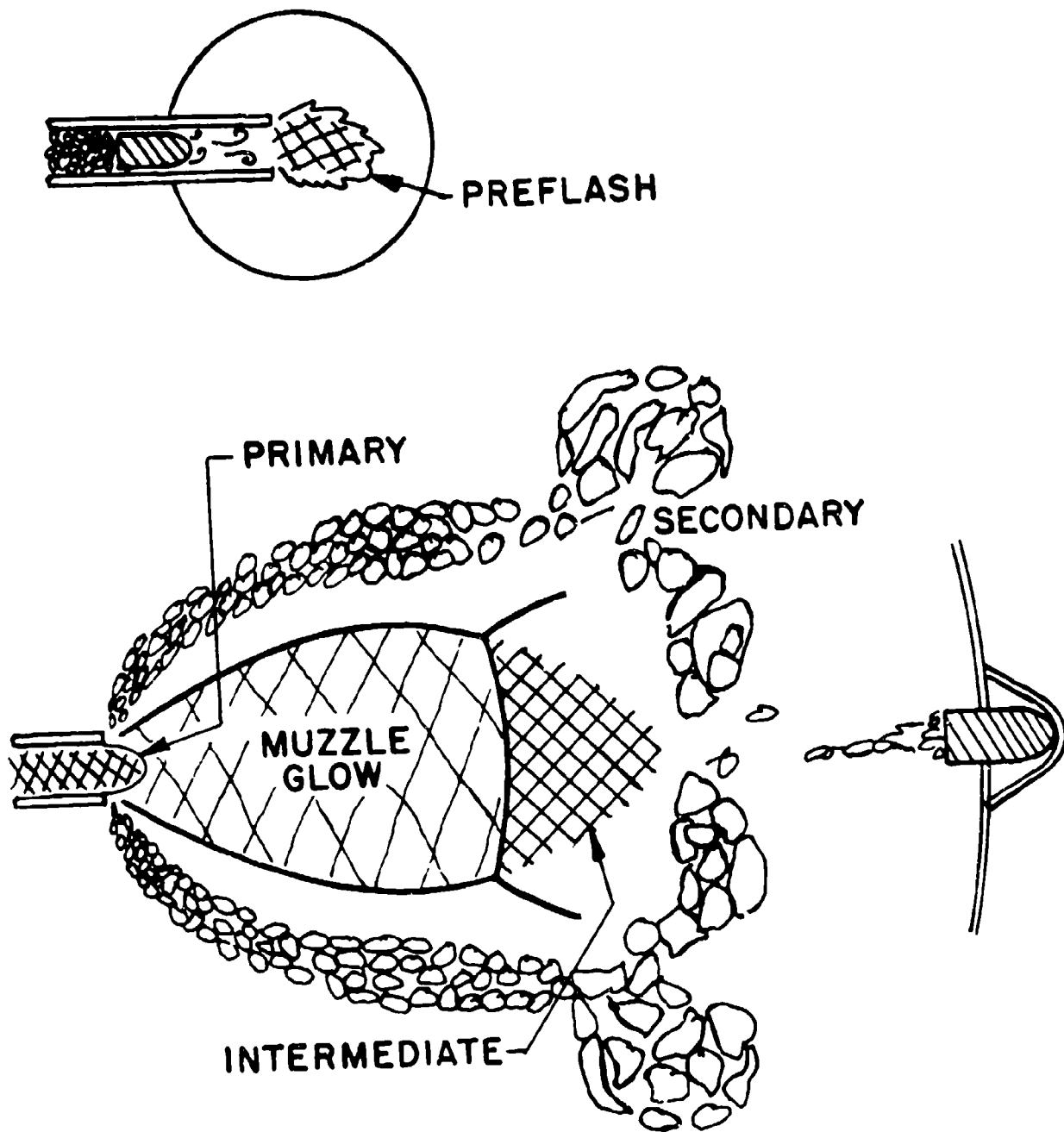


FIGURE 20 FLASH PHENOMENA

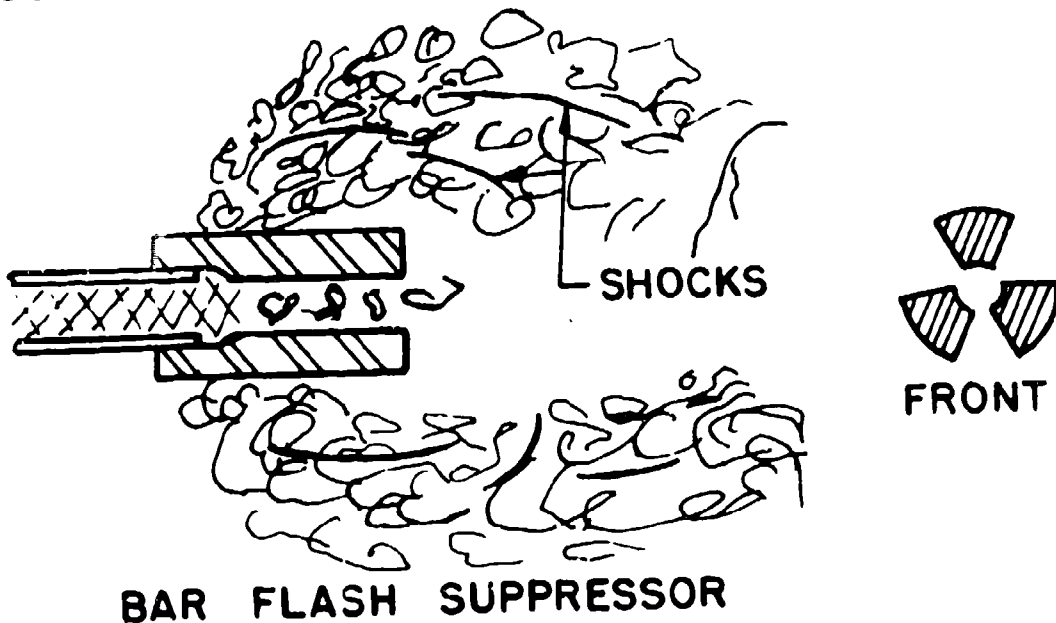
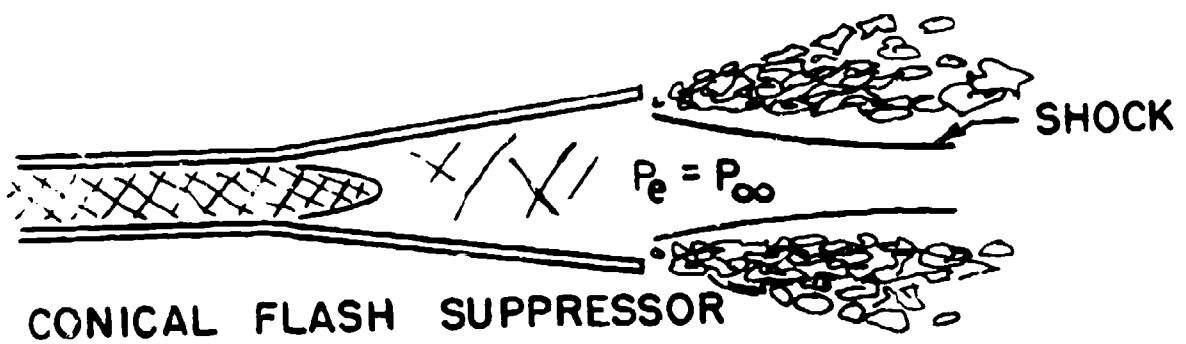
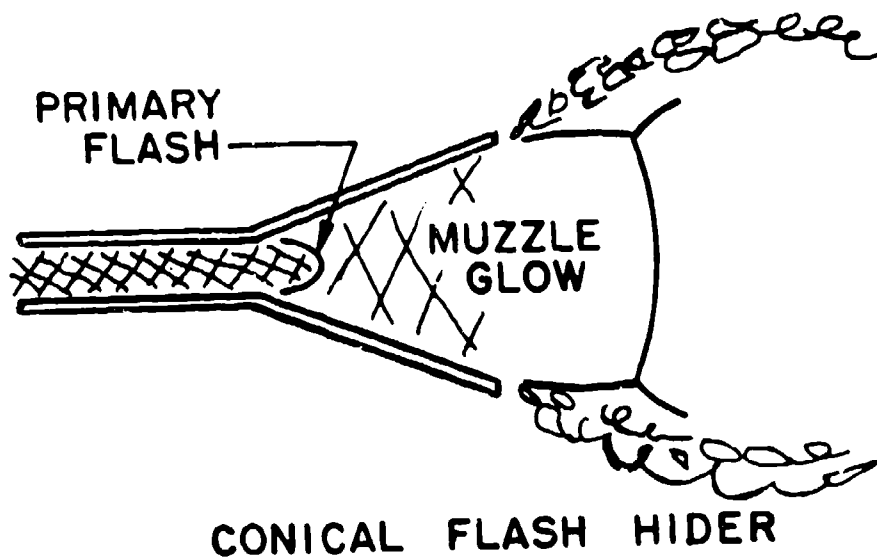


FIGURE 21 FLASH PREVENTIVE DEVICES


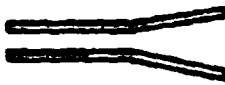

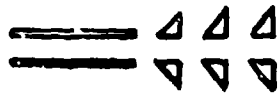





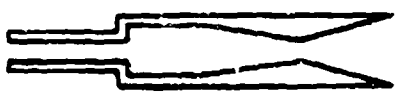
		
CONE		$\eta = 1.4$
BAR		$\eta = 5.4$
MIXING SLOTS		$\eta = 5.4$
MIXING SLOTS + CONVERGING NOZZLE		$\eta = 1.5$
SILENCER SLOTS		$\eta = 8$
SINGLE SLOT		$\eta = 12$
SLOTS + CONE		$\eta = 85$ (SINGLE SLOT + CONE $\eta = 100$)
CONVERGING CONE		$\eta = 8.1$
CONVERGING - DIVERGING CONE		$\eta = 300$

FIGURE 22 WATLING FLASH SUPPRESSOR TESTS

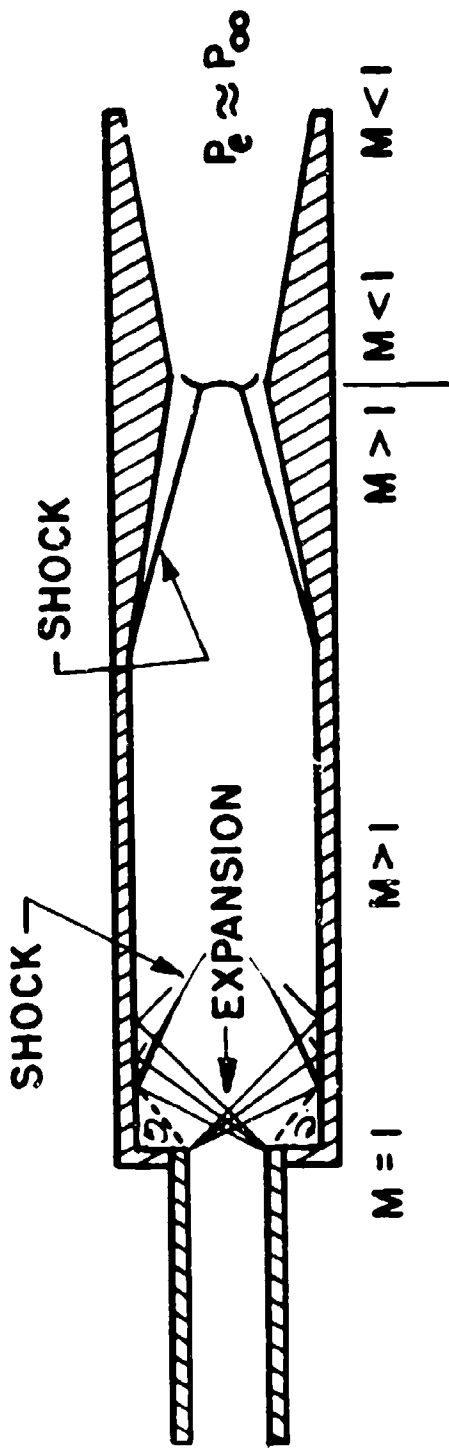
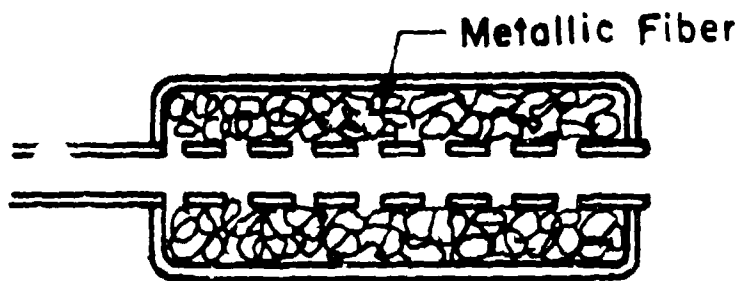
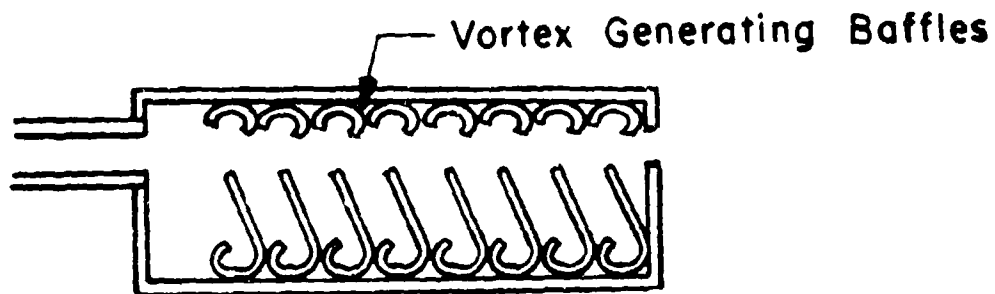


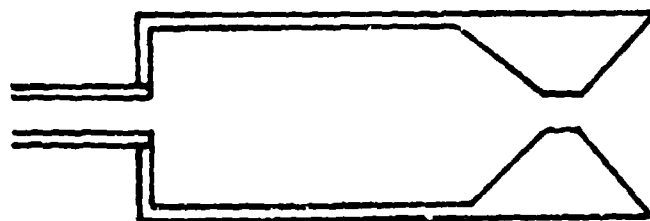
FIGURE 23 SUPERSONIC DIFFUSER SILENCER



ENERGY ABSORPTION



ENERGY DISSIPATOR (MAXIM)



ENERGY CONTAINMENT AND
CONTROLLED RELEASE

FIGURE 24 BLAST SUPPRESSOR CLASSIFICATION

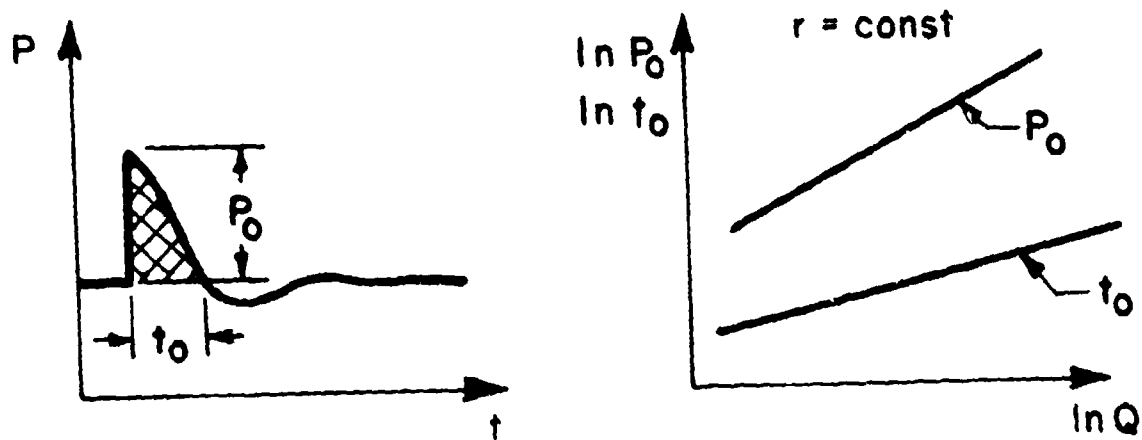


FIGURE 25 FURRER EXPLOSIVE BLAST MEASUREMENTS

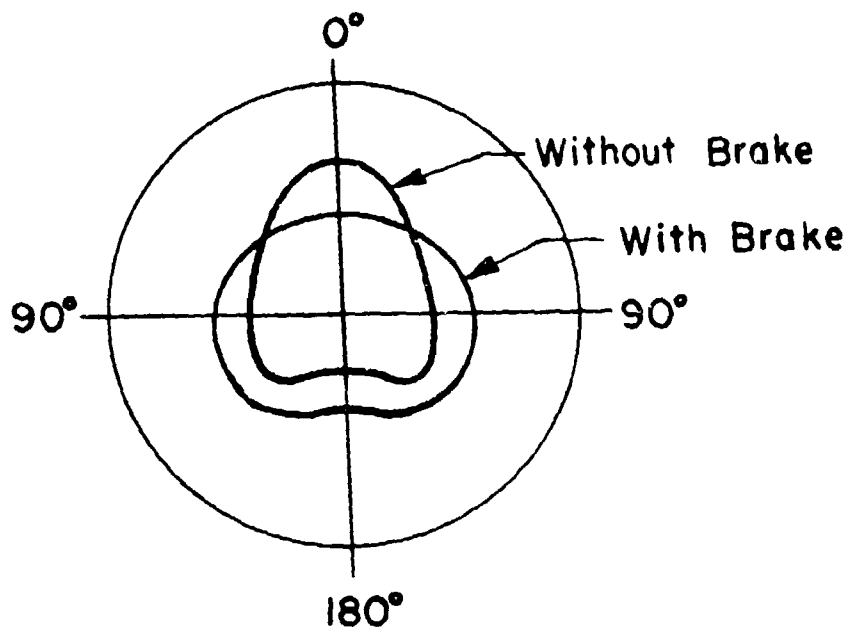


FIGURE 26 THE EFFECT OF MUZZLE BRAKES ON BLAST PRESSURES

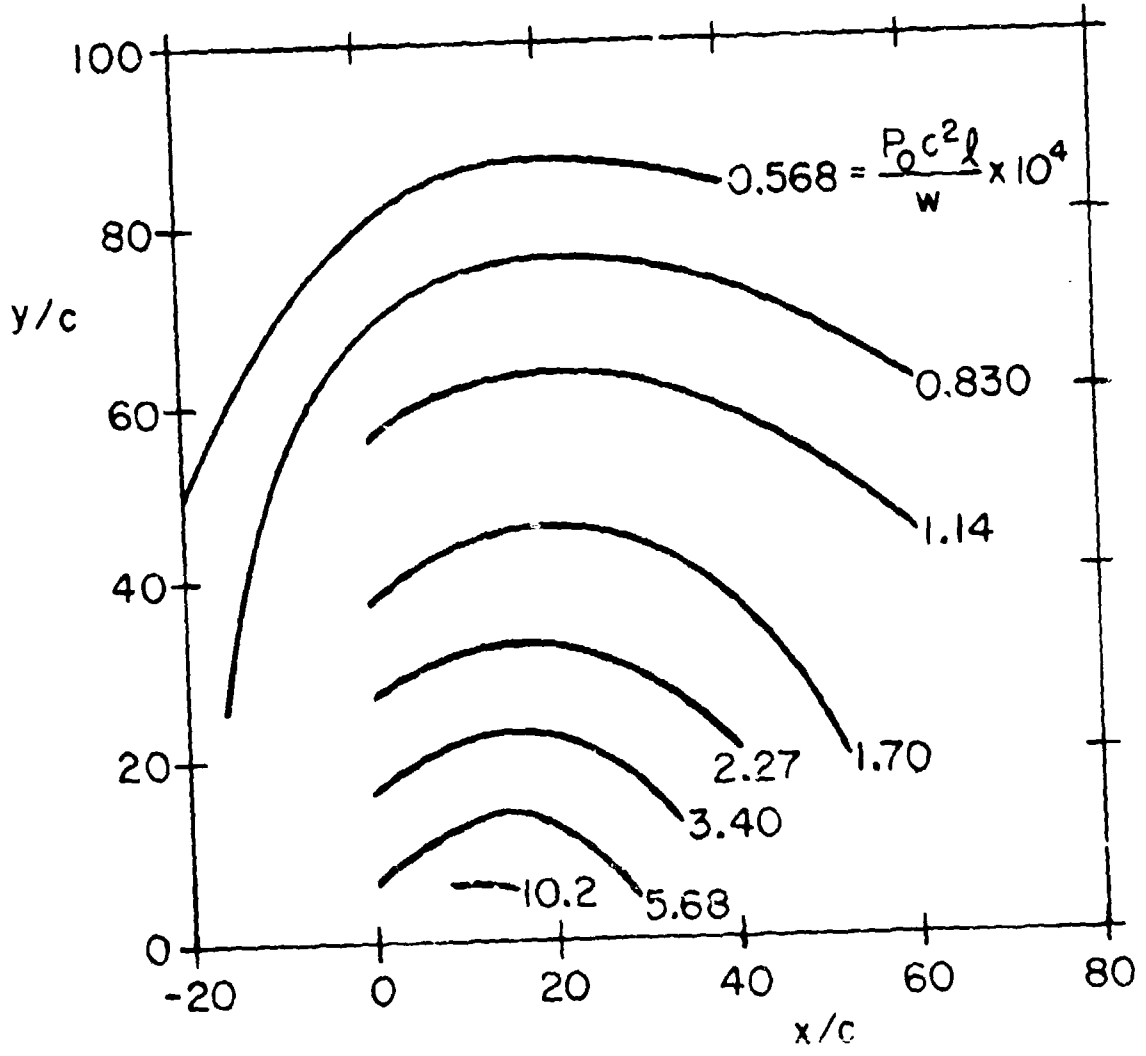
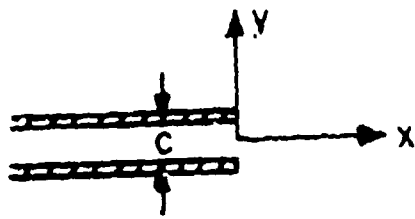


FIGURE 27 WESTINE'S UNIVERSAL GUN BLAST PLOT

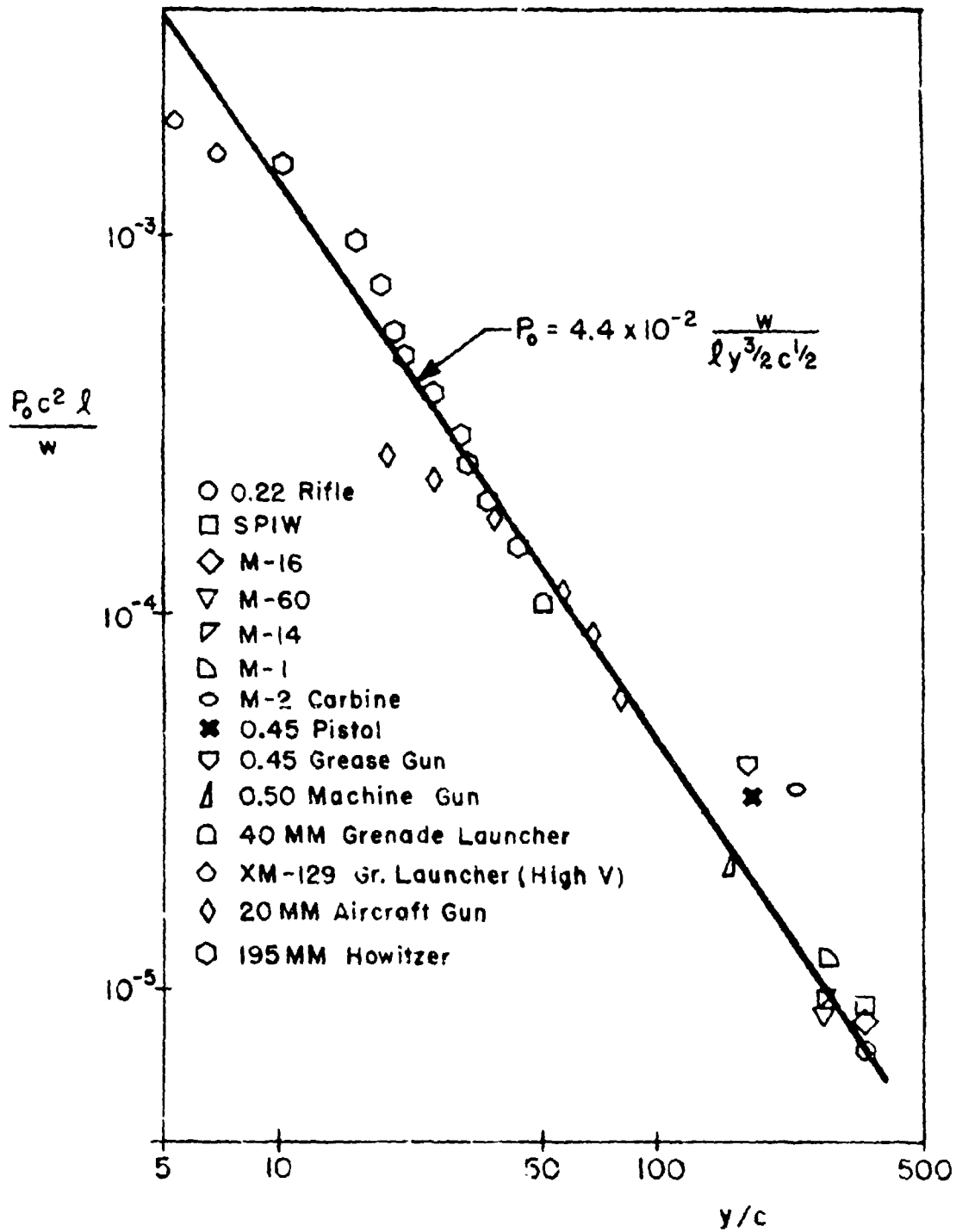


FIGURE 28 CORRELATION OF OVERPRESSURE FACTOR FOR VARIOUS WEAPONS ($x/c = 0$)

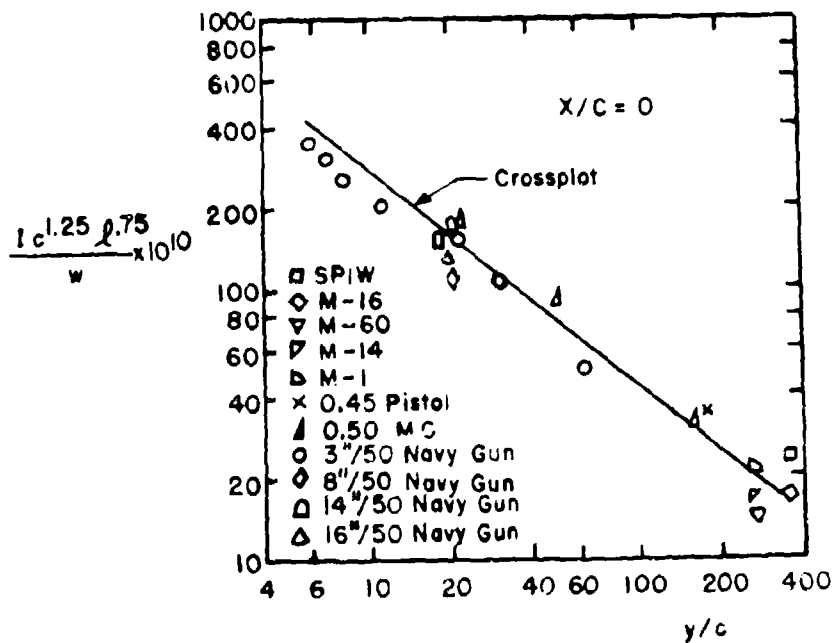
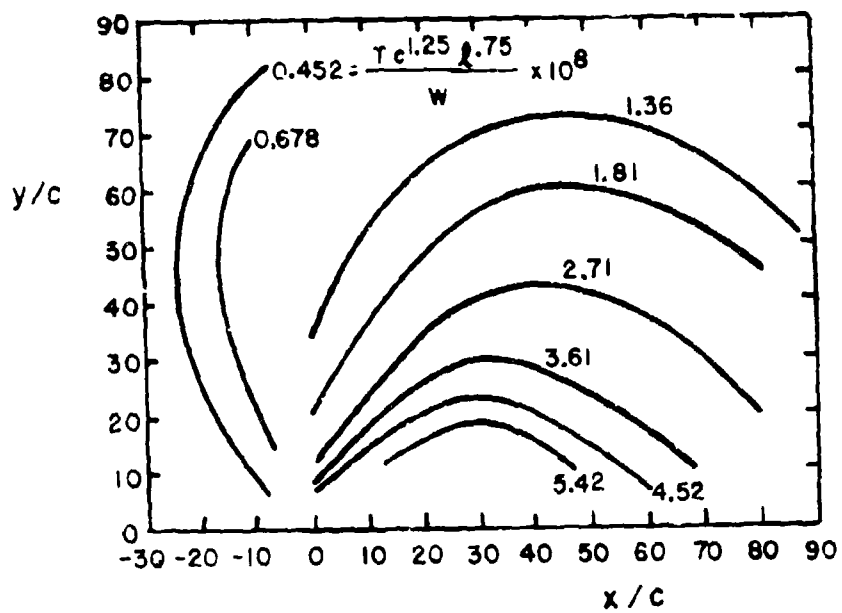


FIGURE 29 UNIVERSAL IMPULSE PLOT AND CORRELATION PLOT

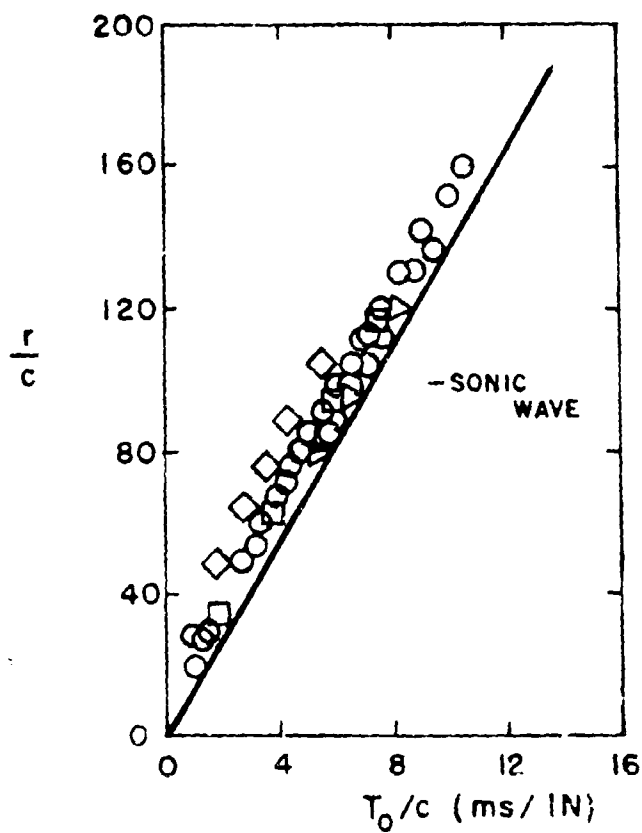
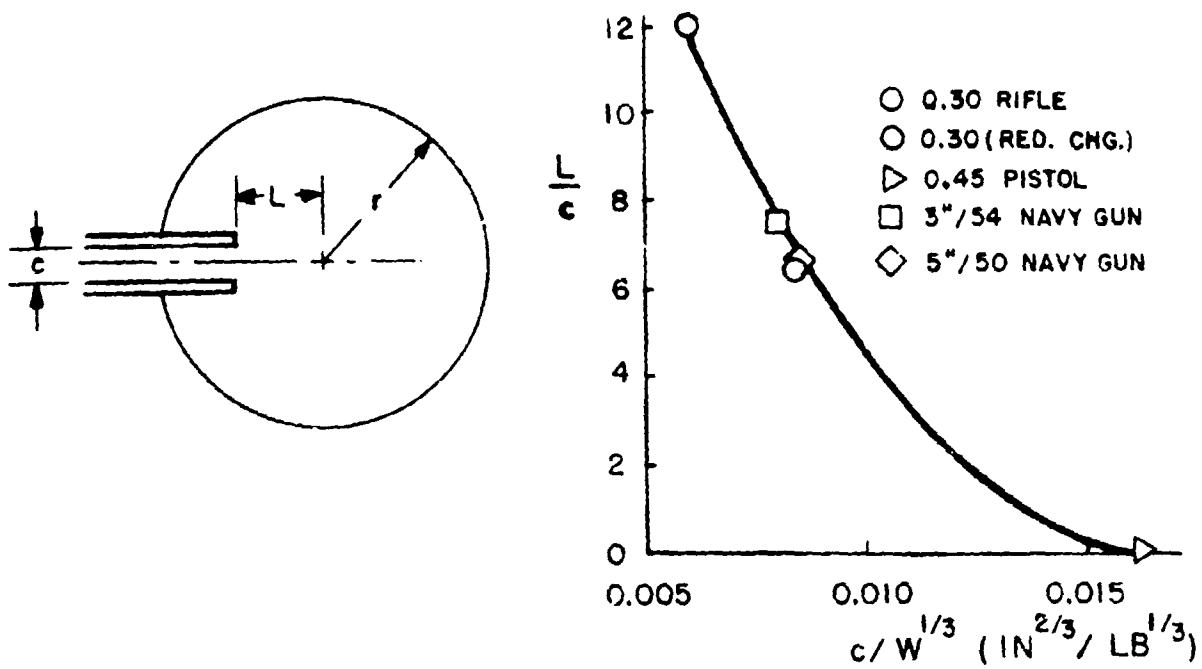
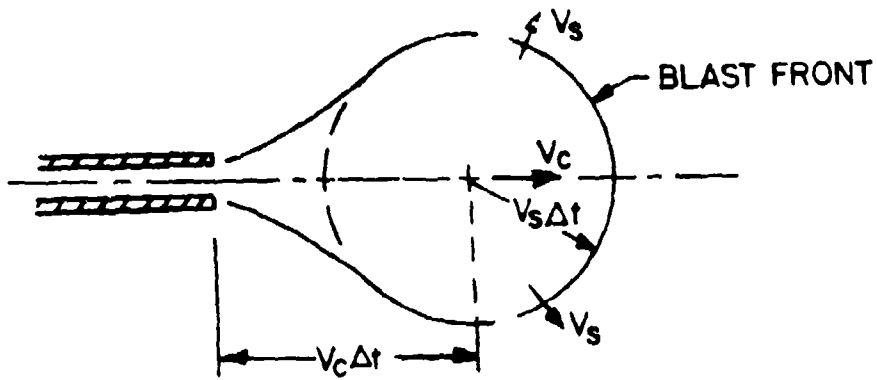
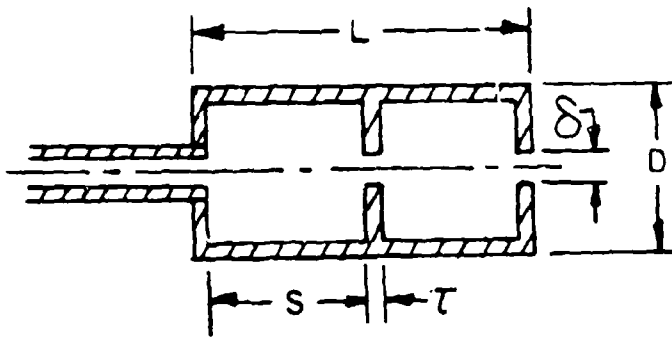


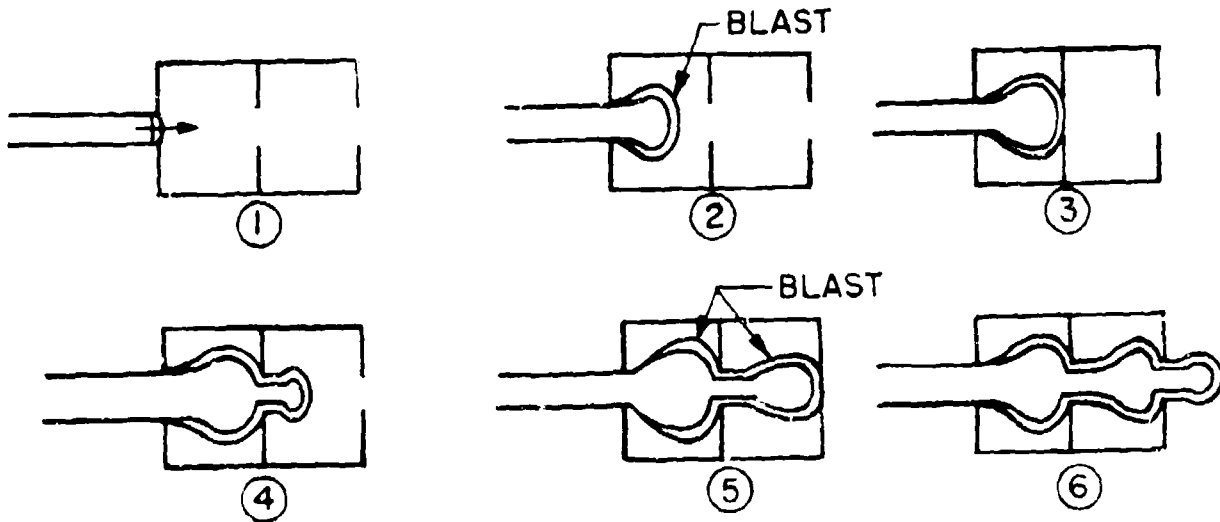
FIGURE 30 TIME OF BLAST ARRIVAL



GEOMETRY OF THE BLAST FIELD



GEOMETRY OF THE BLAST SUPPRESSOR



SEQUENCE OF BLAST PROPAGATION

FIGURE 31 BIXLER BLAST SUPPRESSOR MODEL

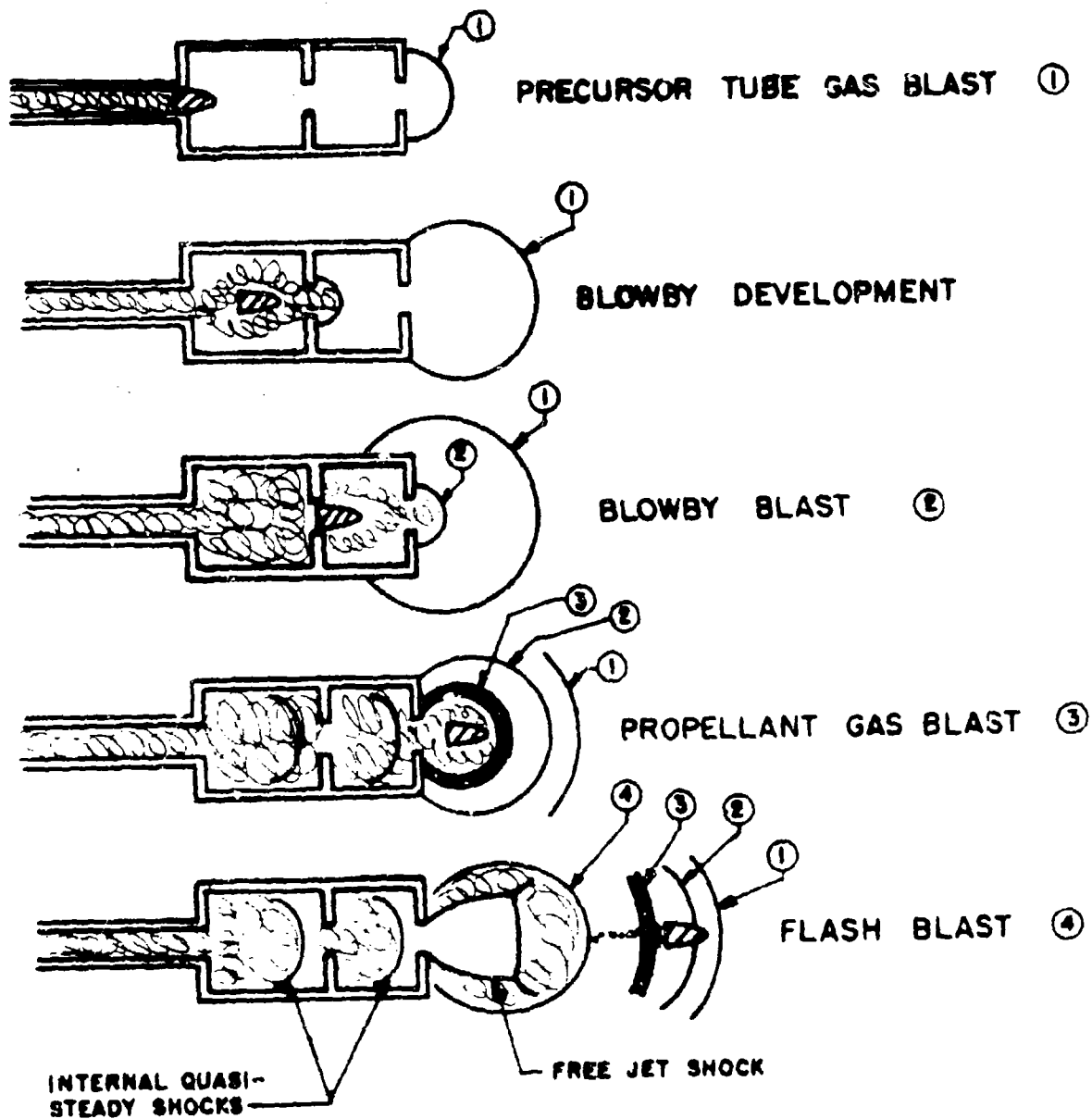
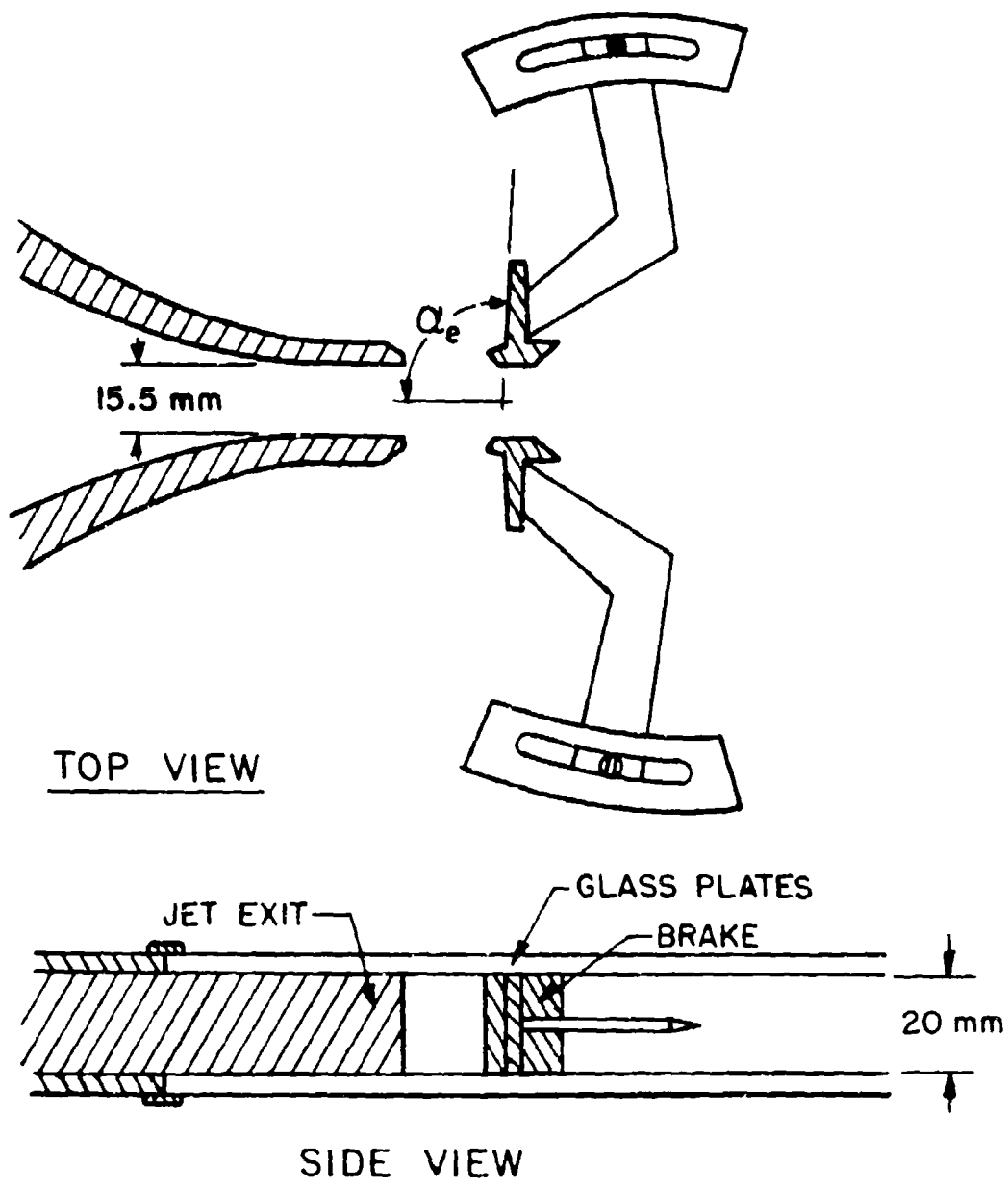


FIGURE 32 SEQUENCE OF MEASURED BLASTS



TEST CONDITIONS

$T_{SE} = 540^\circ R$
 $\gamma_E = 1.4$
 $P_E = 45 \text{ PSIA}$
 $P_\infty = 4.5 \text{ PSIA}$
 NO PROJECTILE

FIGURE 33 OSWATITSCH 2-D MUZZLE FLOW SIMULATOR

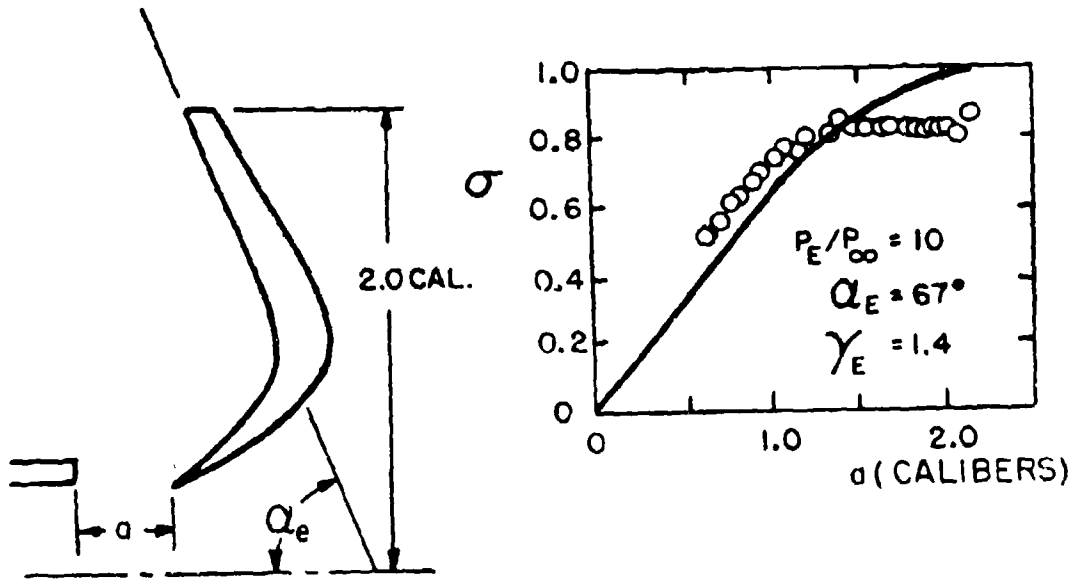


FIGURE 34 EFFICIENCY FACTOR, THEORY AND EXPERIMENT

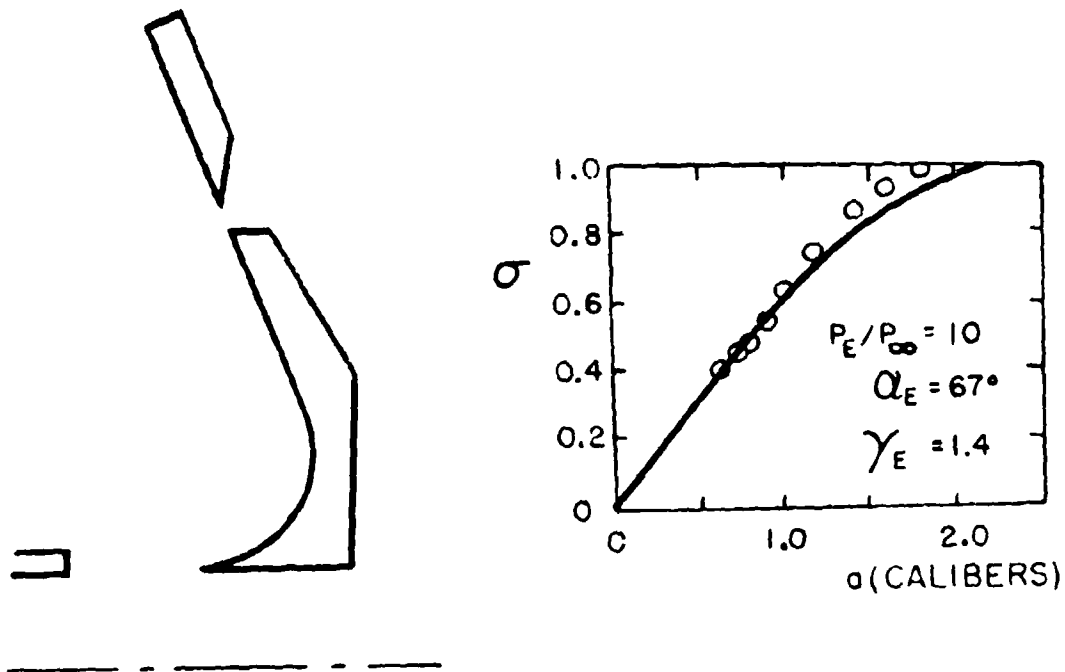


FIGURE 35 EFFICIENCY FACTOR OF EXTENDED BRAKE

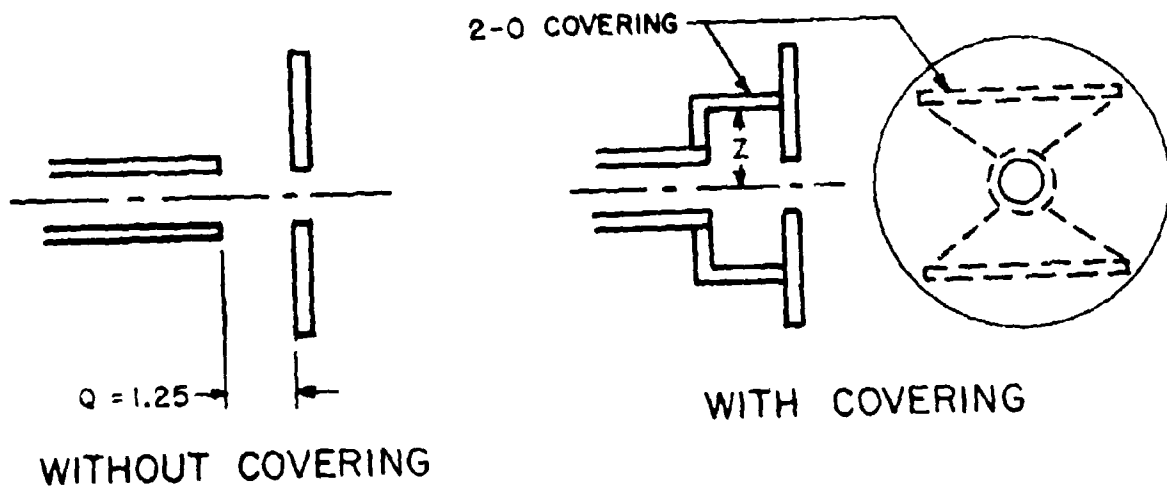


FIGURE 36 AXISYMMETRIC JET WITH BAFFLE

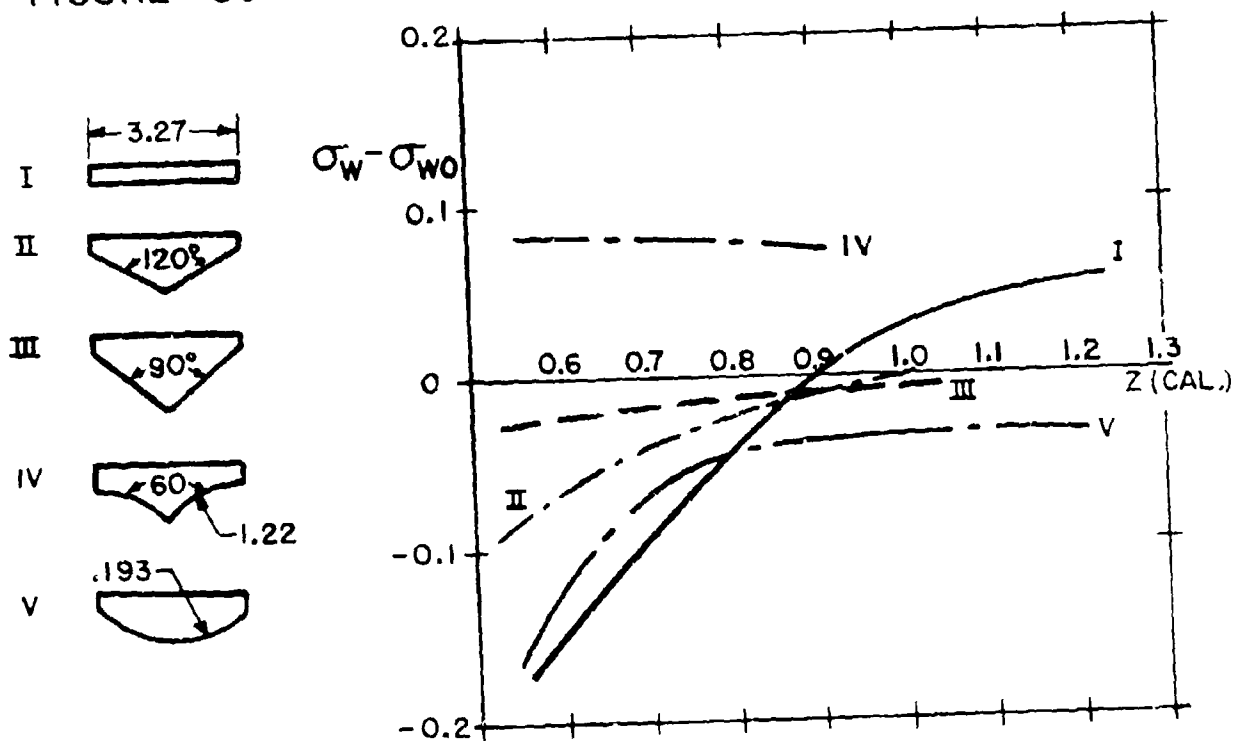


FIGURE 37 COVER TYPES AND EFFECT ON EFFICIENCY

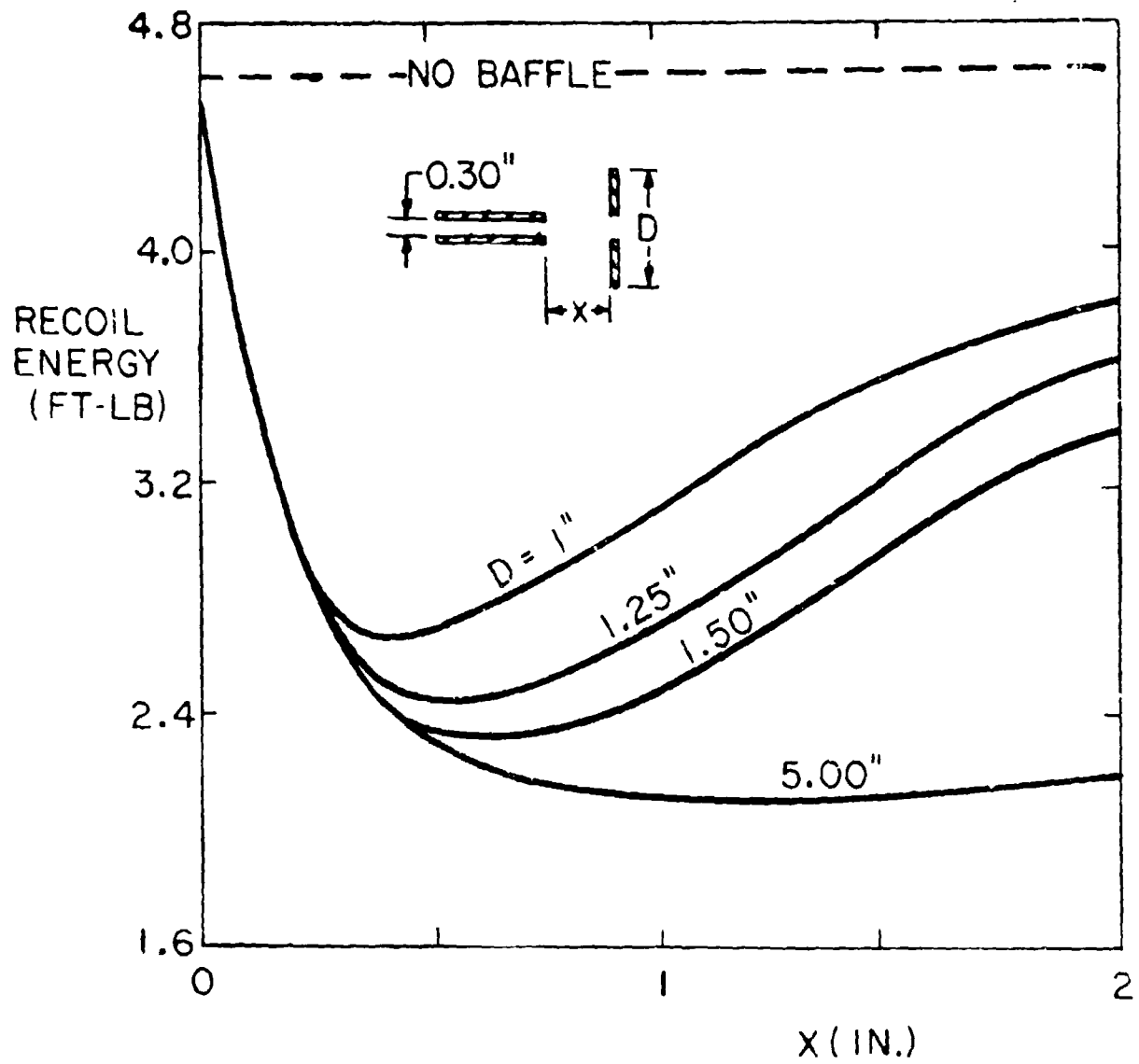


FIGURE 38 SLADE RECOIL MEASUREMENTS

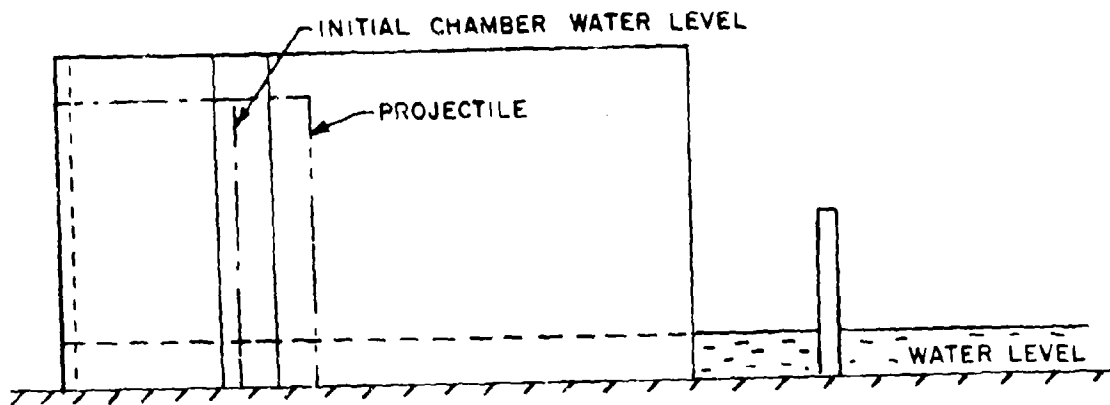
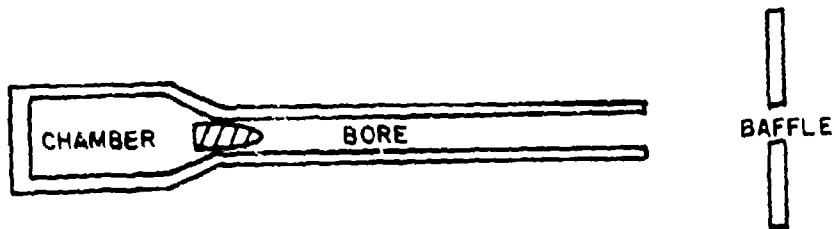


FIGURE 39 SLADE WATER TABLE

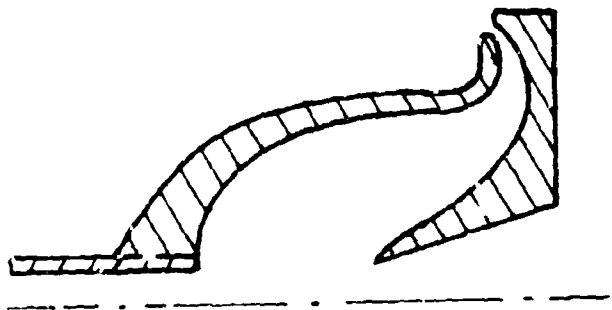
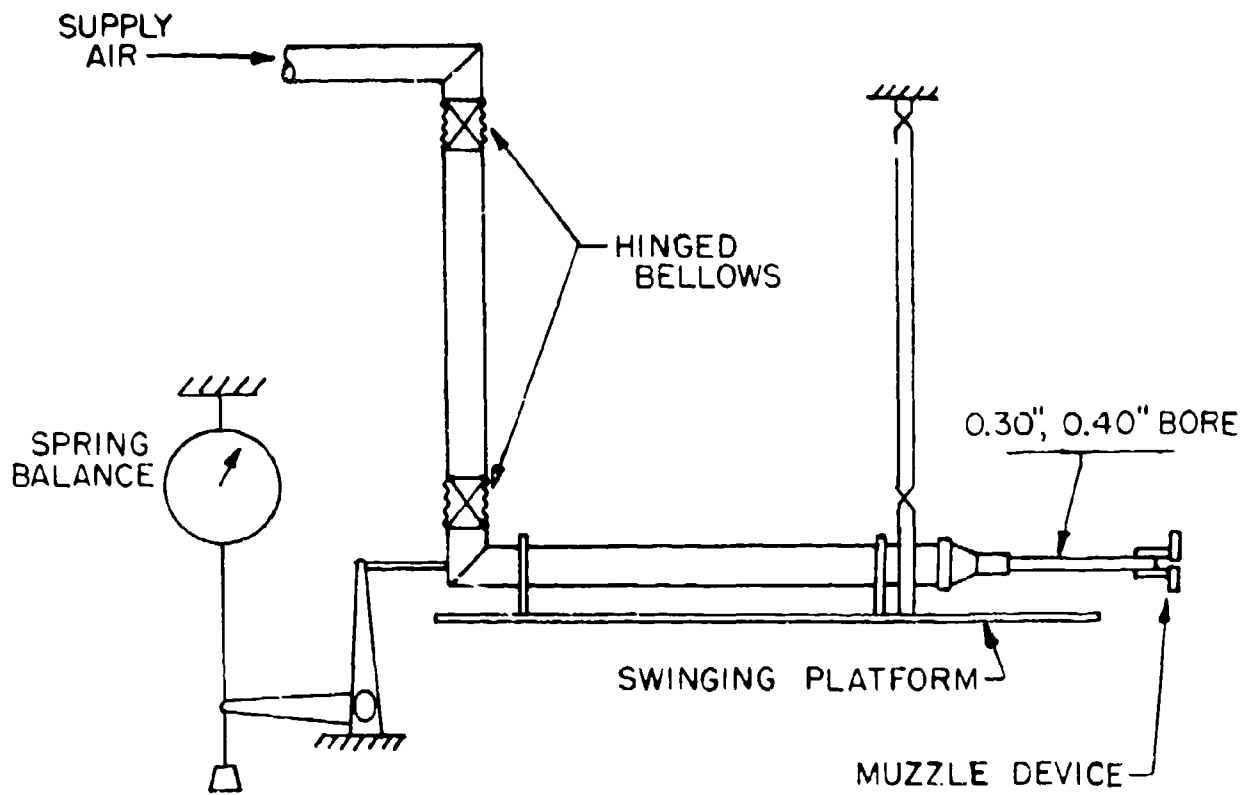


FIGURE 40 SLADE OPTIMAL TURNING VANE



TEST CONDITIONS:

$$T_{se} = 540^{\circ}R$$

$$\gamma_e = 1.40$$

$$P_{eMAX} = 61 \text{ PSIA}$$

$$P_{\infty MIN} = 0.122 \text{ PSIA}$$

NO PROJECTILE

FIGURE 41 SMITH MUZZLE BRAKE RIG

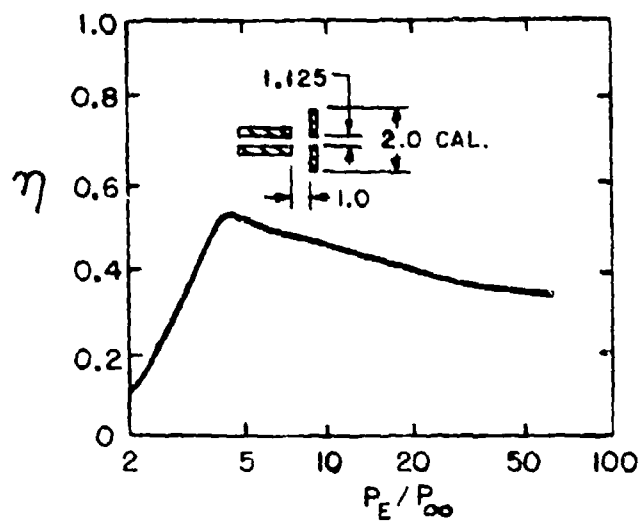


FIGURE 42 AERODYNAMIC INDEX VERSUS PRESSURE RATIO ($\bar{x}=1.0$)

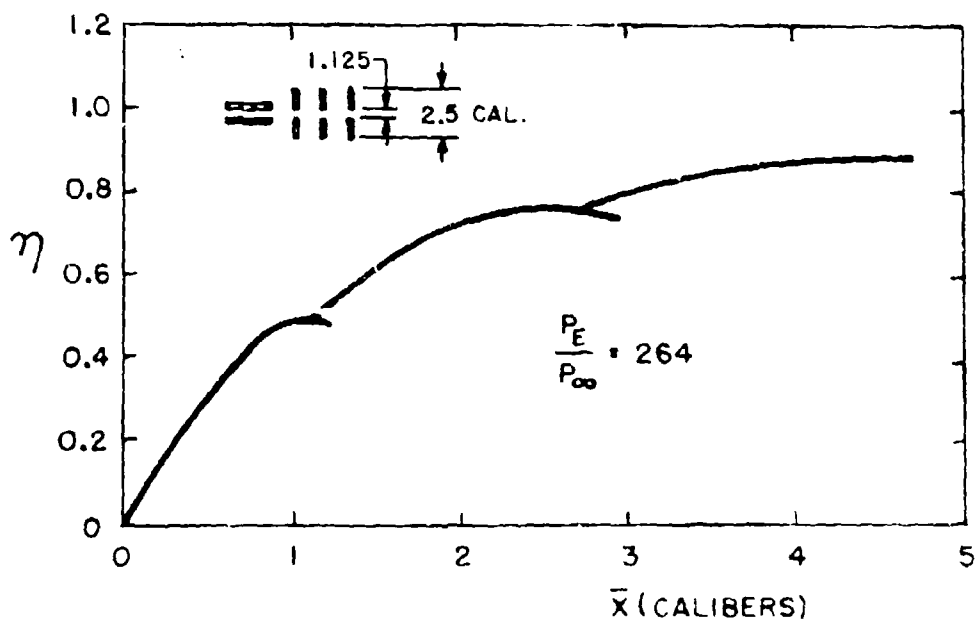
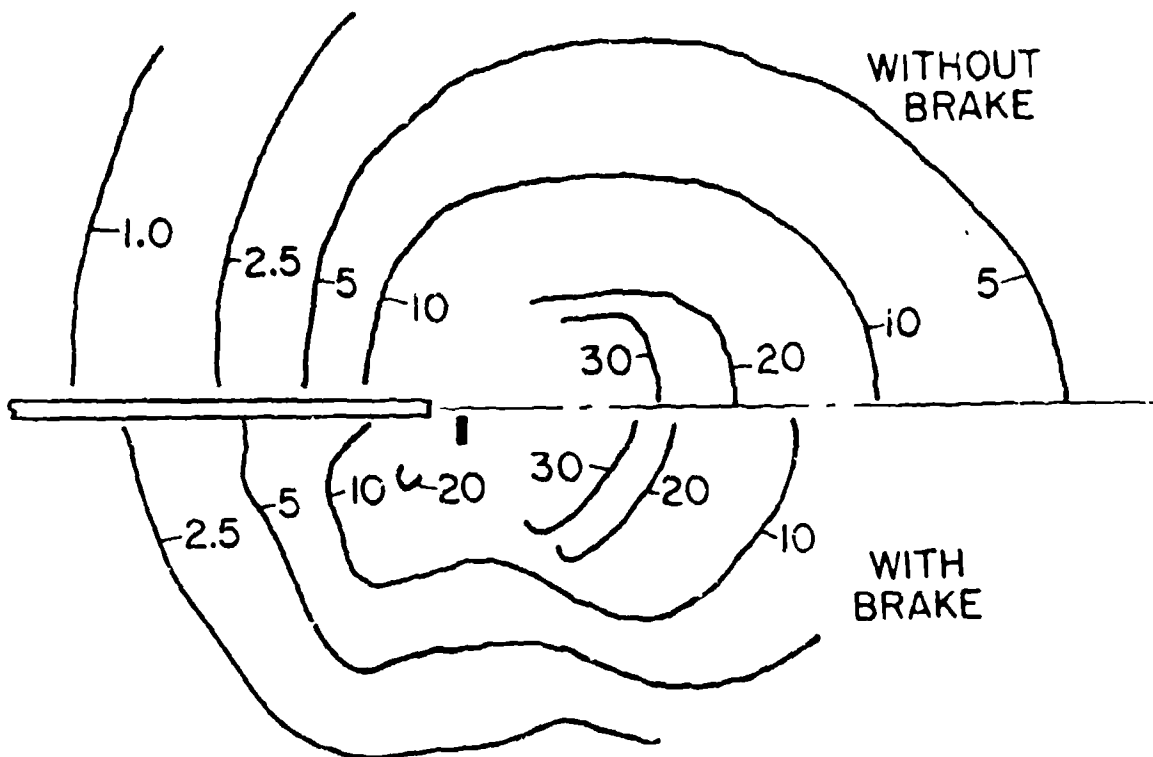


FIGURE 43 AERODYNAMIC INDEX FOR MULTIBAFFLE BRAKES



SCALE:

0 10 20 30 CALIBERS

OVERPRESSURES IN PSI

FIGURE 44 SMITH'S OVERPRESSURE MEASUREMENTS

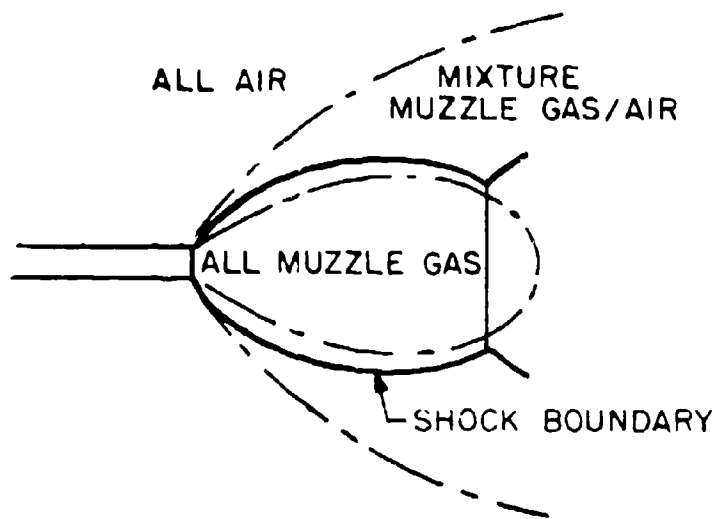
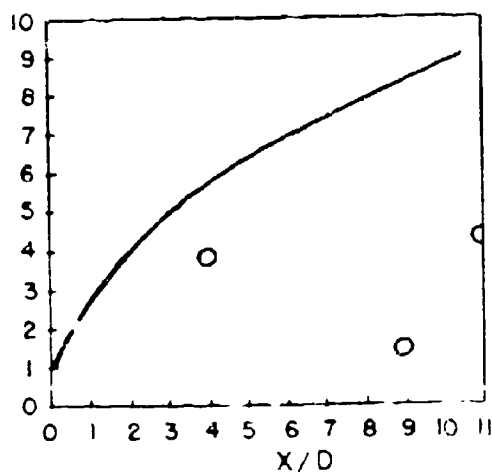
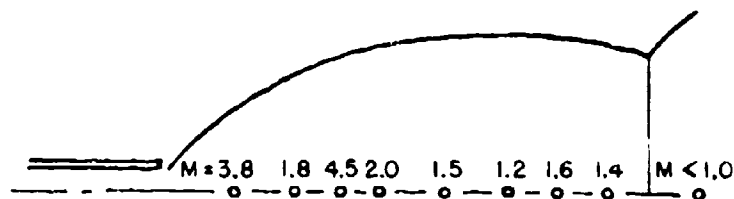


FIGURE 45 CONCENTRATION SCHEMATIC



THEORY: OWEN & THORNHILL⁵⁷

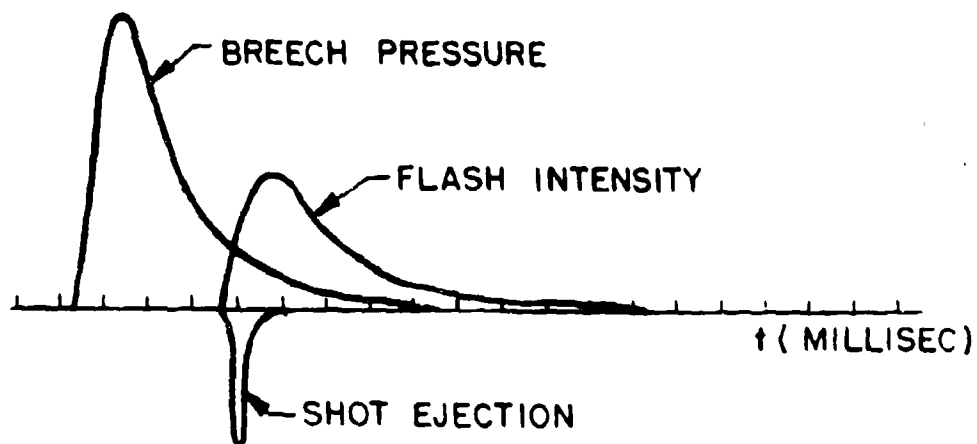
$$P_E / P_\infty = \infty$$

○ EXPERIMENT

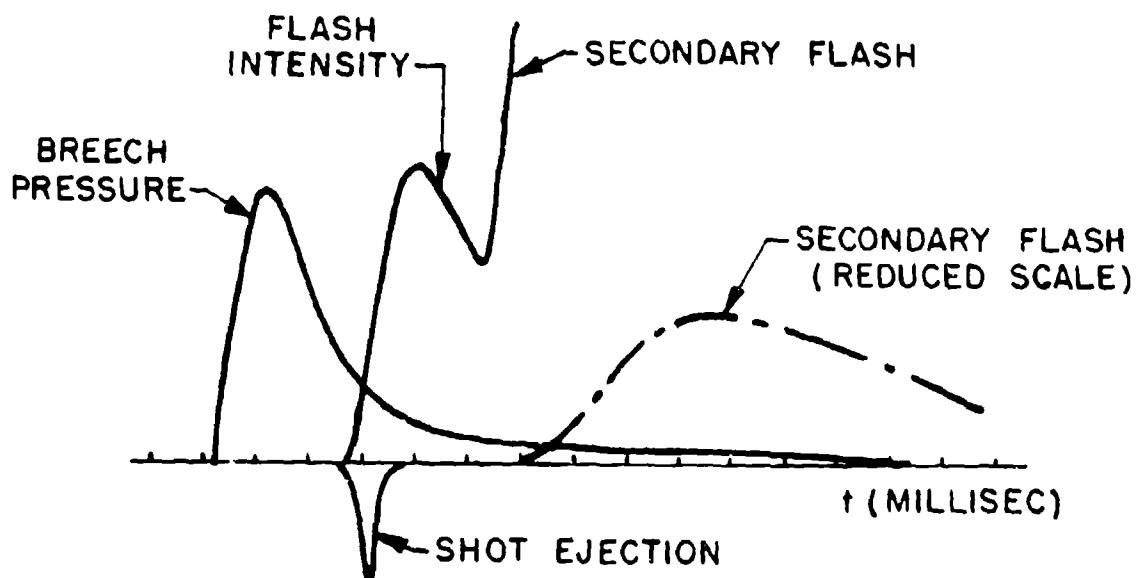
$$P_E / P_\infty = 359$$

$$T_{SE} = 540^\circ R$$

FIGURE 46 MRI MACH NUMBER MEASUREMENTS AND COMPARISON WITH THEORY



WITHOUT SECONDARY FLASH



WITH SECONDARY FLASH

FIGURE 47 RELATIVE TIME AND INTENSITY OF FLASH

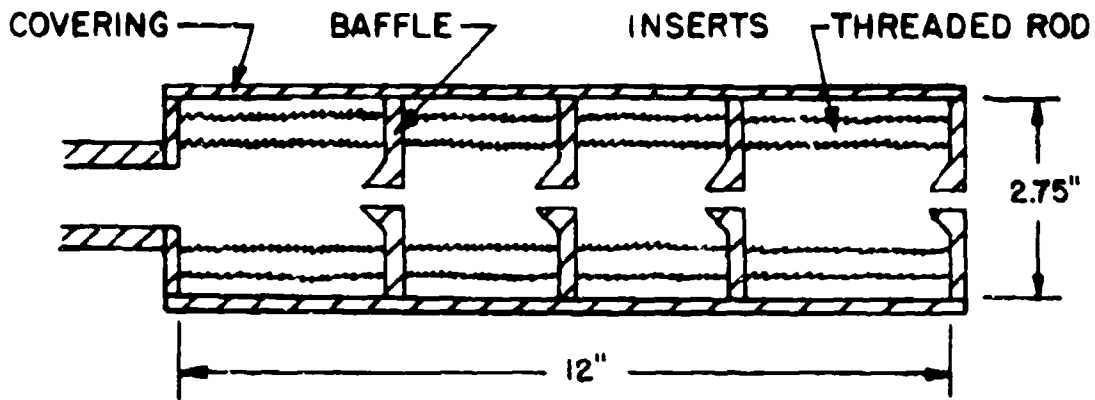


FIGURE 48 BLAST SUPPRESSOR TEST RIG

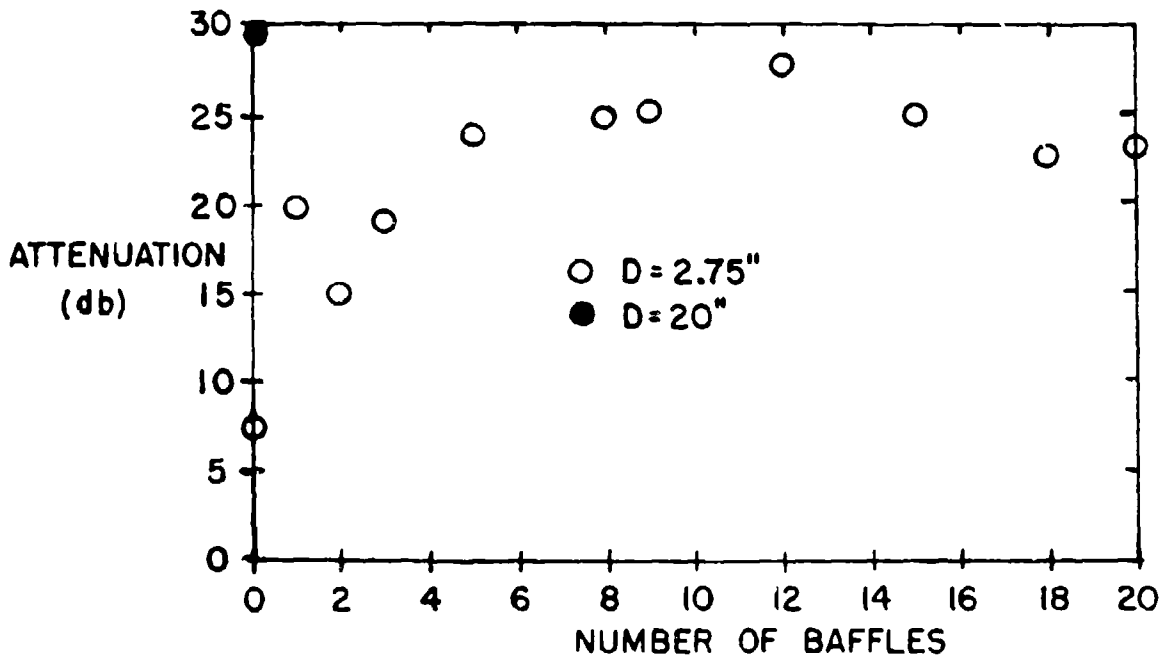


FIGURE 49 ATTENUATION OF CONSTANT LENGTH SUPPRESSOR

REFERENCES

1. E. Schmidt and D. Shear, "Experimental Transitional Ballistics at BRL", Ballistic Research Laboratories Memo Report (to be published).
2. W. A. Hyde, U. S. Navy Ordnance Pamphlet No. 422, 1913.
3. C. Cranz, and B. Glatzel, "Die Ausströmung von Gasen Bei Hohen Anfangsdrucken," Ann. der Physik, Vol. 43, 1914.
4. C. Cranz, Lehrbuch der Ballistik, J. Springer Verlag, Berlin, 1926.
5. P. Quayle, "Spark Photography and its Application to Some Problems in Ballistics," Scientific Papers, Bureau of Standards, Vol. 20, No. 508, 1925.
6. J. J. Slade, "Muzzle Blast: Its Characteristics, Effects, and Control", National Defense Research Council, Report A-391, March 1966.
7. K. Oswatitsch, "Flow Research to Improve the Efficiency of Muzzle Brakes":
 - a. "Part I: Tests on Baffle Surfaces With One-Dimensional Flow", German Air Research Report 6601, July 1943.
 - b. "Part II: Efficiency Factor, Momentum Relation, Two-Dimensional Flow, and Flow With Covering", Research and Development, Army Ordnance, Report 1001, October 1944.
 - c. "Part III: The Axial Symmetric Flow Problem, a Comparison of Tests of Muzzle Brakes Free of Reaction", Gottingen, March 1945.
8. K. Oswatitsch, "Intermediate Ballistics", Deutsche Luft und Raumfahrt FB 64-37, DVL Bericht 358, December 1964.
9. E. Love, C. Grigsby, L. Lee, and M. J. Woodling, "Experimental and Theoretical Studies of Axisymmetric Free Jets", NASA TR R-6, 1959.
10. T. Adamson, and J. Nicholls, "On The Structure of Jets From Highly Underexpanded Nozzles into Still Air", J. of the Aero/Space Sciences. Vol. 26, 1959.
11. W. Sheeran and D. Dosanjh, "Observations on Jet Flows From a Two-Dimensional, Underexpanded Sonic Nozzle", AIAA J., Vol. 6, No. 3, 1968.
12. S. Crist, P. Sherman, and D. Glass, "Study of the Highly Underexpanded Sonic Jet", AIAA J., Vol. 4, No. 1, 1966.

13. H. Ashkenas and F. Sherman, "Structure and Utilization of Supersonic Free Jets in Low Density Wind Tunnels", Rarefied Gas Dynamics Fourth Symposium, Vol. II, Academic Press, New York, 1966.
14. S. Pai, Fluid Dynamics of Jets, D. Van Nostrand, New York, 1954.
15. M. Moe and B. Troesch, "Jet Flows with Shocks", ARS J., 1960.
16. K. Bier and B. Schmidt, "Zur Form der Verdichtungsstose un Frei Expandierenden Gasstrahlen", Z. Angen. Physik, 1961.
17. M. Sibulkin, W. Gallaher, "Far-Field Approximation for a Nozzle Exhausting Into a Vacuum", AIAA J., Vol. 1, No. 6, 1963.
18. A. Charwat, "Boundary of Underexpanded Axisymmetric Jets Issuing Into Still Air", AIAA J., Vol. 2, No. 1, 1964.
19. F. Albini, "Approximate Calculation of Underexpanded Jet Structure", AIAA J., Vol. 3, No. 8, 1965.
20. J. Hill and J. Draper, "Analytical Approximation for the Flow From a Nozzle Into a Vacuum", J. Spacecraft, Vol.3, No. 10, 1966.
21. E. Wedemeyer, "Asymptotic Solutions for the Expansion of Gas Into Vacuum", Ballistic Research Laboratories Report 1278, April 1965. (AD 465 240)
22. F. Boynton, "Highly Underexpanded Jet Structure: Exact and Approximate Calculations", AIAA J., Vol. 5, No. 9, 1967.
23. K. Korkan and L. Knowles, "Boundary of Underexpanded Axisymmetric Jets in Still Air", AIAA J., Vol. 7, No. 2, 1969.
24. E. Muntz, B. Hamel, and B. Maguire, "Some Characteristics of Exhaust Plume Rarefaction", AIAA J., Vol. 8, No. 9, 1970.
25. G. Simons, "Rarefaction Effects in High-Altitude Rocket Plumes", AIAA J., Vol. 10, No. 3, 1972.
26. D. Eastman and L. Radtke, "Location of the Normal Shock Wave in the Exhaust Plume of a Jet", AIAA J., Vol. 2, No. 4, 1964.
27. C. Lewis and D. Carlson, "Normal Shock Location in Underexpanded Gas and Gas-Particle Jets", AIAA J., Vol. 2, No. 4, 1964.
28. M. Werle, D. Shaffner, and R. Driftmeyer, "Freejet Terminal Shocks", AIAA J., Vol. 8, No. 12, 1970.
29. M. Abbett, "Mach Disk in Underexpanded Exhaust Plumes", AIAA J., Vol. 9, No. 3, 1971.

30. J. Hartman and F. Lazarus, "The Air Jet With a Velocity Exceeding That of Sound", *Phil. Mag. and Journ. Sci.*, Ser. 7, Vol. 31, No. 204, 1941.
31. E. Hammer, "Muzzle Brakes, Volume I: History and Volume II: Theory", Franklin Institute, June 1949. (AD 111481)
32. M. Hugoniot, "On the Diversified Movement of a Gas Compressed in a Reservoir Which Empties Freely Into the Atmosphere", *Comptes Rendue*, Vol. 103, 1886.
33. A. Rateau, "The Theory of Muzzle Brakes", *Memorial de L'Artillerie Francaise*, Vol. XI, 1932; *Comptes Rendue*, Vol. 168, 1919.
34. L. Kazincky, "Theoretical Considerations in Regard to the Construction of Muzzle Brakes", *Memorial de L'Artillerie Francaise*, Vol. IX, 1930.
35. E. Ravelli, "A Study of the Theory of Muzzle Brakes", *Rivista di Artiglieria E Genio*, January 1929.
36. M. Gabeaud, "The Theory of Recoil Brakes", *Memorial de L'Artillerie Francaise*, Vol. XI, 1932.
37. M. Gentil, "A Summary of the Studies of Muzzle Brakes", *Memorial de L'Artillerie Francaise*, Vol. XV, 1936.
38. J. Corner, "The Internal Ballistics of a Gun After Shot Ejection", A.C. 4502/1.B 201/Gn. 227, OSRD Liaison Office Reference No. WA-859-1.
39. Engineering Design Handbook, Ballistic Series, Interior Ballistics of Guns, AMCP 706-150, U.S. Army Materiel Command, February 1965.
40. P. Baer and J. Frankle, "The Simulation of Interior Ballistic Performance of Guns by Digital Computer Program", *Ballistic Research Laboratories Report 1183*, December 1962. (AD 299 980)
41. P. Vottis, "Digital Computer Simulation of the Interior Ballistic Process in Guns", *Watervliet Arsenal, WVT-6615*, October 1965. (AD 805 248)
42. O. Heiney, "Simplified Interior Ballistics of Closed Breech Guns", *Air Force Armament Laboratory, AFATL-IR-67-42*, April 1967. (AD 822 447)
43. J. Corner, Theory of Interior Ballistics of Guns, John Wiley and Sons, New York, 1950.
44. F. Hunt, Internal Ballistics, *Philosophical Library*, New York, 1951.

45. C. Thornhill, "A New Special Solution to the Complete Problem of Interior Ballistics", Royal Armament Research and Development Establishment, Report 2/67, April 1967. (AD 818 009)
46. Engineering Design Handbook, Gun Series, Muzzle Devices, AMCP 706-251, U.S. Army Materiel Command, May 1968.
47. "Design Data Sheet, DH5", Armament Design Department, Ministry of Supply, Great Britain, 1943.
48. V. Dear and F. Smithies, "Tests of Muzzle Brakes for the Q.F. 6 PR., 7 cm. Gun", Gun Design Committee, A. C. 4162/GN. 260, June 1943.
49. C. Millikan, E. Secher, and R. Buhler, "A Study of Blast Deflectors, Final Report", National Defense Research Council, Report A-351, October 1945.
40. E. Robinson and E. Wilson, "Reduction of Smoke and Blast Obscuration Effect", National Defense Research Council, Report A-325, May 1945.
51. N. Munch, M. MacKay, and R. Greengrove, "80mm Gun Blast Deflector Development", Power Generators, Inc., Report 1398, September 1955. (AD 836 751)
52. P. Townsend, "Development of a Gas Gun to investigate Obscuration Effects", WECOM, Report 66-3281, November 1966. (AD 804 815)
53. F. Smith, "Model Experiments on Muzzle Brakes", Royal Armament Research and Development Establishment, Report 2/66, June 1966. (AD 487 121)
54. F. Smith, "Model Experiments on Muzzle Brakes, Part III: Measurement of Pressure Distribution", Royal Armament Research and Development Establishment, Report 3/68, February 1968. (AD 845 519)
55. F. Smith, "A Study of Gun Blast in Relation to That From a Moving Source", Royal Armament Research and Development Establishment, Memo 28/70, 1970. (AD 878 659)
56. F. Smith, "Loads on Surfaces Due to Gun Blast", Royal Armament Research and Development Establishment, Memo 29/70, 1970.
57. P. Owen and C. Thornhill, "The Flow in an Axially Symmetric Supersonic Jet From a Nearly Sonic Orifice Into a Vacuum", Royal Armament Research and Development Establishment, Report 30/48, 1948. (AD 57 261)
58. R. Ladenburg, C. Van Voorhis, and J. Winckler, "Interferometric Studies of Faster Than Sound Phenomena, Part II: Analysis of Supersonic Air Jets", Physics Review, Vol. 76, No. 5, September 1949.

59. A. Horton, J. Agnew, et al, "Basic and Technical Work on Military Propellants", Franklin Institute, Final Report F-2092-15, December 1949.
60. E. Stephens, G. Wachtell, and S. Carfagno, "Physical Suppression of Gun Muzzle Flash", Franklin Institute, Interim Report I-2364, September 1953. (AD 21 736)
61. J. Agnew, "Activities in Connection with Basic and Technical Work on Infrared Radiation From the Flash of Military Propellants", Franklin Institute, Progress Report 1897-10, February 1948.
62. L. Herczeg, "Investigation of the Spectral Emittance of Military Propellants", Franklin Institute, Final Report F-2258, August 1954. (AD 66 009)
63. S. Carfagno and G. Wachtell, "Emergence of Muzzle Gases Between Suppressor Bars", Franklin Institute, Interim Report I-A1828-5, January 1958 (AD 300 766)
64. S. Carfagno and O. Rudyi, "Relationship Between Propellant Composition and Flash and Smoke Produced by Combustion Products (U)", Franklin Institute, Final Report F-A2132, December 1960. (AD 321 118)(Confidential)
65. S. Carfagno, "Handbook on Gun Flash (U)", Franklin Institute, November 1961. (AD 327 051) (Confidential)
66. Engineering Design Handbook, "Spectral Characteristics of Muzzle Flash", AMCP 706-255, U.S. Army Materiel Command, June 1967.
67. W. Gillam, S. Fisher, and H. Young, "Smoke and Flash in Small Arms Ammunition", Midwest Research Institute, 1948.
68. H. Young, "Smoke and Flash in Small Arms Ammunition, 1948-1955", Midwest Research Institute, 1954. (AD 88 537)
69. J. Fay, "The Physical Mechanism of Gun Flash", Midwest Research Institute, Progress Report 1, June 1954.
70. E. Hodil and D. Merrill, "Weapon Development, Multiple Flechette Weapon System Development Contract", Winchester-Western, October 1970.
71. J. Wyatt, "Flash Hider for GAU - 2B/A (7.62 Miniguns)", Eglin AFB, June 1969. (AD 864 225L)
72. C. Burket, "Integrated Engineering and Service Test of the Flash Suppressor Assembly for M134, 7.62mm Miniguns", U.S. Army Aviation Test Board, August 1970. (AD 875 334L)

73. R. Ladenburg, "Report on Muzzle Flash", Ballistic Research Laboratories Report No. 426, 1943.
74. R. Ladenburg, "Suppression of Muzzle Flash From Caliber .30 Machine Gun", Ballistic Research Laboratories MR 404, 1945. (AD 492 761)
75. R. Ladenburg, "Studies of the Muzzle Flash and its Suppression", Ballistic Research Laboratories Report 618, 1947. (AD 224 762)
76. W. Watling, "Acoustical and Visual Attenuation Through Dynamic Regulation of Muzzle Gas Flow", Springfield Armory, June 1966. (AD 634 649)
77. A. Karakauskas, "Sudden Expansion of a Bounded Jet at High Pressure Ratio", AIAA J., Vol. 2, No. 9, September 1964.
78. L. Skochko and H. Greveris, "Silencers", Frankford Arsenal, Report R-1896, August 1968.
79. P. Westine, "Structural Response of Helicopters to Muzzle and Breech Blast. Volume I of Final Technical Report: Blast Field About Weapons", Southwest Research Institute, Report 02-2029, November 1968.
80. P. Westine, "Modeling the Blast Field Around Guns and Conceptual Design of a Model Gun Blast Facility", Southwest Research Institute, Report 02-2643-01, September 1970. (AD 875 984).
81. B. Hopkinson, British Ordnance Board Minutes 13565, 1915.
82. G. Schlenker, "Contribution to the Analysis of Muzzle Brake Design", Rock Island Arsenal, Report 62-1794, May 1962.
83. G. Schlenker, "Theoretical Study of the Blast Field of Artillery With Muzzle Brakes", Rock Island Arsenal, Report 62-4257, December 1962.
84. G. Schlenker and S. Olson, "A revised Method of Computing the Overpressure Isobars in the Blast Field of Artillery", Rock Island Arsenal, Tech. Note 65-2, July 1965. (AD 817 024L)
85. H. Brode, "Point Source Explosion in Air", Rand Corporation RM-1824-AEC, December 1956. (AD 133 030)
86. H. Brode, "A Calculation of the Blast Wave From a Spherical Charge of TNT", Rand Corporation, RM-1965, August 1957. (AD 144 302)
87. W. Furrer, "The Acoustics of Detonation", Schweizer Archiv, July 1946.

88. G. Reynolds, "Muzzle Blast Pressure Measurements", Princeton University, Report PMR-21, April 1944.
89. U.S. Navy Gun Blast Committee, "Survey of Research on Blast (U)", First Interim Report, 1946 (Confidential).
90. H. Barton, R. Heyman, and T. Schiffman, "Correlation of Muzzle Blast Pressures Over Flat Surfaces", Armour Research Foundation, 1956.
91. S. Levin, "Concept and Feasibility Studies of Muzzle Brake Blast Suppression Devices for 105mm and 155mm Howitzers", Ordnance Engineering Associates, Report P.N. 2070, February 1964 . (AD 601 728)
92. O. Bixler, H. Kahlke, R. Kaplan, and J. Van Houten, "Analytical and Experimental Studies of Weapon Muffling", Ling Tempco Vought, TR O-71200/7TR-123, August 1967. (AD 821 879L)
93. G. Whitham, "On the Propagation of Shock Waves Through Regions of Non-uniform Area or Flow", J. Fluid Mech., Vol. 4, 1958.
94. G. Garinther and J. Moreland, "Transducer Techniques for Measuring the Effect of Small Arms Noise on Hearing", U.S. Army Human Engineering Laboratories, TM 11-65, July 1965.
95. N. Ethridge, "A Procedure for Reading and Smoothing Pressure-Time Data From H.E. and Nuclear Explosions", Ballistic Research Laboratories Memorandum Report 1691, September 1965. (AD 479 775)
96. R. Reisler, R. Raley, and D. Lefevre, "Air Blast Measurements Recorded by Standard and Developmental Instrumentation", P.O.R. 4030, Operation Sailor Hat, NDA, July 1967. (AD 819 459)
97. Materiel Test Procedure, "Airblast Pressure Measurement-Electric", Test and Evaluation Command, July 1970. (AD 875 696)
98. C. Kingery, "Parametric Analysis of Sub-Kiloton Nuclear and High Explosive Air Blast", Ballistic Research Laboratories, February 1968. (AD 833 698)

DISTRIBUTION LIST

<u>No. of Copies</u>	<u>Organization</u>	<u>No. of Copies</u>	<u>Organization</u>
2	Commander Defense Documentation Center ATTN: TIPCR Cameron Station Alexandria, Virginia 22314	1	Commander U.S. Army Materiel Command ATTN: AMCRD-W 5001 Eisenhower Avenue Alexandria, Virginia 22304
1	Director Defense Nuclear Agency Washington, DC 20305	1	Commander U.S. Army Aviation Systems Command ATTN: AMSAV-E 12th & Spruce Streets St. Louis, Missouri 63166
1	Commander U.S. Army Materiel Command ATTN: AMCDL 5001 Eisenhower Avenue Alexandria, Virginia 22304	1	Director U.S. Army Air Mobility Research and Development Laboratory Ames Research Center Moffett Field, California 94035
1	Commander U.S. Army Materiel Command ATTN: AMCRD, MG S. C. Meyer 5001 Eisenhower Avenue Alexandria, Virginia 22304	2	Commander U.S. Army Electronics Command ATTN: AMSEL-CE AMSEL-RD Fort Monmouth, New Jersey 07703
1	Commander U.S. Army Materiel Command ATTN: AMCRD, Dr. J.V.K.Kaufman 5001 Eisenhower Avenue Alexandria, Virginia 22304	2	Commander U.S. Army Missile Command ATTN: AMSMI-R AMSMI-RBL Redstone Arsenal, Alabama 35809
1	Commander U.S. Army Materiel Command ATTN: AMCRD-TP 5001 Eisenhower Avenue Alexandria, Virginia 22304	5	Commander U.S. Army Missile Command ATTN: AMSMI-RDK Mr. R. Becht (4 cys) Mr. R. Deep Redstone Arsenal, Alabama 35809
1	Commander U.S. Army Materiel Command ATTN: AMCRD-TE 5001 Eisenhower Avenue Alexandria, Virginia 22304	1	Commander U.S. Army Tank Automotive Command ATTN: AMSTA-RHFL Warren, Michigan 48090
1	Commander U.S. Army Materiel Command ATTN: AMCRD-MT 5001 Eisenhower Avenue Alexandria, Virginia 22304		

DISTRIBUTION LIST

<u>No. of Copies</u>	<u>Organization</u>	<u>No. of Copies</u>	<u>Organization</u>
2	Commander U.S. Army Mobility Equipment Research & Development Center ATTN: Tech Docu Ctr, Bldg. 315 AMSME-RZT Fort Belvoir, Virginia 22060	4	Commander U.S. Army Weapons Command ATTN: AMSWE-RE AMSWE-RES AMSWE-RDF AMCPM-RS Rock Island, Illinois 61202
2	Commander U.S. Army Munitions Command ATTN: AMSMU-RE AMSMU-RE-M Dover, New Jersey 07801	1	Commander US Army Watervliet Arsenal Watervliet, New York 12189
5	Commander U.S. Army Frankford Arsenal ATTN: SMUFA-U2100 Mr. J. Mitchell SMUFA-U3100 Mr. S. Fulton SMUFA-U3300 Mr. S. Hirshman SMUFA-U3300 Mr. A. Cianciosi L4100-150-2 Mr. C. Sleischer, Jr. Philadelphia, Pennsylvania 19137	1	Commander U.S. Army Safeguard Systems Command Huntsville, Alabama 35804
		1	Director U.S. Army Advanced Materiel Concepts Agency 2461 Eisenhower Avenue Alexandria, Virginia 22314
		1	Commander U.S. Army Harry Diamond Laboratories ATTN: AMXDO-TD/002 Washington, DC 20438
7	Commander U.S. Army Picatinny Arsenal ATTN: SMUPA-DR-D, Mr. S. Wasserman SMUPA-DR-V, Mr. A. Loeb Mr. D. Mertz SMUPA-D, Mr. Lindner SMUPA-V, Mr. E. Walbrecht Mr. S. Verner SMUPA-VE, Dr. Kaufman Dover, New Jersey 07801	1	Commander U.S. Army Materiel and Mechanics Research Center ATTN: AMXMR-ALL Watertown, Massachusetts 02172
		1	Commander U.S. Army Natick Laboratories ATTN: AMXRE, Dr. D. Sieling Natick, Massachusetts 01762
1	PLASTECH U.S. Army Picatinny Arsenal ATTN: SMUPA-FR-M-D Dover, New Jersey 07801	1	Deputy Assistant Secretary of the Army (R&D) ATTN: Mr. C. L. Poor Washington, DC 20310

DISTRIBUTION LIST

<u>No. of Copies</u>	<u>Organization</u>	<u>No. of Copies</u>	<u>Organization</u>
1	Commander U.S. Army Research Office (Durham) ATTN: CRD-AA-EH Box CM, Duke Station Durham, North Carolina 27706	4	Director U.S. Naval Research Laboratory ATTN: Tech Info Div Code 7700, Dr. A. Kolb Code 7720, Dr. E. McClean Mr. I. Vitkovitsky Washington, DC 20390
1	Director U.S. Army Advanced Ballistics Missile Defense Agency P. O. Box 1500 Huntsville, Alabama 35809	3	Commander U.S. Naval Weapons Laboratory ATTN: Code GX, Dr. W. Kemper Code V213, Mr. J. Edwards Code MAS, Mr. M. Jones Dahlgren, Virginia 22448
3	Commander U.S. Naval Air Systems Command ATTN: AIR-604 Washington, DC 20360	2	Commander U.S. Naval Ordnance Station Indian Head, Maryland 20640
3	Commander U.S. Naval Ordnance Systems Command ATTN: ORD-9132 Washington, DC 20360	1	AEDC (AER) Arnold AFS Tennessee 37389
2	Commander and Director U.S. Naval Ship Research and Development Center ATTN: Tech Lib Aerodynamic Lab Washington, DC 20007	2	ADTC (ADBPS-12) Eglin AFB Florida 32542
3	Commander U.S. Naval Weapons Center ATTN: Code 753, Tech Lib Code 50704, Dr. W. Haseltine Code 3007, Mr. A. Rice China Lake, California 93555	1	AFATL (DLR) Eglin AFB Florida 32542
4	Commander U.S. Naval Ordnance Laboratory ATTN: Code 031, Dr. K. Lobb Code 312, Mr. R. Regan Mr. S. Hastings Code 730, Tech Lib Silver Spring, Maryland 20910	1	AFATL (DLRD) Eglin AFB Florida 32542
		1	AFATL (DLRV) Eglin AFB Florida 32542
		2	AFATL (DLRA, Mr. F. Burgess; Tech Lib) Eglin AFB Florida 32542

DISTRIBUTION LIST

<u>No. of Copies</u>	<u>Organization</u>	<u>No. of Copies</u>	<u>Organization</u>
1	AFWL (DEV) Technical Library Kirtland AFB New Mexico 87117	2	Director National Aeronautics and Space Administration George C. Marshall Space Flight Center ATTN: MS-1, Lib R-AERO-AE, Mr. A. Felix Huntsville, Alabama 35812
1	ARD (ARIL) Wright Patterson AFB Ohio 45433	1	Director National Aeronautics and Space Administration Langley Research Center ATTN: MS 185, Tech Lib Langley Station Hampton, Virginia 23365
1	ARL Wright-Patterson AFB Ohio 45433	1	Director National Aeronautics and Space Administration Lewis Research Center ATTN: MS 60-3, Tech Lib 21000 Brookpark Road Cleveland, Ohio 44135
1	ASD (ASBEE) Wright-Patterson AFB Ohio 45433	1	Advanced Technology Laboratories ATTN: Dr. J. Erdos 400 Jericho Turnpike Jericho, New York 11753
1	RTD (FDPE, Mr. Sedderke) Wright-Patterson AFB Ohio 45433	2	ARO, Inc. ATTN: Tech Lib Arnold AFS Tennessee 37389
1	Director National Bureau of Standards ATTN: Tech Lib U.S. Department of Commerce Washington, DC 20234	1	Technical Director Solt Firearms Corporation 150 Huyshore Avenue Hartford, Connecticut 14061
1	Headquarters National Aeronautics & Space Administration ATTN: Code EP, M. Adams Washington, DC 20546	1	General Electric Corporation Armaments Division ATTN: Mr. R. Whyte Lakeside Avenue Burlington, Vermont 05401
1	Director NASA Scientific & Technical Information Facility ATTN: SAK/DL P. O. Box 33 College Park, Maryland 20740		
1	Director Jet Propulsion Laboratory ATTN: Tech Lib 4800 Oak Grove Drive Pasadena, California 91105		

DISTRIBUTION LIST

<u>No. of Copies</u>	<u>Organization</u>	<u>No. of Copies</u>	<u>Organization</u>
1	Winchester-Western Division Olin Corporation ATTN: Mr. D. Mertill New Haven, Connecticut 06504	1	Massachusetts Institute of Technology Department of Aeronautics and Astronautics ATTN: Tech Lib 77 Massachusetts Avenue Cambridge, Massachusetts 02139
1	Sandia Corporation ATTN: Aerodynamics Dept Org. 9320, R. Maydew P. O. Box 5800 Albuquerque, New Mexico 87115	1	Director Guggenheim Aerospace Labs New York University New York Heights New York, New York 10053
1	California Institute of Technology Aeronautics Department ATTN: Prof. H. Liepmann Pasadena, California 91102	1	Ohio State University Department of Aeronautics and Astronautical Engineering ATTN: Tech Lib Columbus, Ohio 43210
1	Guggenheim Aeronautical Laboratory California Institute of Technology ATTN: Tech Lib Pasadena, California 91104	1	Polytechnic Institute of Brooklyn Graduate Center ATTN: Dr. G. Morretti Farmingdale, New York 11735
3	Calspan Corporation ATTN: Mr. J. Martin Dr. W. Wurster Dr. G. Skinner P. O. Box 235 Buffalo, New York 14221	1	Director Forrestal Research Center Princeton University Princeton, New Jersey 08540
2	Franklin Institute ATTN: Dr. Carfagno Dr. Wachtell Race & 20th Streets Philadelphia, Pennsylvania 19103	1	Princeton University Forrestal Laboratories ATTN: Dr. S. I. Cheng Princeton, New Jersey 08540
1	Director Applied Physics Laboratory The Johns Hopkins University 8621 Georgia Avenue Silver Spring, Maryland 20910	2	University of Michigan Department of Aeronautical Engineering ATTN: Dr. A. Kuethe Dr. M. Sichel East Engineering Building Ann Arbor, Michigan 48104

DISTRIBUTION LIST

No. of
Copies Organization

Aberdeen Proving Ground

Ch, Tech Lib
Marine Corps Ln Ofc
CDC Ln Ofc
CO, USALWL
CO, USASASA (5 cys)
 ATTN: Mr. B. Jezek
CDR, USATECOM
 ATTN: AMSTE-BE
 Mr. Morrow
 AMSTE-TA-R
 Mr. Wise
Dir, USAMSAA
 ATTN: Dr. J. Sperrazza

UNCLASSIFIED
Security Classification

DOCUMENT CONTROL DATA - R & D

(Security classification of title, body of abstract and indexing annotation must be entered when the overall report is classified)

1. ORIGINATING ACTIVITY (Corporate author) U. S. Army Ballistic Research Laboratories Aberdeen Proving Ground, Maryland 21005		2a. REPORT SECURITY CLASSIFICATION Unclassified	
2b. GROUP			
3. REPORT TITLE MUZZLE DEVICES, A STATE-OF-THE-ART SURVEY. VOLUME I: HARDWARE STUDY			
4. DESCRIPTIVE NOTES (Type of report and inclusive dates)			
5. AUTHOR(S) (First name, middle initial, last name) EDWARD M. SCHMIDT			
6. REPORT DATE FEBRUARY 1973		7a. TOTAL NO. OF PAGES 114	7b. NO. OF REFS 98
8a. CONTRACT OR GRANT NO.		8b. ORIGINATOR'S REPORT NUMBER(S) BRL MEMORANDUM REPORT NO. 2276	
8c. PROJECT NO. RDT&E 1J562604A607		9a. OTHER REPORT NO(S) (Any other numbers that may be assigned this report)	
10. DISTRIBUTION STATEMENT Distribution limited to US Government agencies only. Other requests for this document must be referred to Director, USA Ballistic Research Laboratories, ATTN: AMXBR-XM-SE, Aberdeen Proving Ground, Maryland 21005. 26 APR 1973 TBC			
11. SUPPLEMENTARY NOTES		12. SPONSORING MILITARY ACTIVITY U. S. Army Materiel Command Washington, D. C. 20315	
13. ABSTRACT A review of the salient literature addressing the engineering design of muzzle devices is presented. Both theoretical and experimental techniques applicable to specific hardware items are discussed. The types of devices considered include: muzzle brakes, compensators, blast deflectors, blast suppressors, and flash suppressors. The second volume of this report addresses specific gas dynamic theories which are applicable, but, in general, have not been utilized in the analysis of muzzle gas flow fields.			

DD FORM 1473

REPLACES DD FORM 1473, 1 JAN 64, WHICH IS OBSOLETE FOR ARMY USE.

UNCLASSIFIED
Security Classification

UNCLASSIFIED
Security Classification

14. KEY WORDS	LINK A		LINK B		LINK C	
	ROLE	WT	ROLE	WT	ROLE	WT
Muzzle Devices						
Muzzle Brakes						
Silencers						
Flash Suppressors						
Blast Suppressors						

UNCLASSIFIED
Security Classification